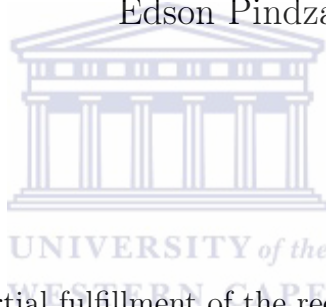


Robust Spectral Methods for Solving Option Pricing Problems

Edson Pindza



A Thesis submitted in partial fulfillment of the requirements for the degree of Doctor of Philosophy in the Department of Mathematics and Applied Mathematics at the Faculty of Natural Sciences, University of the Western Cape

Supervisor: Prof. Kailash C. Patidar

June 2012

KEYWORDS

Financial derivatives

European and American options

Exotic options

Jump-diffusion models

Volatility models

Spectral methods

Rational approximations

Time integration methods

Penalty methods.



ABSTRACT

Robust Spectral Methods for Solving Option Pricing Problems

by

Edson Pindza

**PhD thesis, Department of Mathematics and Applied Mathematics, Faculty of
Natural Sciences, University of the Western Cape**

Ever since the invention of the classical Black-Scholes formula to price the financial derivatives, a number of mathematical models have been proposed by numerous researchers in this direction. Many of these models are in general very complex, thus closed form analytical solutions are rarely obtainable. In view of this, we present a class of efficient spectral methods to numerically solve several mathematical models of pricing options. We begin with solving European options. Then we move to solve their American counterparts which involve a free boundary and therefore normally difficult to price by other conventional numerical methods. We obtain very promising results for the above two types of options and therefore we extend this approach to solve some more difficult problems for pricing options, viz., jump-diffusion models and local volatility models. The numerical methods involve solving partial differential equations, partial integro-differential equations and associated complementary problems which are used to model the financial derivatives. In order to retain their exponential accuracy, we discuss the necessary modification of the spectral methods. Finally, we present several comparative numerical results showing the superiority of our spectral methods.

June 2012.

DECLARATION

I declare that *Robust Spectral Methods for Solving Option Pricing Problems* is my own work, that it has not been submitted before for any degree or examination at any other university, and that all sources I have used or quoted have been indicated and acknowledged by complete references.

Edson Pindza

June 2012

Signed

ACKNOWLEDGEMENT

My praise and gratitude to NDZAMI who always inspires me in any aspect of my life.

I would first like to express the deepest appreciation to my advisor, Professor Kailash C. Patidar for his inspiration, constant encouragement and tremendous help on this research work.

Special thanks go to his wife for her welcoming and hospitality during after hour work at their house.

I would like to thank my parents, brothers and sisters for their belief in me, they never question me on what I was doing in South Africa during these years.

I am extremely grateful to Nathalie Van Landuyt for her support, patience and love.

I would like to express my deepest gratitude to, my brother from another mother, Edgard Ngounda. Many thanks to your fiancée Vegalia Komba for your support during the most challenging moments of my life, you never give up on me.

To all my friends, Stephane, Elvis, Tadi, Serge, Hermanno, Nina, Arsene, Roland, I say thank you for your calls and encouragement.

I would like to thank the Department of Mathematics and Applied Mathematics at the University of the Western Cape for the working facilities.

Lastly, I would appreciate the financial support of the Gabonese government through the Agence Nationale des Bourses du Gabon.

DEDICATION

To my Parents

Pindza Jean Urbain and Bakani Georgette



Contents

| | |
|---|----------|
| Keywords | i |
| Abstract | ii |
| Declaration | iii |
| Aknowledgement | iv |
| Dedication | v |
| List of Tables | xiii |
| List of Figures | xvii |
| List of Publications | xviii |
| 1 General introduction | 1 |
| 1.1 Option pricing | 1 |
| 1.2 A quick tour to spectral methods and their applications | 4 |
| 1.2.1 Rational spectral collocation approximation | 5 |
| 1.2.2 Clenshaw-Curtis quadrature formula | 9 |
| 1.2.3 Grid transformations | 11 |
| 1.3 Literature Review | 17 |
| 1.4 Outline of the thesis | 22 |



| | | |
|----------|---|-----------|
| 2 | A fully spectral collocation methods for pricing European style standard and non-standard options | 25 |
| 2.1 | Introduction | 26 |
| 2.2 | The mathematical model | 27 |
| 2.3 | Spectral space discretisation of the PDE | 30 |
| 2.4 | Sinc function time approximations and related properties | 30 |
| 2.4.1 | Single Exponential (SE) Sinc method | 31 |
| 2.4.2 | Double Exponential (DE) Sinc method | 33 |
| 2.4.3 | Full discretisation | 35 |
| 2.5 | Numerical results | 37 |
| 2.5.1 | Valuation of European call options | 38 |
| 2.5.2 | Valuation of European put options | 42 |
| 2.5.3 | Valuation of European digital call options | 43 |
| 2.5.4 | Valuation of supershare options | 46 |
| 2.6 | Summary and discussions | 47 |
| 3 | Implicit-explicit predictor-corrector methods combined with rational spectral methods for pricing European options | 49 |
| 3.1 | Introduction | 50 |
| 3.2 | The mathematical model | 51 |
| 3.3 | Spectral space discretisation of the PDE | 52 |
| 3.4 | Implicit-explicit predictor-corrector time discretisation | 53 |
| 3.5 | Convergence and stability results for the implicit-explicit predictor-corrector methods | 57 |
| 3.6 | Numerical results | 60 |
| 3.6.1 | Valuation of European call options | 60 |
| 3.6.2 | Valuation of European put options | 66 |
| 3.6.3 | Valuation of European digital call options | 68 |
| 3.6.4 | Valuation of Butterfly spread options | 69 |

| | | |
|----------|---|------------|
| 3.7 | Summary and discussions | 71 |
| 4 | Rational spectral collocation method for pricing American options | 72 |
| 4.1 | Introduction | 72 |
| 4.2 | The mathematical model | 74 |
| 4.3 | Spectral space discretisation of the nonlinear PDE | 75 |
| 4.4 | Numerical results | 78 |
| 4.4.1 | Valuation of American put options | 78 |
| 4.4.2 | Valuation of American butterfly spread options | 82 |
| 4.5 | Summary and discussions | 84 |
| 5 | Spectral methods for pricing European and American options under local volatility | 86 |
| 5.1 | Introduction | 87 |
| 5.2 | The mathematical model | 88 |
| 5.3 | Spectral space discretisation of the PDEs | 91 |
| 5.4 | Numerical results | 92 |
| 5.4.1 | Valuation European options under local volatility | 94 |
| 5.4.2 | Valuation of American options under local volatility | 97 |
| 5.5 | Summary and discussions | 99 |
| 6 | Robust spectral method for numerical valuation of European options under Merton's jump-diffusion model | 101 |
| 6.1 | Introduction | 102 |
| 6.2 | The mathematical model | 102 |
| 6.3 | Spectral space discretisation of the PIDE | 104 |
| 6.4 | Time integration | 107 |
| 6.4.1 | Convergence and stability results for the implicit-explicit predictor-corrector methods | 108 |
| 6.5 | Numerical results | 110 |

| | | |
|----------|---|------------|
| 6.5.1 | Valuation of European call options | 110 |
| 6.5.2 | Valuation of European butterfly spread options | 115 |
| 6.6 | Summary and discussions | 118 |
| 7 | Spectral collocation methods to price American options with jump-diffusion processes | 120 |
| 7.1 | Introduction | 121 |
| 7.2 | The mathematical model | 123 |
| 7.3 | Spectral space discretisation of the nonlinear PIDE | 125 |
| 7.4 | Numerical results | 128 |
| 7.4.1 | Valuation of American jump-diffusion model under constant volatility | 129 |
| 7.4.2 | Valuation of American jump-diffusion model under local volatility | 131 |
| 7.5 | Summary and discussions | 134 |
| 8 | Concluding remarks and scope for the future research | 135 |
| | Bibliography | 138 |

List of Tables

| | |
|---|----|
| 2.5.1 Convergence of the SE Sinc method for European call option. | 39 |
| 2.5.2 Convergence of the DE Sinc method for European call option. | 39 |
| 2.5.3 Comparison of European call option valuation by using the rational collocation (RC) method on CGL grid and the finite difference (FD) method on uniform grid. | 40 |
| 2.5.4 Comparison of European call option valuation by using the rational collocation (RC), finite difference (FD) and the TGB ([127]) methods using adaptive grid. | 41 |
| 2.5.5 Comparison of European put option valuation by using the rational collocation (RC), the finite difference (FD) and ([127]) methods using adaptive grid. | 43 |
| 2.5.6 Numerical results for valuing digital call options using the rational collocation (RC), finite difference (FD) and TGB [127] methods on adaptive grid, using parameters: $E = 45$, $T = 0.5$, $r = 0.05$, $\sigma = 0.2$, $\delta = 0.03$, $\beta = 10^6$, $M = 32$ | 45 |
| 2.5.7 Numerical results for valuing supershare options using the rational collocation (RC), finite difference (FD) and TGB [127] methods on adaptive grid using parameters: $E = 45$, $T = 0.5$, $r = 0.05$, $\sigma = 0.2$, $\delta = 0.03$, $\beta = 10^6$, $M = 32$, $S_{\max} = 200$, $S_{\min} = 0$ | 46 |
| 3.6.1 Comparison of European call option valuation using barycentric Lagrange collocation (BLC) with Chebyshev Gauss Labatto (CGL) points and finite difference method (FD) with uniform grid points. | 62 |

| | |
|--|----|
| 3.6.2 Comparison of European call option valuation using barycentric Lagrange collocation (BLC) with transformed Chebyshev Gauss Labatto (CGL) points and finite difference method (FD) with non-uniform grid points. | 62 |
| 3.6.3 Comparison of European put option valuation using barycentric Lagrange collocation (BLC) with transformed Chebyshev Gauss Labatto (CGL) points and finite difference method (FD) with uniform grid points. | 63 |
| 3.6.4 Comparison of European digital call option valuation using barycentric Lagrange collocation (BLC) with transformed Chebyshev Gauss Labatto (CGL) points and finite difference method (FD) with uniform grid points. | 64 |
| 3.6.5 Comparison of European butterfly spread option valuation using barycentric Lagrange collocation (BLC) with transformed Chebyshev Gauss Labatto (CGL) points and finite difference method (FD) with uniform grid points. . . | 65 |
| 4.4.1 Data used to value American put options. | 78 |
| 4.4.2 Results of the rational spectral collocation (RSC) method with respect to the penalty term for valuing American put options with the set of parameters given in Table 4.4.1. | 79 |
| 4.4.3 Comparison of the rational spectral collocation (RSC) method with other existing methods for valuing American put options with the set of parameters given in Table 4.4.1. | 80 |
| 4.4.4 Data used to value American butterfly spread options | 82 |
| 4.4.5 Comparison of the convergence of the rational spectral collocation (RSC) method with other existing methods for valuing American butterfly spread options at strike price E_1 with the set of parameters given in Table 4.4.4. . . | 83 |
| 4.4.6 Comparison of the convergence of the rational spectral collocation (RSC) method with other existing methods for valuing American butterfly spread options at strike price E_2 with the set of parameters given in Table 4.4.4. . . | 83 |

| | |
|--|-----|
| 4.4.7 Comparison of the convergence of the rational spectral collocation (RSC) method with other existing methods for valuing American butterfly spread options at strike price E_3 with the set of parameters given in Table 4.4.4. . . | 83 |
| 5.4.1 Results for the fully discrete numerical method for solving European options under local volatility using the set of parameters $T = 0.5$, $E = 100$, $r = 0.1$, $\delta = 0.0$. Benchmark solution: 7.39883446. | 94 |
| 5.4.2 Results for the fully discrete numerical method for solving European options under local volatility using the set of parameters $T = 0.5$, $E = 100$, $r = 0.1$, $\delta = 0.07$. Benchmark solution: 5.2274224. | 95 |
| 5.4.3 Errors in spectral discretisation method for solving European options under local volatility using the set of parameters $T = 0.5$, $E = 100$, $r = 0.1$, $\delta = 0.0$. $TOL = 10^{-10}$, Benchmark solution: 7.39883446. | 96 |
| 5.4.4 Errors in spectral discretisation method for solving European options under local volatility using the set of parameters $T = 0.5$, $E = 100$, $r = 0.1$, $\delta = 0.07$. $TOL = 10^{-10}$, Benchmark solution: 5.2274223. | 96 |
| 5.4.5 Convergence of the rational spectral method with respect to the penalty term for valuing American put options with the set of parameters $T = 0.5$, $E = 100$, $r = 0.1$, $\delta = 0.0$ | 98 |
| 5.4.6 Results of the of the rational spectral method for valuing American put options under local volatility using $T = 0.5$, $E = 100$, $r = 0.1$, $\delta = 0.0$, $\epsilon = 10^{-5}$, $TOL = 10^{-5}$ | 99 |
| 5.4.7 Results of the rational spectral method for valuing American put options using $T = 0.5$, $E = 100$, $r = 0.1$, $\delta = 0.07$, $\epsilon = 10^{-5}$, $TOL = 10^{-5}$ | 99 |
| 6.5.1 Data used to value a vanilla call option under Merton's model | 112 |
| 6.5.2 Numerical results for pricing European call options under jump-diffusion process at the spot price $S = 100$ using parameters given in Table 6.5.1. The other parameters are $\alpha = 10^4$, $x_{\min} = -1.5$, $x_{\max} = 1.5$, $N = 80$ and $M = 800$ | 114 |
| 6.5.3 Data used to value a butterfly spread option under Merton's model | 115 |

| | |
|--|-----|
| 6.5.4 Numerical results for pricing European butterfly spread options under jump-diffusion process at the spot price $S = 100$ using parameters given in Table 6.5.3. The other parameters are $\alpha = 10^4$, $x_{\min} = -1.5$, $x_{\max} = 1.5$, $N = 80$ and $M = 800$ | 116 |
| 7.4.1 Data used to value American options under Merton's model | 129 |
| 7.4.2 Results for the fully discrete numerical method for solving jump-diffusion for American options with constant volatility using parameters given in Table 7.4.1 and $TOL = 10^{-5}$. Benchmark solution: 5.5676747. | 130 |
| 7.4.3 Errors in spectral discretisation numerical method for solving jump-diffusion model for American options with constant volatility; and using parameters given in Table 7.4.1 and $\epsilon = 10^{-6}$, $TOL = 10^{-6}$. Benchmark solution: 5.5676747. | 130 |
| 7.4.4 Results for the fully discrete numerical method for solving jump-diffusion model for American options with local volatility using parameters given in Table 7.4.1 and $TOL = 10^{-5}$. Benchmark solution: 4.7194288. | 132 |
| 7.4.5 Errors in spectral discretisation numerical method for solving jump-diffusion model for American options with local volatility; and the set of parameters given in Table 7.4.1 and $\epsilon = 10^{-6}$, $TOL = 10^{-6}$, Benchmark solution: 4.7194288 | 132 |

List of Figures

| | |
|--|----|
| 1.1.1 Payoff function of a plain vanilla option at $t = T$ | 3 |
| 1.2.1 Function $g(x)$ and its inverse $g^{-1}(x)$ for one region of rapid change (left figure) and for three regions of rapid changes (right figure) using the ‘tan’ transformation. | 12 |
| 1.2.2 Function $g(x)$ and its inverse $g^{-1}(x)$ for one region of rapid changes (left figure) and for three regions of rapid changes (right figure) using the ‘sinh’ transformation. | 15 |
| 1.2.3 Solution to (1.2.40) with $\beta = 10^3$ obtained using the rational spectral method with 100 grid points defined by g (left). The improvement in convergence of the transformed grid (solid dotted line) over the Chebyshev grid (dashed line) as the number of collocation points N increases (right). | 17 |
| 2.5.1 Convergence of the rational collocation (RC), finite difference (FD) and the TGB ([127]) methods using adaptive grid with $M = 32$, $N = 80$, $\beta = 10^4$, $S_{\min} = 0$, $S_{\max} = 200$, $r = 0.05$, $\sigma = 0.2$, $\delta = 0.00$, $E = 45$ at $T = 0.5$ | 42 |
| 2.5.2 Valuation of Digital call options (top left figure); approximation errors (bottom left figure); and Δ (top right figure) and Γ (bottom right figure) using the rational collocation (RC) method with $M = 32$, $N = 80$, $\beta = 10^6$, $S_{\min} = 0$, $S_{\max} = 200$, $r = 0.05$, $\sigma = 0.2$, $\delta = 0.03$, $E = 45$, $T = 0.5$ | 44 |

| | |
|--|----|
| 2.5.3 Valuation of supershare options (top left figure); approximation errors (bottom left figure); and Δ (top right figure) and Γ (bottom right figure) using the rational collocation (RC) method with $M = 32$, $N = 80$, $\beta = 10^6$, $S_{\min} = 0$, $S_{\max} = 200$, $Q = 20$, $d = 20$, $r = 0.05$, $\sigma = 0.2$, $\delta = 0.03$, $E = 45$, $T = 0.5$ | 47 |
| 3.5.1 Stability regions of schemes (3.5.9) (left figure) and (3.5.10) (right figure) | 60 |
| 3.6.1 Performance of different IMEX-PC method for pricing European call options with $N = 200$, $r = 0.1$, $\sigma = 0.2$, $\delta = 0.0$, $E = 45$ and $\alpha = 2 \times 10^5$ at $T = 0.5$ | 64 |
| 3.6.2 Convergence of the mapped BLC method for European call options with $M = 1000$, $S_{\min} = 0$, $S_{\max} = 200$, $r = 0.1$, $\sigma = 0.2$, $\delta = 0.0$, $E = 45$, $T = 0.5$ | 65 |
| 3.6.3 Valuation of the European call options (top left), its Error (top right), Δ (bottom left) and Γ (bottom right) using the the barycentric Lagrange collocation (BLC) method with $M = 1000$, $N = 80$, $S_{\min} = 0$, $S_{\max} = 200$, $r = 0.1$, $\sigma = 0.2$, $\delta = 0.0$, $E = 45$, $T = 0.5$ | 66 |
| 3.6.4 Valuation of the European digital call options (top left), its Error (top right), Δ (bottom let) and Γ using the the barycentric Lagrange collocation (BLC) method with with $M = 1000$, $S_{\min} = 0$, $S_{\max} = 200$, $r = 0.1$, $\sigma = 0.2$, $\delta = 0.0$, $E = 45$, $T = 0.5$ | 68 |
| 3.6.5 Valuation of butterfly spread option by the barycentric Lagrange collocation (BLC) method with $M = 1000$, $S_{\min} = 0$, $S_{\max} = 200$, $r = 0.1$, $\sigma = 0.2$, $\delta = 0.0$, $E_1 = 45$, $E_3 = 80$, $T = 0.5$ | 70 |
| 4.4.1 Values of the American put option (top figure), Δ (left bottom figure) and Γ (right bottom figure) using parameters given in Table 4.4.1. The other parameters are $S_m = 0$, $S_M = 200$ and $\beta = 20$ | 81 |
| 4.4.2 Values of the American butterfly spread option (top figure), Δ (left bottom figure) and Γ (right bottom figure) using parameters given in Table 4.4.4. The other parameters are $S_m = 0$, $S_M = 200$ and $\beta = 50$ | 84 |

| | |
|---|-----|
| 5.4.1 Local volatility function at different times | 93 |
| 5.4.2 Values of European call options under local volatility (top figure), Δ (left bottom figure) and Γ (right bottom figure) using the parameters given as $T = 0.5$, $E = 100$, $r = 0.1$, $\delta = 0.0$ and $\delta = 0.7$. The other parameters are $S_m = 0$, $S_M = 200$ and $\beta = 10^4$ | 97 |
| 5.4.3 Values of the American put option under local volatility (top figure), Δ (left bottom figure) and Γ (right bottom figure) using the parameters given as $T = 0.5$, $E = 100$, $r = 0.1$, $\delta = 0.0$ and $\delta = 0.7$. The other parameters are $S_m = 0$, $S_M = 200$ and $\beta = 10^4$ | 100 |
| 6.4.1 Stability regions of schemes (6.4.9) (left figure) and (6.4.10) (right figure) | 110 |
| 6.5.1 Numerical and analytical solutions of European call under jump and pure diffusion models (left figure) and difference between values of European call under jump and pure diffusion (right figure) with parameters given in Table 6.5.1. The other parameters $\alpha = 10^4$, $x_{\min} = -1.5$, $x_{\max} = 1.5$, $N = 80$ and $M = 800$ | 112 |
| 6.5.2 Numerical and analytical values of the Δ (left figure) and Γ (right figure) European call under jump-diffusion and pure diffusion model, with parameters given in Table 6.5.1. The other parameters are $\alpha = 10^4$, $x_{\min} = -1.5$, $x_{\max} = 1.5$, $N = 80$ and $M = 800$ | 113 |
| 6.5.3 Error vs. N at spot price $S = 100$, for the spectral collocation (with different values of α) and the finite difference methods for pricing European call options (top figure), Δ (left bottom figure) and Γ (right bottom figure) using the parameters given in Table 6.5.1. The other parameters are $x_{\min} = -1.5$, $x_{\max} = 1.5$ and $M = 800$ | 114 |

| | |
|---|-----|
| 6.5.4 Numerical and analytical solutions of European butterfly spread options under jump and pure diffusion models (left figure) and difference between values of European butterfly spread options under jump and pure diffusion (right figure) using parameters given in Table 6.5.3. The other parameters are $\alpha = 10^4$, $x_{\min} = -1.5$, $x_{\max} = 1.5$, $N = 80$ and $M = 800$ | 116 |
| 6.5.5 Numerical and analytical values of the Δ (left figure) and Γ (right figure) European butterfly spread options under jump-diffusion and pure diffusion model, using parameters given in Table 6.5.3. The other parameters are $\alpha = 10^4$, $x_{\min} = -1.5$, $x_{\max} = 1.5$, $N = 80$ and $M = 800$ | 117 |
| 6.5.6 Error vs. N at spot price $S = 100$, for the spectral collocation (with different values of α) and the finite difference methods for pricing European butterfly spread options (top figure), Δ (left bottom figure) and Γ (right bottom figure) using parameters given in Table 6.5.1. The other parameters are $x_{\min} = -1.5$, $x_{\max} = 1.5$ and $M = 800$ | 118 |
| 7.4.1 American put option under jump-diffusion process value (top), Δ (left bottom) and Γ (right bottom) using the data as in Table 7.4.1. The other parameters are $s_m = -1$, $s_M = 1$ and $\beta = 35$ | 131 |
| 7.4.2 American put option under local volatility jump-diffusion process value (top), Δ (left bottom) and Γ (right bottom) using the data as in Table 7.4.1. The other parameters are $s_m = -1$, $s_M = 1$ and $\beta = 35$ | 133 |

List of Publications

Part of this thesis has been submitted in the form of the following research papers submitted to international journals for publications.

1. E. Pindza, K.C. Patidar and E. Ngounda, A fully spectral collocation methods for pricing European style standard and nonstandard options, submitted for publication.
2. E. Pindza, K.C. Patidar and E. Ngounda, Implicit-explicit predictor-corrector methods combined with improved spectral methods for pricing European style vanilla and exotic options, submitted for publication.
3. E. Pindza, K.C. Patidar and E. Ngounda, Robust spectral method for numerical valuation of European options under Merton's jump-diffusion model, submitted for publication.
4. E. Pindza, K.C. Patidar and E. Ngounda, Rational spectral collocation method for pricing American options, submitted for publication.
5. E. Pindza, K.C. Patidar and E. Ngounda, Spectral methods for pricing European and American options under local volatility, submitted for publication.
6. E. Pindza, K.C. Patidar and E. Ngounda, Spectral collocation methods to price American options with jump-diffusion processes, submitted for publication.

Chapter 1

General introduction

As stock markets have become increasingly more sophisticated during the last decades, more complex contracts than simple buy/sell trades, such as financial *Options* have been introduced. These contracts can give investors various kinds of opportunities to tailor their dealings to their investment needs. They are usually modeled by partial differential and partial-integro differential equations which in most cases do not possess analytical solutions. In this thesis, therefore, we propose a robust numerical method, namely, spectral method to efficiently solve such option pricing problems.

In this chapter, we present some basic terminologies, literature review and outline of the thesis.

1.1 Option pricing

Options belong to a certain family of financial instruments called *Derivatives* whose values rely on financial assets such as mutual funds, stocks, index, bonds, etc. Empirical observations of stock markets show that financial asset values are not unquestionably given by their history records. Indeed, many purchase or sell operations are not foreseeable. Often, they utilise elements that do not belong to the history of the stock markets and modify their trends. Many of these follow a stochastic process which is modeled by the Brownian motion.

An Option is a contract that gives the holder the right (but not the obligation) to buy or to sell an asset (S , the underlying asset) by a given time (t , expiration date) for a specific price (E , strike price or exercise price). Conversely, the other party to the contract, known as the writer of the contract, is obliged to buy or sell the asset depending on the holder's decision. If the holder decides to buy or sell the asset according to the terms of the contract, the option is said to be exercised. A call option allows its owner to buy whereas a put option allows its owner to sell its underlying asset, at a certain time for a fixed strike price.

Options can broadly be classified into two types: plain vanilla (standard) options and exotic (non-standard) options. Vanilla options, actively traded at an exchange, are those whose values are determined "market-to-market", i.e., by looking up their prices on the market. Exotic options are combinations of diverse plain vanilla options, designed to fit the needs of their writer's clients. There is no active market for them, so their value is gained by "market-to-model", i.e., by using a model to determine the premium. Some of these options may be further classified into European, American, Asian, Bermudan, Japanese and Russian options. Note the names of options are not based on the geographical classifications. They represent different types of exercise rights. For instance, European options can only be exercised at maturity time ($t = T$), whereas American options can be exercised at anytime before the maturity time.

When an option is exercised, there is no actual transfer of the underlying asset, but a cash flow of the gained money. To understand the cash flows better, we consider a vanilla European call option with strike price E . Let S_T denote the price of the underlying asset on the expiration date T . If $S_T > E$, then the holder of the call option will choose to exercise the option since he can buy the asset, worth S_T , at the cost of only E . The net profit is then $S_T - E$. However, if $S_T < E$, then the holder will forfeit the right to exercise the option since he can now purchase the asset in the market at a cost less than or equal to the strike price E . In this case, the net profit is zero and the holder will lose all his investment. Thus the terminal payoff of a vanilla

European call is

$$h(S_T) = \max(S_T - E, 0). \quad (1.1.1)$$

Similarly, the terminal payoff of a vanilla European put option can be given by

$$h(S_T) = \max(E - S_T, 0), \quad (1.1.2)$$

since the put option will be exercised only if $S_T < E$, and the holder of the option can sell the asset at a higher price of E instead of S_T .

In a similar manner, we can say that, the payoff of a vanilla American call option at time t , is

$$h(S_t) = \max(S_t - E, 0), \quad (1.1.3)$$

where S_t is the price of the asset at time t . That is to say, should the holder of a vanilla American call option choose to exercise it at time t , he will receive the amount $\max(S_t - E, 0)$. Naturally, the payoff of a vanilla American put option at time t is

$$h(S_t) = \max(E - S_t, 0). \quad (1.1.4)$$

Figure (1.1.1) represents the payoff function of a plain option at exercised time. So,

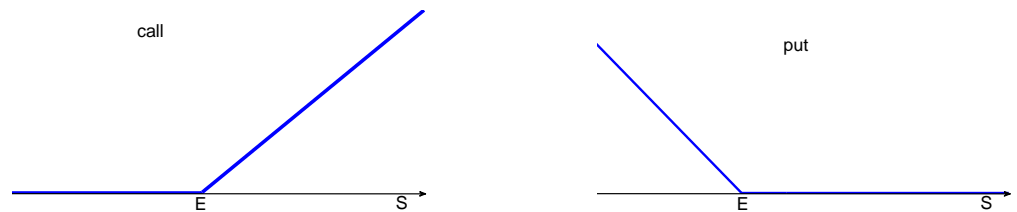


Figure 1.1.1: Payoff function of a plain vanilla option at $t = T$.

in theory, a holder of an option could earn a maximum of E for a put, and an infinite amount of money for a call. Conversely, the loss on a short call position is unlimited.

There are two main reasons an investor would use options: to *speculate* and to *hedge*. A speculator would expect the value of an asset to fall in the future. (S)he

could make money by buying the asset and a put option. If the same person expects an asset to increase dramatically, he would buy a call option. Options for hedging can serve as security for a portfolio. For instance, if someone owns shares of a company and expects a significant drop in their value, the person could buy put options. If the market goes down, the puts prevent a big loss and, if it remains stable, the options would expire.

In practice, there is a wide variety of options, which can be used for different kinds of speculation and hedging. More details on derivatives can be found in a number of texts on financial engineering, see, for example, Hull [77].

1.2 A quick tour to spectral methods and their applications

Spectral methods are a class of spatial discretisation methods for differential equations. They distinguish themselves from finite difference or finite element methods by the fact that they use global representations of functions by high order polynomials, rational polynomials or Fourier series. Spectral methods can yield greater accuracy, in fact exponential for problems having smooth solutions, with far fewer nodes and therefore take less computational time than the finite difference and finite element methods. The main idea behind spectral methods is to approximate the solution of a given problem by a linear combination of the trial functions (also called the expansion or approximating functions) and the test functions (also known as weight functions). The trial functions, which are linear combinations of suitable trial basis functions, are used to provide the approximate representation of the solution. The test functions are used to ensure that the differential equation and perhaps some boundary conditions are satisfied as closely as possible by the truncated series expansion.

Spectral methods are further classified as : Galerkin, Tau and the collocation methods. The main difference lies in the choice of the weight functions. Galerkin's method

was first implemented by Silberman [117] and later on used for other practical problems by Orszag [107, 108]. Eliassen *et al.* [57] developed Galerkin's methods to calculate sum of convolutions. The tau method, for its part, has been developed by Lanczos [92]. Both methods use coefficients of global series, with small differences in the way of treating boundary conditions for non-periodic problems. In contrast, in the method of collocation, a linear combination of basis functions must satisfy the differential equation at collocation points. The collocation method was first used by Slater [118] and Kantorovic [82]. Frazer *et al.* [62] used spectral collocation methods to solve the ordinary differential equations. Lanczos [92] discovered that a good choice of basis functions and collocation points is crucial for the convergence of the solution. This work was regarded as the first one which was concerned with the orthogonal collocation. The method was further explored by Clenshaw [40], Clenshaw and Norton [42], Wright [144] and Villadsen and Stewart [133] where they used Chebyshev polynomials for solving initial value problems.

The first applications of the spectral collocation method to solve partial differential equations were performed for periodic problems by Kreiss and Oliger [88], and Orszag [109] for non-periodic problems.

In this thesis, we will focus on several applications of the rational collocation method. Therefore, below we present some of the key ideas dealing with this methods.

1.2.1 Rational spectral collocation approximation

Rational collocation approximations have recently emerged as promising tools for the development of spectral methods for problems with localised regions of rapid change [15]. It is common to write these approximations in barycentric form [14, 19], which provides a general framework that includes both polynomial and rational approximations [130]. Below we discuss some basic results dealing with these rational spectral methods which can be useful for the discretisation of the problems considered in this thesis. More details on rational collocation methods can be found in [10, 18] and the

references therein.

The barycentric form of a rational function $r_N(x)$ which interpolates the function $f(x)$ at grid points $\{x_j\}_{0 \leq j \leq N}$ is defined as ([20]):

$$r_N(x) = \frac{\sum_{j=0}^N \frac{\omega_j}{x - x_j} f(x_j)}{\sum_{j=0}^N \frac{\omega_j}{x - x_j}}, \quad (1.2.1)$$

where $x_0, x_1 \dots x_N$ are the collocation points and $\omega_0, \omega_1 \dots \omega_N$ are called the barycentric weights given by

$$\omega_j = 1 / \prod_{i \neq j} (x_j - x_i). \quad (1.2.2)$$

For fixed $\omega = [\omega_0, \dots, \omega_N]^T$, $\omega_j \neq 0$, we associate the linear space, denoted by $\mathcal{R}_N^{(\omega)}$ and spanned by the functions

$$L_j^{(\omega)}(x) = \frac{\omega_j}{x - x_j} / \sum_{k=0}^N \frac{\omega_k}{x - x_k}, \quad j = 0, \dots, N, \quad (1.2.3)$$

which satisfy the Langrange property

$$L_j^{(\omega)}(x_i) = \delta_{ij}. \quad (1.2.4)$$

In the rational collocation method (in barycentric form), we approximate the unknown solution $u(x, t)$ at the nodes x_j , as

$$\tilde{u}(x) = \sum_{j=0}^N \tilde{u}(x_j) L_j^{(\omega)}(x) \in \mathcal{R}_N^{(\omega)}, \quad j = 0, \dots, N. \quad (1.2.5)$$

An advantage of the barycentric representation of \tilde{u} is the simplicity of the formula for the elements of the first and the second order differentiation matrices $D^{(1)}$ and $D^{(2)}$

which arise in the discretisation. Entries of the matrices can be given in ([8]) as

$$D_{jk}^{(1)} = \begin{cases} \frac{\omega_k}{\omega_j(x_j - x_k)} & \text{if } j \neq k, \\ -\sum_{i=0, i \neq j}^N D_{ji}^{(1)} & \text{if } j = k, \end{cases} \quad (1.2.6)$$

and

$$D_{jk}^{(2)} = \begin{cases} 2D_{jk}^{(1)} \left(D_{jj}^{(1)} - \frac{1}{x_j - x_k} \right) & \text{if } j \neq k, \\ -\sum_{i=0, i \neq j}^N D_{ji}^{(2)}, & \text{if } j = k, \end{cases} \quad (1.2.7)$$

where $j, k = 0, 1, \dots, N$. Note that for every set of points x_j , there corresponds a unique set of barycentric weights ω_j up to a multiplicative constant, such that (1.2.1) represents a polynomial interpolant. In the case of Chebyshev approximations, these weights are given by $\omega_0 = c/2$, $\omega_j = (-1)^j c$ for $j = 1, \dots, N-1$, and $\omega_N = (-1)^N c/2$ for some nonzero constant c (see [19]). In view of this setting, the rational collocation interpolant (1.2.1) enjoys exponential convergence property as stated in the following theorem:

Theorem 1.2.1 ([8]). *Let $\mathcal{D}_1, \mathcal{D}_2$ be domains in \mathbb{C} containing $J = [-1, 1]$ and a real interval I respectively. Let $g : \mathcal{D}_1 \rightarrow \mathcal{D}_2$ be a conformal map such that $g(J) = I$. Suppose that $h : \mathcal{D}_2 \rightarrow \mathbb{C}$ is a function such that the composition $u \circ g : \mathcal{D}_1 \rightarrow \mathbb{C}$ is analytic inside and on an ellipse E_ρ , $\rho > 1$, with foci at ± 1 and the sum of its lengths of semi-major and semi-minor axes is equal to ρ . Let $r_N(x)$ be the rational function, interpolating $u(x)$ between transformed Chebyshev points x_j with barycentric weights. Then for all $x \in [-1, 1]$*

$$|r_N(x) - u(x)| = \mathcal{O}(\rho^{-N}). \quad (1.2.8)$$

Proof. See [8].

Remark 1.2.2. Theorem 1.2.1 suggests that in order to have an approximation of u

which is more accurate than the one obtained by using the Chebyshev spectral method with the same number of grid points, one should choose a conformal map g such that the ellipse of analyticity of $u \circ g$ is larger than the ellipse of analyticity of u , and apply g in a spectral method based on rational interpolant of the form (1.2.1). A detailed literature on how to choose and construct g can be found in [130].

Theorem 1.2.1 above does not make any assertion about the convergence of the derivatives, which is of paramount importance in the design of spectral method for solving PDEs. The following theorem asserts the exponential convergence of the derivatives.

Theorem 1.2.3 ([129]). *In the same notation and condition as in Theorem 1.2.1, $r_N^{(p)}$ the p -th derivative of r_N also has exponential convergence*

$$|r_N^{(p)}(x) - u^{(p)}(x)| = \mathcal{O}(\rho^{-N}). \quad (1.2.9)$$

Proof. See [129].

A significant advantage of the rational spectral collocation method based on rational interpolation in barycentric form, is that tedious transformations using the chain rule to approximate the derivatives of f are not required as it is usual in other spectral collocation methods.

Before proceeding further, we note that some classes of pricing problems we solve in this thesis involve non-local integrals. In order to retain high accuracy in our approach while dealing with these integrals, we introduce a spectrally converging quadrature formula, namely, Clenshaw-Curtis quadrature formula, as described in the next subsection.

1.2.2 Clenshaw-Curtis quadrature formula

Let f be a continuous function on $[a, b]$, then a quadrature rule is a numerical method to approximate the definite integral

$$I_{[a,b]}(f) = \int_a^b f(z)dz. \quad (1.2.10)$$

Assume that both a and b are finite, then without loss of generality, solving the problem (1.2.10) on the interval $[a, b]$ becomes equivalent to solve it on the interval $[-1, 1]$ if the transformation $2y = (b - a)z + (b + a)$ is used which turns into

$$I_{[a,b]}(f) = \frac{1}{2}(b - a)I_{[-1,1]}(f \circ y). \quad (1.2.11)$$

For simplicity, we denote $I_{[-1,1]}(f) = I$ and we seek to approximate the integral

$$I = \int_{-1}^1 f(z)dz. \quad (1.2.12)$$

In general (1.2.10) does not have analytical solution and therefore, we resort to efficient and accurate numerical methods. The quadrature rule for the above integral is the sum

$$I_N = \sum_{k=0}^N w_k f(z_k) \quad (1.2.13)$$

where z_k are specific nodes and w_k are weights specific depending on the nature of the quadrature rule. The Clenshaw-Curtis [41] quadrature formula relies on using Chebyshev points $z_k = \cos(\pi k/N)$. In order to accommodate more points around the regions of singularity, it is useful to consider the map g . The problem (1.2.10) can be reformulated as follows: let f and g be analytic functions in Ω_ρ subset of the complex plane containing $[-1, 1]$ and in some ellipse E_ρ , respectively, with $g(E_\rho) \subseteq \Omega_\rho$ and $g(\pm 1) = \pm 1$. By the Cauchy's integral theorem for analytic functions, the problem

(1.2.10) can be rewritten as

$$I = \int_{-1}^1 g'(z) f(g(z)) dz. \quad (1.2.14)$$

The quadrature formula for the above integral is given by

$$\begin{aligned} I_N(g'(f \circ g)) &= \sum_{k=0}^N w_k g'(z_k) f(g(z_k)), \\ &= \sum_{k=0}^N \tilde{w}_k f(\tilde{z}_k), \quad \tilde{w}_k = w_k g'(z_k), \quad \tilde{z}_k = g(z_k), \end{aligned} \quad (1.2.15)$$

The Clenshaw-Curtis quadrature enjoys the following convergence result:

Theorem 1.2.4 ([49]). *Let f be an analytic function in $[-1, 1]$ and analytically continuable with $|f(z)| < M$ in the closed ellipse E_ρ . The error of $I_N(f)$ (Clenshaw-Curtis quadrature of degree N) to $I(f)$ will decay geometrically with the bound*

$$|I - I_N| \leq \frac{64M\rho}{15(\rho^2 - 1)(\rho^{N-1} - \rho^{-(N-1)})}, \quad N \geq 3. \quad (1.2.16)$$

In other words,

$$|I - I_N| = \mathcal{O}(\rho^{-N}). \quad (1.2.17)$$

Proof. See [49].

The main advantage with the Clenshaw-Curtis quadrature rule is that its weights and nodes can be computed efficiently via a fast Fourier transform (FFT) in only $(\mathcal{O}(N \ln N))$ operations.

Spectral methods for solving partial differential equations with smooth initial conditions have been proved to have exponential accuracy [35, 60, 124]. However, the option pricing problems possess the initial conditions that are usually non-smooth. This has a detrimental effect on the stability of the computational scheme. In the next subsection, therefore we present two conformal mappings that can be used to design

adaptive grids so as to achieve high accuracy results with spectral methods.

1.2.3 Grid transformations

In the most common pseudo-spectral Chebyshev methods, the interpolation points in the interval $[-1, 1]$ are the Chebyshev-Gauss-Lobatto (CGL) collocation points $y_j = \cos\left(\frac{j\pi}{N}\right)$ for $j = 0, \dots, N$. The CGL points are clustered near the boundaries of $[-1, 1]$. However, we need to accumulate these points in the vicinity of the region(s) of rapid change. One way to do this is to use adaptive grids via coordinate transformations. To begin with, let $x = g(y)$, where g is defined as in Theorem 1.2.1, maps a domain \mathcal{D}_1 containing $[-1, 1]$ conformally onto a domain \mathcal{D}_2 containing $[-1, 1]$. The CGL nodes $y_j = \cos\left(\frac{j\pi}{N}\right)$ are now chosen in the new coordinate space. The nodes in the physical space are then chosen as $x_j = g(y_j)$.

In this thesis, we consider two types of conformal maps, one is based on the ‘tan’ transformation, whereas the second one is based on the sinh transformation. The first conformal map g was derived in [12]:

$$x = g(y) = \beta + \frac{1}{\alpha} \tan[\lambda(y - \mu)], \quad (1.2.18)$$

where

$$\lambda = \frac{\gamma + \delta}{2}, \quad \mu = \frac{\gamma - \delta}{\gamma + \delta}, \quad (1.2.19)$$

with

$$\gamma = \tan^{-1}[\alpha(1 + \beta)], \quad \delta = \tan^{-1}[\alpha(1 - \beta)]. \quad (1.2.20)$$

Here β and α , respectively determine the location and the magnitude of the region(s) of rapid change. To the best of our knowledge, this mapping has never been used in option pricing problems earlier. The conformal map g is constructed from

$$y = g^{-1}(x) = \mu + \frac{1}{\lambda} \tan^{-1}[\alpha(x - \delta)]. \quad (1.2.21)$$

The behavior of g and its inverse g^{-1} on specific grids is depicted in Figure 1.2.1.

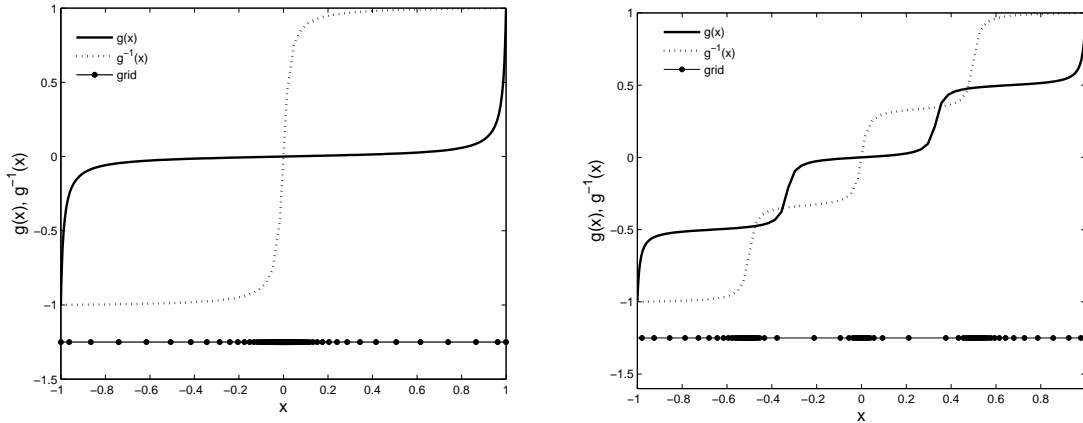


Figure 1.2.1: Function $g(x)$ and its inverse $g^{-1}(x)$ for one region of rapid change (left figure) and for three regions of rapid changes (right figure) using the ‘tan’ transformation.

In the case of multiple regions of singularity, it is possible to combine a single point of singularity maps in order to accommodate more points around these regions. One way is to split the initial domain I into sub-domains and to consider approximating the solution on each of them, but this procedure ruins the spectral accuracy [12]. Therefore, for every region of singularity, we address such problems with a single conformal map involving two parameters α_k and β_k . The construction of such maps with R singularities is done through the inverse map as

$$y(x) = g^{-1}(x) = \mu + \frac{1}{\lambda} \sum_{k=1}^R \tan^{-1}[\alpha_k(x - \beta_k)], \quad (1.2.22)$$

where λ and μ are parameters that satisfy

$$g^{-1}(-1) = -1 \quad \text{and} \quad g^{-1}(1) = 1. \quad (1.2.23)$$

Therefore, the solution of the system (1.2.23) yields the same values of λ and μ as in

(1.2.19), with

$$\gamma = \sum_{k=1}^R \tan^{-1}[\alpha_k(1 + \beta_k)] \quad (1.2.24)$$

and

$$\delta = \sum_{k=1}^R \tan^{-1}[\alpha_k(1 - \beta_k)]. \quad (1.2.25)$$

By the conformality, g^{-1} is itself monotonically increasing from -1 to 1 since it is the sum of monotonically increasing functions in some neighbourhood of $[-1, 1]$. Consequently, we have $g^{-1}(x) = y$. For R singularities $g(y) = x$ is computed pointwise by solving the non linear equation

$$\sum_{k=1}^R \tan^{-1}[\alpha_k(x - \beta_k)] = \lambda(y - \mu). \quad (1.2.26)$$

If $R = 1$, then $g(y)$ is defined as in (1.2.18). For $R > 1$, (1.2.26) is computed by means of numerical methods, e.g., Newton method or by noticing that the sum of arc tangents may be written as a single arc tangent, then solving (1.2.26) becomes equivalent to solve a polynomial of order R .

For $R = 2$, we have to solve a quadratic equation

$$ax^2 + bx + c = 0, \quad (1.2.27)$$

with

$$\begin{aligned} a &= \alpha_1\alpha_2t \\ b &= [(\alpha_1 + \alpha_2) - a(\beta_1 + \beta_2)], \\ c &= (\alpha_1\alpha_2\beta_1\beta_2 - 1)t - (\alpha_1\beta_2 + \alpha_2\beta_1), \\ t &= \tan[\lambda(y - \mu)]. \end{aligned} \quad (1.2.28)$$

For $R = 3$, equation (1.2.26) yields a cubic equation

$$ax^3 + bx^2 + cx + d = 0, \quad (1.2.29)$$

with

$$\begin{aligned} a &= \alpha_1 \alpha_2 \alpha_3, \\ b &= -t(\alpha_1 \alpha_2 + \alpha_1 \alpha_3 + \alpha_2 \alpha_3) - a(\beta_1 + \beta_2 + \beta_3), \\ c &= t[\alpha_1 \alpha_2(\beta_1 + \beta_2) + \alpha_1 \alpha_3(\beta_1 + \beta_3) + \alpha_2 \alpha_3(\beta_2 + \beta_3)] \\ &\quad + a(\beta_1 \beta_2 + \beta_1 \beta_3 + \beta_2 \beta_3) - (\alpha_1 + \alpha_2 + \alpha_3), \\ d &= t(1 - \alpha_1 \alpha_2 \beta_1 \beta_2 - \alpha_1 \alpha_3 \beta_1 \beta_3 - \alpha_2 \alpha_3 \beta_2 \beta_3) - a\beta_1 \beta_2 \beta_3 \\ &\quad + (\alpha_1 \beta_1 + \alpha_2 \beta_2 + \alpha_3 \beta_3), \\ t &= \tan[\lambda(y - \mu)]. \end{aligned} \quad (1.2.30)$$

We choose solutions of equations (1.2.29) and (1.2.28) for which $g^{-1}(x)$ is satisfied. Figure 1.2.1 (left) represents the function g and its inverse g^{-1} for $\alpha = 50$ and $\beta = 0.0$. Figure 1.2.1 (right) represents the same for $\alpha = 50$ in the three cases and $\beta = [-0.5 \ 0.0 \ 0.5]$.

Another conformal map we consider in this thesis was derived in [130]:

$$g(y) = \beta + \varepsilon \sinh \left[\left(\sinh^{-1} \left(\frac{1 - \beta}{\varepsilon} \right) + \sinh^{-1} \left(\frac{1 + \beta}{\varepsilon} \right) \right) \frac{x - 1}{2} + \sinh^{-1} \left(\frac{1 - \beta}{\varepsilon} \right) \right],$$

where β is the point of singularity in the interval $[-1, 1]$ and ε is the parameter of points redistribution around β . This particular map has been previously used in option pricing to reduce at-the-money pricing biases [128]. Using the change of variables $\varepsilon = 1/\alpha$, we can write g in the form

$$x = g(y) = \beta + \frac{1}{\alpha} \sinh [\lambda(y - \mu)], \quad (1.2.31)$$

where

$$\lambda = \frac{\gamma + \delta}{2}, \quad \mu = \frac{\gamma - \delta}{\gamma + \delta}, \quad (1.2.32)$$

with

$$\gamma = \sinh^{-1}[\alpha(1 + \beta)], \quad \delta = \sinh^{-1}[\alpha(1 - \beta)]. \quad (1.2.33)$$

Again as in the previous case, β and α determine the location and the magnitude of the regions of rapid change.

Using (1.2.31), the conformal map g is constructed from its inverse

$$y = g^{-1}(x) = \mu + \frac{1}{\lambda} \sinh^{-1}[\alpha(x - \delta)]. \quad (1.2.34)$$

Figure 1.2.2 (left) represents the function g and its inverse g^{-1} for $\alpha = 10^3$ and $\beta = 0.0$. In the case of multiple regions of singularities, the construction of such maps (with R

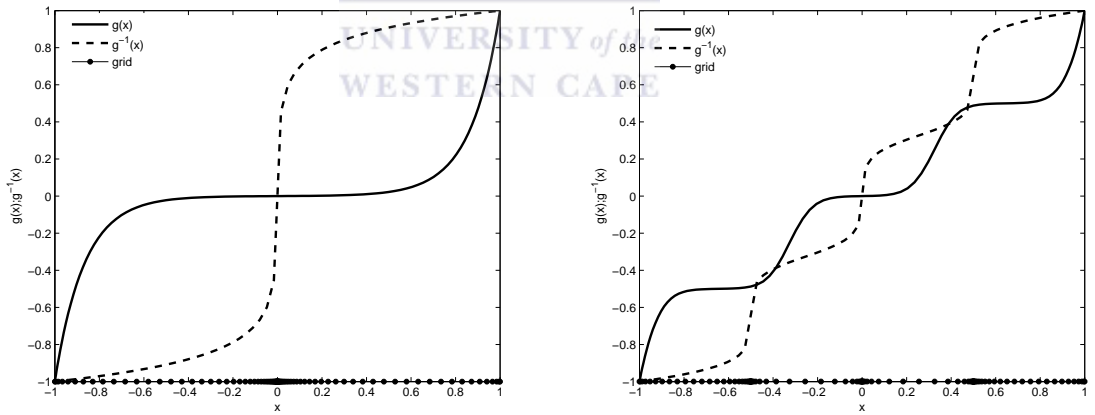


Figure 1.2.2: Function $g(x)$ and its inverse $g^{-1}(x)$ for one region of rapid changes (left figure) and for three regions of rapid changes (right figure) using the ‘sinh’ transformation.

singularities) is done through the inverse map g^{-1} as

$$y(x) = g^{-1}(x) = \mu + \frac{1}{\lambda} \sum_{k=1}^R \sinh^{-1}[\alpha_k(x - \beta_k)], \quad (1.2.35)$$

where λ and μ are parameters that satisfy

$$g^{-1}(-1) = -1 \quad \text{and} \quad g^{-1}(1) = 1. \quad (1.2.36)$$

Therefore, the solution of the system (1.2.36) yields the same values of λ and μ as in (1.2.32), with

$$\gamma = \sum_{k=1}^R \sinh^{-1}[\alpha_k(1 + \beta_k)] \quad (1.2.37)$$

and

$$\delta = \sum_{k=1}^R \sinh^{-1}[\alpha_k(1 - \beta_k)]. \quad (1.2.38)$$

By the conformality, g^{-1} is itself monotonically increasing from -1 to 1 since it is the sum of monotone increasing functions in some neighbourhood of $[-1, 1]$. Consequently, we have $g^{-1}(x) = y$. For R singularities $g(y) = x$ is computed pointwise by solving the non-linear equation

$$\sum_{k=1}^R \sinh^{-1}[\alpha_k(x - \beta_k)] = \lambda(y - \mu). \quad (1.2.39)$$

If $R = 1$, $g(y)$ is defined as in (1.2.31). For $R > 1$, (1.2.39) can be computed using a generic nonlinear solver. Figure 1.2.2 (right) represents the function g and its inverse g^{-1} for $\alpha = 10^3$ in the three cases and $\beta = [-0.5 \ 0.0 \ 0.5]$.

In order to illustrate the effect of the conformal mappings on numerical convergence of the rational spectral method, we consider the following two-point boundary value problem

$$u''(x) - \left(1 + \frac{1}{x - 0.01}\right) u'(x) - \frac{u(x)}{x - 0.01} = 0, \quad u(-1) = e^{-1}, \quad u(0) = 1. \quad (1.2.40)$$

The analytical solution of (1.2.40) is

$$u(x) = e^x. \quad (1.2.41)$$

This ODE appears in [10]. Figure 1.2.3 (left) shows the solution to (1.2.40) using

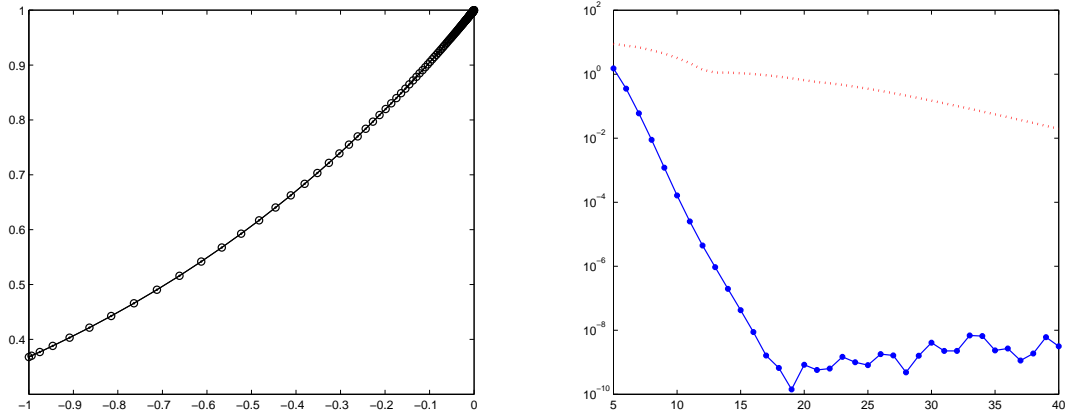


Figure 1.2.3: Solution to (1.2.40) with $\beta = 10^3$ obtained using the rational spectral method with 100 grid points defined by g (left). The improvement in convergence of the transformed grid (solid dotted line) over the Chebyshev grid (dashed line) as the number of collocation points N increases (right).

the map in (1.2.31) for $\beta = 10^3$, and Figure 1.2.3 (right) displays the convergence of the mapped rational spectral collocation approach with the standard rational spectral collocation approach as the number of collocation points increases. We observe a significant improvement of the convergence when a conformal map is used to accommodate more points in the vicinity of the pole $x = 0.01$. In view of the above observation, we use the mapped rational spectral collocation method throughout this thesis to solve option pricing problems.

In the next section, we review historical records of some numerical methods that have been used to value option pricing problems.

1.3 Literature Review

Options were introduced in financial markets many years ago. Initially, options were non-exchange traded because agreements were made between two traders, in which case they were called over-the-counter [140] derivatives. In America, options were exercised in the early 19th century and were simply known as privileges. However,

the rate of growth of the options was not very attractive, although such options were legally accepted in America and many other European countries. In late 1960's, it was found what was wrong within the financial markets of options. The Chicago Board of Trade discovered many distortions within the markets of options. In order to eliminate the distortions and to strengthen the options made by traders in the financial markets, it was necessary to standardise the exercise prices, expiry dates, option prices and other important factors that came along with the financial markets. In view of the standardisations, several mathematical models for pricing financial derivatives emerged, some of which were described through the various forms of the celebrated Black-Scholes equations [21]. However, depending on the nature and complexities of these Black-Scholes PDEs, analytical solutions in closed form can be rarely obtained and therefore one usually relies on numerical methods. In literature three types of numerical methods have been used. These are classified as Monte Carlo, Lattice and finite difference method.

Monte Carlo methods involve generating large numbers of numerically simulated realizations of the random walk followed by the underlying asset and averaging the derivative prices obtained from these realizations. The detailed analysis of the Monte Carlo algorithms presented in [11, 31, 96, 113, 131]. Monte-Carlo methods are usually slow and inflexible. One of the main considerations in Monte-Carlo simulations is the implementation of an unbiased random number generator. Already we see that this can present a problem. The main disadvantage is that it is either very difficult or impossible to implement American-style features such as early exercise opportunities.

Lattice methods, which include the binomial and trinomial models, assume that the underlying stochastic process is discrete i.e. the underlying asset “jumps” to a finite number of values (each associated with a certain probability) with a small advancement in time[26, 47, 74, 139]. Lattice methods can be very efficient for valuing simple calls and puts, however, they become less efficient when valuing more complicated options.

Finite-difference methods (FDM) consists of discretising the PDE and the given boundary conditions to form a set of difference equations which can either be solved

directly or iteratively [27, 28, 101, 140]. Finite-difference grids/meshes are more desirable over Binomial (or Trinomial) trees because the transition from a differential equation to a difference equation is easier when the tree/grid/mesh is simple and regular. Moreover, there are many ways in which the FDM can be improved upon, making it faster and more accurate.

Below we review some of these works. Numerous ways have been proposed to enhance the convergence of FD methods.

Clark and Parrot [39] used a coordinate transformation that stretched grids around the strike price where there is discontinuity in the first derivative of the final condition and found that the accuracy of their implicit FD method was improved. Another way of obtaining more grid points around the discontinuity is to use adaptive grid points as in Persson and von Sydow [110]. Oosterlee et al. [106] obtained a fourth order accurate solution for European options using the grid stretching transformation [128] in combination with the fourth order spatial discretisation based on a five points stencil and the fourth order backward differencing formula (BDF4) for time discretisation. Tangman et al. [126], considered the higher order compact (HOC) schemes and used a grid stretching that concentrates the grid nodes at the strike price for the European options.

Numerical solution of American options, subject to free boundary conditions, were early proposed by Brennan and Schwartz [27]. Later, Courtadon [45] used a Finite Difference (FD) scheme for finding the value of an American option. Brennan and Schwarz employ an iterative projection method to solve the remaining inequality. In [13] an optimal stopping-time problem was formulated as free boundary value problem, variational inequality and linear complementarity problem (LCP). Although the name is not mentioned explicitly there, this problem (LCP) expresses exactly the pricing process of American options. This conclusion was drawn by Jaillet, Lamberton and Lapeyre [79], who formalized the connection between the valuation of American options and variational inequalities, and derived some regularity properties from that coincidence.

Dempster and Hutton [52] continued along the lines of Jaillet *et al.* [79] and additionally suggested a LCP for American options. They employ an FD scheme for both a (LCP) and their linear problem, and solve them with projected successive overrelaxation (PSOR) and a dual simplex algorithm, respectively. Later, Borici and Lüthi [22] proved that a complementary feasible basis alluded by [52] exists and gave the corresponding algorithm which finds it. Wu and Kwok [145] introduced a front-fixing method, which transforms the initially unknown free boundary into a known fixed line, the solution can then be found by an FD scheme, without the need to solve an inequality. Other numerical approaches are the Method of Lines, applied to the free boundary value problem by Meyer and van der Hoek [103], the Differential Quadrature method by Wu and Ding [146], a moving index method to solve the LCP, introduced by Koulisianis and Papatheodorou [87], the penalty methods of Forsyth and Vetzal [61] and the artificial boundary conditions of Han and Wu [71].

In response to the shortcomings encountered in the Black-Scholes model when valuing assets whose prices move rapidly, a variety of jump-diffusion models have been proposed. For instance, Merton proposed a jump-diffusion model with log-normally distributed jumps, while Kou suggested one with double exponentially distributed jumps. Under certain assumptions, such models lead to partial integro-differential equations (PIDEs). The popularity of these models resides in the analytic tractability of their solutions. Indeed for many commonly used options, such as lookbacks, barriers and butterfly spreads, closed-form analytical solutions are hardly available. Hence, it is often necessary to use numerical methods. In jump-diffusion models, numerical methods for finding option prices are related to solving partial integro-differential equations (PIDEs).

In literature, several classes of numerical methods have been proposed and used to solve these PIDEs. Briani *et al.* [29] used the fully explicit schemes, although their approach required very restrictive conditions for stability. Cont and Volchkova [44] used implicit schemes to treat the differential part. The use of the Crank-Nicolson time stepping for the PDE portion and evaluation of the convolution integral term explicitly

were tested by Tavella and Randall [128]. However, such an asymmetric treatment of PDE and integral part introduces biases in the viscosity solution. More specifically, the second order convergence is not achieved for long dated options. d'Halluin *et al.* [55] employed the Crank-Nicolson scheme with the Rannacher time smoothing to the PIDE with a fixed point iterative procedure as the system solver and obtained second order convergence even for long dated options.

Andersen and Andreasen [5] derived a forward PIDE for European call options and applied it to the calibration problem. They also used an unconditionally stable operator splitting ADI finite difference method and accelerated it using the fast Fourier transform (FFT). Almendral and Oosterlee [4] proposed a matrix splitting technique to price European options under jump-diffusion processes. To avoid the wrap around effect, they embedded the resulting Toeplitz matrix into a circulant matrix. Feng and Linetsky [58] proposed an approach that combined extrapolation and implicit-explicit Euler (IMEX-Euler). Their approach improved significantly the classical IMEX-Euler scheme and proved strong competence for short maturity options. Mayo [100] showed how to use the operator splitting of Andersen and Andreasen to reduce the solution of the pricing equation in the Kou and similar models to a sequence of ODEs that can be solved efficiently. Sachs and Strauss [116] proposed an efficient second order fully implicit method. Their approach relied on transforming the PIDE to eliminate the convection term and the use of finite differences on uniform grids. This exhibited a structure that can be solved efficiently by a circulant preconditioned conjugate gradient method. For higher order schemes, Lee and Sun [93] implemented a fourth order compact boundary value method in order to achieve the fourth order in space and time.

In this thesis, we will explore the spectral methods to discretise the option pricing problems in the asset (spatial) direction. Spectral methods are a class of approximation methods that are well-known for the solution of partial differential equations [111]. For smooth enough solutions, they are exponentially convergent in the number of degrees of freedom [35, 60, 124]. Although widely used in fields such as fluid mechanics, their use in option pricing have been rare. The main drawback for their direct applications to

option pricing is that the payoff functions for typical options or the initial conditions in the governing PDEs are nonsmooth. Thus, the collocation approximations are reduced to low order accuracy, making them not competitive with existing finite difference methods. The literature is rich with ideas for overcoming this problem. One approach is to regularize the initial condition as proposed by Greenberg [66]. Suh [122, 123] used the Broadie-Detemple approach and obtained a significant improvement of the pseudo-spectral method over the finite difference methods (FDM) while solving PDEs and PIDEs (partial integro-differential equations) in finance. Tangman *et al.* [127] presented a new approach which consisted on dividing the set of Chebyshev points into two at strike price E . To this end, the new set of points will cluster grid nodes not only at the boundaries located at but also at the singularity located at the strike price for an European option. Zhu [149] proposed a spectral element based on the regularisation approach of Greenberg [66] to price European options with and without jumps in one and two dimensions. Some other relevant works can be found in [66, 149] and references therein. Furthermore, some specific works are reviewed in individual chapters.

In what follows, we present an overview of this thesis.

1.4 Outline of the thesis

The rest of this thesis is organised as follows:

In Chapter 2, we design and implement a fully spectral collocation method for solving European style vanilla and exotic options. The method is initially designed to solve problems for European call and put, and then further extended to solve digital and supershare option pricing problems. The method is coupled with rational interpolation using prescribed barycentric weights and mapped Chebyshev points in asset (space) direction. We also investigate the convergence analysis of the proposed approach. Numerical results are checked against available analytical solutions and compared in a number of settings.

In Chapter 3, we propose a semi-discrete spectral method for pricing European,

digital and butterfly spread options modeled via reaction-diffusion-advection partial differential equation. The method is based on a pseudo-spectral formulation of the PDE discretised by the means of an improved Lagrange formula. Implicit-Explicit (IMEX) Predictor-Corrector (PC) schemes are used for time integration; in which the diffusion term is integrated implicitly, whereas the reaction and advection terms are integrated explicitly. We analyse the stability of the method, and perform numerical experiments in order to illustrate the efficiency of the proposed method.

In Chapter 4, we present a robust rational spectral collocation method for pricing American options. Due to the free boundary conditions associated with the PDEs, we first reformulate the problem as a variational inequality. Then, by adding a penalty term, the resulting variational inequality is transformed into a nonlinear advection-diffusion-reaction equation on fixed boundaries. This nonlinear PDE is discretised in asset (space) direction by means of rational spectral collocation method, resulting into a system of stiff nonlinear ODEs which is then integrated using the implicit forth-order Lobatto time integration method. We carry out extensive comparisons with other results obtained by using some existing methods found in literature.

In Chapter 5, we consider European and American options under local volatility on both dividend and non-dividend paying assets. In the case of European options, the PDE is discretised directly in space, by the mean of rational spectral method while a penalty approach is used to solve the partial differential complementary problem that arises from American options resulting into a nonlinear partial differential equation. Then the nonlinear PDE is discretised in asset direction by means of a rational spectral collocation approximation, which uses the “sinh” transformation in order to accommodate more grids at a desired region. We obtain a system of ordinary differential equations that we solve using the implicit fifth-order RADAU time integration method. Then we finally present numerical results illustrating the robustness of our method.

Chapter 6 deals with a more challenging problem which involves non-local integral. We solve European vanilla and butterfly spread options under Merton’s jump-diffusion

model. This model leads to a partial integro-differential equation (PIDE). The differential and integral parts of the PIDE are approximated by the rational spectral collocation and the Clenshaw-Curtis quadrature methods, respectively, resulting into a system of ODEs. We use the implicit-explicit predictor-corrector (IMEX-PC) schemes to integrate the ODEs in which the diffusion term is integrated implicitly, and the convolution integral, reaction and advection terms are integrated explicitly. We analyse the stability of IMEX-PC and then perform numerical experiments.

In Chapter 7, we extend our approach to solve jump-diffusion models of American options. These type of problems are modelled by partial integro-differential complementary (PIDC) problems. We first reformulate the PIDC problem as a variational inequality, and then transform it into a nonlinear partial integro-differential equation (PIDE) on fixed boundaries by adding a penalty term. We discretise the resulting nonlinear PIDE in asset (space) direction by means of a spectral method using suitable barycentric weights and transformed Chebyshev points. The application of spectral collocation methods to the PIDE leads to a system of ordinary differential equations which is solved using the implicit forth-order Lobatto time integration method. Then we present numerical results to investigate the performance of our method.

Finally, Chapter 8 provides some concluding remarks and scope for future research.

Chapter 2

A fully spectral collocation methods for pricing European style standard and non-standard options



This chapter demonstrates the applications of a fully spectral collocation numerical methods for solving European style vanilla and exotic options. In particular, we solve problems for European call, put, digital and supershare options. The method was originally designed to solve problems for European call and put, and then further extended to solve digital and supershare option pricing problems. The method is coupled with rational interpolation using prescribed barycentric weights and mapped Chebyshev points in asset (space) direction. The Sinc collocation method is used to approximate the indefinite integral. These two approximations result in a system of algebraic equations which are then solved to obtain the approximate solution of the problem. As compared to the approach of Suh [123] which relies heavily on the techniques of Broadie and Detemple [30] to improve the efficiency of the pseudo-spectral method (PSM), we use conformal mappings in PSM in order to improve the accuracy the underlying method. Numerical results are checked against available analytical solutions and compared in a number of settings.

2.1 Introduction

Option pricing problems are often modeled by stochastic processes. Such problems were initially introduced in financial institution late in 1960's. The famous stochastic model for the equilibrium condition between the expected return on the option, the expected return on the stock and the risk-less interest rate is the celebrated Black-Scholes equation which was derived by Black and Scholes in 1973 ([21]).

Due to inherent complexity in the modelling equations, one can rarely find closed-form analytical solutions to these Black-Scholes PDEs, and therefore one has to resort to numerical methods. In literature, four main families of methods have been developed and used extensively to solve option pricing problems. These are lattice methods [26, 47, 74, 139], Monte Carlo simulations [11, 31, 96, 113, 131], finite difference (FD) methods [27, 28, 101, 140] and analytical approximations [37, 63, 70, 80]. The first two of these methods are classified as stochastic simulation methods since they approximate the underlying process directly. The other two methods are usually performed on the Black-Scholes PDEs with appropriate approximate boundary conditions. Some detailed comparisons [30, 64] have been made in order to select approximation methods that encompass the above mentioned characteristics.

This chapter investigates fully spectral methods for pricing European style options. Spectral and pseudo-spectral methods for solving partial differential equations with smooth initial conditions are proved to have exponential accuracy [35, 60, 124], whereas the prospects of using such methods for problems with non-smooth initial conditions remain more controversial. This can be attributed mainly to the presence of the Gibbs phenomenon, that appear when approximating non-smooth solutions using polynomial interpolations. This has usually a detrimental effect on the stability of the computational scheme. Thus, it is often perceived that spectral methods are too sensitive and lack robustness to allow the modeling of problems of realistic complexity which, by their very nature, are often non-smooth. The literature is rich with ideas for overcoming this lack of robustness. One approach is to use adaptive grids methods in

order to concentrate more grid points and achieve high resolution around the region of rapid variation. The standard approach in adaptive spectral methods has been to use coordinate transformations [85, 130].

The procedure of discretising using Chebyshev rational polynomials for spatial derivatives and Sinc approximation to the indefinite integral in time, gives rise to a Sylvester system where coefficient matrix for the temporal discretisation is full. This idea has been proposed and used in [1, 2, 3, 94, 98, 97] where the Sinc method was used both for the spatial and time discretisations. The utility of Sinc method can be justified from numerical considerations. Because the plain call or put is highly stiff during the first time steps, high resolution grids, like those used for the singular perturbation problems, are therefore required to achieve high accuracy results and rapid convergence. This is possible due the flexibility of conformal mapping in Sinc methods.

The rest of the chapter is organized as follows. Section 2.2 is devoted to a brief review of the four option pricing problems that we intend to solve. In Section 2.3, we give a semi-discretisation of the various Black-Scholes PDEs using rational spectral collocation method. Section 2.4 describes Sinc function properties and interpolations. In Section 2.5, we solve European options and estimate the error of numerical solutions against available analytical solutions. Finally, the last section contains a summary and discussions.

2.2 The mathematical model

Consider the financial market model $\mathcal{M} = (\Omega, \mathcal{F}, \mathbb{P}, (\mathcal{F}_\tau)_{\tau \geq 0}, (S_\tau)_{\tau \geq 0})$ where Ω is the set of all possible outcomes of the experiment known as the sample space, \mathcal{F} is the set of all events, i.e. permissible combinations of outcomes, \mathbb{P} is a map $\mathcal{F} \longrightarrow [0, 1]$ which assigns a probability to each event, $(\mathcal{F}_\tau)_{\tau \geq 0}$ is a natural filtration and S_τ a risky underlying asset price process. The triplet $(\Omega, \mathcal{F}, \mathbb{P})$ is defined as a probability space. Let $(B_\tau)_{\tau \geq 0}$ a \mathbb{P} -Brownian motion, $\sigma > 0$ the volatility of the underlying asset, $r > 0$ a risk-free interest rate and $\delta \geq 0$ a continuous dividend yield. Without loss of generality,

we assume that both the risk-free interest rate and the dividend yield are constants. Then under the equivalent martingale measure \mathbb{Q} , the dynamics of the Black-Scholes model satisfies the stochastic differential equation

$$dS_\tau = (r - \delta)S_\tau d\tau + \sigma S_\tau dB_\tau. \quad (2.2.1)$$

Using the Ito's formula we derive from the above equation a PDE for European style options

$$\frac{\partial V}{\partial t} = \frac{1}{2}\sigma^2 S^2 \frac{\partial^2 V}{\partial S^2} + (r - \delta)S \frac{\partial V}{\partial S} - rV, \quad (2.2.2)$$

where $t = T - \tau$. The boundary and the final conditions make the difference between American and European style options as well as between put and call and other types of options. The solution of the European vanilla call option is uniquely determined by

$$\left. \begin{aligned} V_t &= \frac{1}{2}\sigma^2 S^2 \frac{\partial^2 V}{\partial S^2} + (r - \delta)S \frac{\partial V}{\partial S} - rV, \\ V(S, 0) &= \max(S - E, 0), \\ V(0, t) &= 0, \\ V(S, t) &= Se^{-\delta t} - Ee^{-rt}, \text{ as } S \rightarrow \infty, \end{aligned} \right\}$$

where T is the expiry time and $t = T - \tau$ is the time to maturity. Similarly, the solution of the European put option can be uniquely determined by

$$\left. \begin{aligned} V_t &= \frac{1}{2}\sigma^2 S^2 \frac{\partial^2 V}{\partial S^2} + (r - \delta)S \frac{\partial V}{\partial S} - rV, \\ V(S, 0) &= \max(E - S, 0), \\ V(S, t) &= Ee^{-rt}, \text{ as } S \rightarrow 0^+, \\ V(S, t) &= V(S, t) = 0, \text{ as } S \rightarrow \infty, \end{aligned} \right\}$$

where T is the expiry time and $t = T - \tau$ is the time to maturity.

On the other hand, European digital options are priced through

$$\left. \begin{aligned} V_t &= \frac{1}{2}\sigma^2 S^2 \frac{\partial^2 V}{\partial S^2} + (r - \delta)S \frac{\partial V}{\partial S} - rV, \\ V(S, t) &= 0, \quad \text{as } S \rightarrow 0^+, \\ V(S, t) &= Qe^{-rt}, \quad \text{as } S \rightarrow \infty, \end{aligned} \right\}$$

with initial conditions

$$V(S, 0) = \begin{cases} Q, & \text{for } S \geq E, \\ 0, & \text{for } S \leq E, \end{cases} \quad (2.2.3)$$

where Q is a given constant, whereas the European super share options are expressed as

$$\left. \begin{aligned} V_t &= \frac{1}{2}\sigma^2 S^2 \frac{\partial^2 V}{\partial S^2} + (r - \delta)S \frac{\partial V}{\partial S} - rV, \\ V(S, t) &= 0, \quad \text{as } S \rightarrow 0^+, \\ V(S, t) &= 0, \quad \text{as } S \rightarrow \infty, \end{aligned} \right\}$$

with initial conditions

$$V(S, 0) = \begin{cases} 0, & \text{for } S < E, \\ \tilde{Q}/d, & \text{for } E < S < E + d, \\ 0, & \text{for } S > E + d, \end{cases} \quad (2.2.4)$$

where \tilde{Q} and d are given constants.

In order to solve these equation numerically, various researchers have used numerous methods (see section 2.1). Recently, Suh [123] used Pseudo-Spectral Chebyshev Methods (PSCM) to price options and extended the advantages of PSMs over Finite difference methods (FDM). However, his methods relies heavily on the techniques of Broadie and Detemple [30] to improve efficiency of the Pseudo-spectral method. We use conformal mappings in PSCM in order to improve the accuracy of the underlying method.

2.3 Spectral space discretisation of the PDE

An overview of the rational spectral collocation method can be found in Chapter 1. We apply this discretisation technique to 2.2.2 and obtain the following system of ODEs

$$\frac{du}{dt} = Au + g(t), \quad u(0) = u_0. \quad (2.3.1)$$

where $u = V_{ii}$, $i = 2, \dots, N-1$, $u(t) = (u_1(t), \dots, u_N(t))^T$, $A = P_{ii}D_{ii}^{(2)} + Q_{ii}D_{ii}^{(1)} - rI_{ii}$ with $P = \frac{1}{2}\sigma^2 L^{-2} \text{diag}(S^2)$ and $Q = (r - \delta)L^{-1} \text{diag}(S)$ are $N \times N$ diagonal matrices. The function $g(t)$ represents the boundary conditions. For European call options, the function g is given by

$$g(t) = \left(P_{ii}D_{iN}^{(2)} + Q_{ii}D_{iN}^{(1)} - rI_{iN} \right) (S_{max}e^{-\delta t} - Ee^{-rt}), \quad (2.3.2)$$

whereas for European put options, g is expressed as

$$g(t) = \left(P_{ii}D_{i1}^{(2)} + Q_{ii}D_{i1}^{(1)} - rI_{i1} \right) (Ee^{-rt}). \quad (2.3.3)$$

Note that for European digital call option, we have

$$g(t) = \left(P_{ii}D_{iN}^{(2)} + Q_{ii}D_{iN}^{(1)} - rI_{iN} \right) (Qe^{-rt}), \quad (2.3.4)$$

whereas for European supershare options the boundary function $g(t)$ is 0.

2.4 Sinc function time approximations and related properties

Sinc numerical methods for solving ordinary and partial differential equations have increasingly become popular and extensively studied, in particular for problems on unbounded domain and those having singularity at boundary. The first Sinc method

was introduced by Stenger [121] to solve two-point boundary value problems for second order differential equation. Excellent overviews of the existing Sinc methods for solving ODEs, PDEs and integral equations can be found in [98, 120]. In this section, we introduce some useful definitions and pertinent theorems of the Sinc function needed for time discretisation for the problems considered in this chapter.

2.4.1 Single Exponential (SE) Sinc method

We denote by \mathbb{Z} the set of all integers, \mathbb{R} the set of all real numbers and \mathbb{C} the set of all complex numbers. Let u be a function defined on \mathbb{R} and h the step-size. Then the Wittaker function is defined by the following series

$$C(u, h)(x) = \sum_{j=-\infty}^{\infty} u(jh)S(j, h)(x), \quad (2.4.1)$$

where $S(j, h)$ is given as follows

$$S(j, h) = \text{Sinc}\left(\frac{x - jh}{h}\right), \quad j = 0, \pm 1, \pm 2 \dots \quad (2.4.2)$$

and the Sinc function defined on the real line \mathbb{R} is given by

$$\text{Sinc}(x) = \begin{cases} \frac{\sin(\pi x)}{\pi x}, & x \neq 0 \\ 1, & x = 0. \end{cases} \quad (2.4.3)$$

Note in the above that h denotes the step-size in space direction. However, the description of the method is same for both space and time discretisations so at later stage, when we deal with the numerical simulations, we will rather use Δt to denote the time step-size instead of h above so as to comply with conventional notations and terminology.

Now, whenever the series given in equation (2.4.1) converges, u is approximated by using the finite number of terms. Therefore, for positive integer N , equation (2.4.1)

implies

$$C_N(u, h)(x) = \sum_{j=-N}^N u(jh)S(j, h)(x). \quad (2.4.4)$$

The sinc functions form an interpolatory set of functions, i.e.,

$$S(j, h)(kh) = \delta_{jk}^{(0)} \begin{cases} 1, & j = k \\ 0, & j \neq k. \end{cases} \quad (2.4.5)$$

Let

$$\delta_{kj}^{(-1)} = \frac{1}{2} + \int_0^{k-j} \frac{\sin(\pi t)}{\pi t} dt, \quad (2.4.6)$$

and define a matrix $I^{(-1)} = [\delta_{kj}^{(-1)}]$ whose (k, j) th entry is given by $\delta_{kj}^{(-1)}$.

The following results (taken from [97, 98, 120, 121, 125]) will be useful for the discussion in the rest of the chapter:

Definition 2.4.1. Let $d > 0$, and let D_d denotes the region $D_d = \{z = x + iy : |y| < d\}$ in the complex plane \mathbf{C} , and ϕ the conformal map of a simply connected domain D in the complex plane onto D_d such that $\phi(a) = -\infty$ and $\phi(b) = \infty$, where a and b are boundary points of D , i.e., $a, b \in \partial D$. Let ψ denote the inverse map of ϕ , and let the arc Γ , with endpoints a and b such that $(a, b) \notin \Gamma$, be given by $\Gamma = \psi^{-1}(-\infty, \infty)$. For $h > 0$, let the points x_j on Γ be given by $x_j = \psi(jh)$, $j \in \mathbb{Z}$, and $\rho(z) = e^{\phi(z)}$. The conformal map ϕ is chosen such that $\phi(z) = \log \left(\frac{z-a}{b-z} \right)$.

Definition 2.4.2. Let $L_\alpha(D)$ denote the family of all analytic functions u for which there exists a constant $C > 0$ such that

$$|u(z)| \leq C \frac{|\rho(z)|^\alpha}{[1 + |\rho(z)|]^{2\alpha}}, \quad \forall z \in D, \quad 0 < \alpha \leq 1. \quad (2.4.7)$$

Theorem 2.4.3 ([120]). Let $\frac{u}{\phi'} \in L_\alpha(D)$, let N be a positive integer and let h be selected by the formula

$$h = \left(\frac{\pi d}{\alpha N} \right)^{\frac{1}{2}}, \quad (2.4.8)$$

then there exist positive constant c_1 , independent of N , such that

$$\left| \int_{\Gamma} u(z) dz - h \sum_{k=-N}^N \frac{u(z_j)}{\phi'(z_j)} \right| \leq c_1 e^{(-\pi d \alpha N)^{\frac{1}{2}}}. \quad (2.4.9)$$

Proof. See [120].

Corollary 2.4.4. Let $\frac{u}{\phi'} \in L_{\alpha}(D)$, and let h be selected by the formula (2.4.8), then there exists a positive constant c_2 , such that

$$\left| \int_{\Gamma} [u(z) S(j, h) \circ \phi(z)] dz - h \frac{u(z_j)}{\phi'(z_j)} \right| \leq c_2 e^{(-\pi d \alpha N)^{\frac{1}{2}}}. \quad (2.4.10)$$

Theorem 2.4.5 ([120]). Let $\frac{u}{\phi'} \in L_{\alpha}(D)$, with $\alpha > 0$, and $d > 0$, let $\delta_{kj}^{(-1)}$ and h be defined as in (2.4.6) and (2.4.8) respectively. Then there exists a positive constant c_3 , independent of N , such that

$$\left| \int_a^{z_j} u(t) dt - h \sum_{k=-N}^N \delta_{kj}^{(-1)} \frac{u(z_j)}{\phi'(z_j)} \right| \leq c_3 e^{(-\pi d \alpha N)^{\frac{1}{2}}}. \quad (2.4.11)$$

Proof. See [120].

2.4.2 Double Exponential (DE) Sinc method

Results presented in the previous subsection imply that the error bound of the approximate solution and its integrals is $O(e^{(c\sqrt{N})})$, $c > 0$, where N is a parameter representing the number of terms in the Sinc approximation. Although this convergence rate is much faster than that of polynomial order, it is still not optimal because this convergence rate is based on the SE transformation. We therefore employ the optimal DE transformation instead of the SE transformation.

Definition 2.4.6. Let $d > 0$, and let D_d denotes the region $D_d = \{z = x + iy : |y| < d\}$ in the complex plane \mathbf{C} , and ϕ the conformal map of a simply connected domain D in the complex plane onto D_d such that $\phi(a) = -\infty$ and $\phi(b) = \infty$, where a and b are

boundary points of D , i.e., $a, b \in \partial D$. We denote ϕ^{-1} the inverse of ϕ . Let $H^1(D_d)$ be the family of all functions u analytic in D_d such that

$$\mathcal{N}_1(u, D_d) = \lim_{\epsilon \rightarrow 0} \int_{\partial D_{d(\epsilon)}} |u(z)| |dz| < \infty, \quad (2.4.12)$$

where $D_{d(\epsilon)} = \{z \in \mathbb{C} : |Re z| < \epsilon, \quad |Im|z| < d(1 - \epsilon)\}$.

Definition 2.4.7. A function u is said to decay double exponentially if there exist positive constants α and C such that

$$|u(z)| \leq C e^{-\alpha e^{|z|}}, \quad z \in (-\infty, \infty), \quad (2.4.13)$$

or a function u is said to decay double exponentially with respect to the conformal map ϕ if there exists positive constants α and C such that

$$|u(\phi(z))\phi'(z)| \leq C e^{-\alpha e^{|z|}}, \quad z \in (-\infty, \infty). \quad (2.4.14)$$

It is in this sense that ϕ satisfying (2.4.14) is called the DE transformation. Let $K_\phi^\alpha(D_d)$ denotes the family of functions where $u(\phi(z))\phi'(z)$ belongs to $H^1(D_d)$ and decays double exponentially with respect to ϕ and with constant α as (2.4.14).

Theorem 2.4.8. Let $u \in K_\phi^\alpha(D_d)$, let N a positive integer and let h be selected by the formula

$$h = \frac{1}{N} \log \frac{2\pi dN}{\alpha}, \quad (2.4.15)$$

then there exist a positive constant C_1 such that

$$\left| \int_a^b u(z) dz - h \sum_{j=-N}^N \frac{u(z_j)}{\phi'(z_j)} \right| \leq C_1 e^{\left(\frac{2\pi dN}{\log(2\pi dN/\alpha)}\right)}. \quad (2.4.16)$$

Theorem 2.4.9 ([104]). Let $u \in K_\phi^\alpha(D_d)$, let N a positive integer and let h be selected by the formula

$$h = \frac{1}{N} \log \frac{\pi dN}{\alpha}, \quad (2.4.17)$$

then there exist a positive constant C_2 such that

$$\left| \int_a^{z_j} u(t) dt - h \sum_{j=-N}^N \frac{u(z_j)}{\phi'(z_j)} \delta_{kj}^{(-1)} \right| \leq C_2 \frac{\log(N)}{N} e^{\left(\frac{\pi d N}{\log \frac{\pi d N}{\alpha}} \right)}. \quad (2.4.18)$$

Proof. See [104].

From the above results, it is clear that the convergence rate of the DE Sinc method is $O(e^{-cN/\log N})$.

2.4.3 Full discretisation

In order to proceed with the full discretisation of the governing PDE, we introduce the following notations and terminologies:

Definition 2.4.10. For an $m \times n$ matrix $B = [b_{ij}]$, $1 \leq i \leq m$, $1 \leq j \leq n$

$$B = [b_1 \ b_2 \ \dots \ b_n] \text{ where } b_j = \begin{bmatrix} b_{1j} \\ b_{2j} \\ \vdots \\ b_{mj} \end{bmatrix} \quad (2.4.19)$$

the concatenation of B is the $mn \times 1$ vector

$$co(B) = \begin{bmatrix} b_1 \\ b_2 \\ \vdots \\ b_n \end{bmatrix} \quad (2.4.20)$$

Definition 2.4.11. Let A be an $m \times n$ matrix and B an $p \times q$ matrix. The Kronecker

or tensor product of A and B is the matrix

$$A \otimes B = \begin{pmatrix} a_{11}B & a_{12}B & \cdots & a_{1n}B \\ a_{21}B & a_{22}B & \cdots & a_{2n}B \\ \vdots & \vdots & & \vdots \\ a_{m1}B & a_{m2}B & \cdots & a_{mn}B \end{pmatrix} \quad (2.4.21)$$

Theorem 2.4.12. Consider the linear system for the unknown matrix X be given as

$$A_1XB_1 + A_2XB_2 + \cdots + A_kXB_k = C \quad (2.4.22)$$

where A_i are $m \times m$, X , C are $m \times n$ and B_i are $n \times m$. This is equivalent to

$$Gco(X) = co(C), \quad (2.4.23)$$

where $G = B_1^T \otimes A_1 + B_2^T \otimes A_2 + \cdots + B_k^T \otimes A_k$.

Now the full discretisation of the semi-discrete system (2.3.1) is obtained by performing the usual integration as

$$u(t) = \int_0^t [Au(t) + g(t)] dt + u_0. \quad (2.4.24)$$

We next collocate with respect to the time variable t by using the indefinite integration formula (2.4.11) with the conformal map $\phi(t) = \log(t/T - t)$.

Let $B = hI^{(-1)}\mathcal{D}(1/\phi'(t_j))$ where $t_j = \phi^{-1}(j\Delta t)$, $j = -M, \dots, M$, we can find a $N \times (2M + 1)$ rectangular matrix $U = u(x_i, t_j)$ as the solution of the Sylvester system

$$U = (AU + g)B^T + U_0, \quad (2.4.25)$$

for which the explicit form is

$$I_x UI_t - AUB^T = gB^T + U_0. \quad (2.4.26)$$

This is equivalent to

$$\mathbf{G}co(\mathbf{U}) = co(\mathbf{C}). \quad (2.4.27)$$

where $\mathbf{G} = \mathbf{I}_t^T \otimes \mathbf{I}_x - \mathbf{B} \otimes \mathbf{A}$ and $\mathbf{C} = \mathbf{g}\mathbf{B}^T + \mathbf{U}_0$.

Note in (2.4.25) that the matrix \mathbf{U}_0 has the same dimensions as the matrix \mathbf{U} , whose columns are the replication of the column vector u_0 .

2.5 Numerical results

Numerical results are obtained using the maturity time as $T = 0.5, 1$ and 2 , $S_{\min} = 0$, $S_{\max} = 200$ and the strike price $E = 45$. At a typical time or space level, the accuracy of the proposed method was measured by means of the maximum error

$$L_\infty = \max_{i=1, \dots, N} |u_i - V_i|, \quad (2.5.1)$$

and the root mean square error

$$L_2 = \sqrt{\frac{1}{N} \sum_{i=1}^N (u_i - V_i)^2}, \quad (2.5.2)$$

where N is the number points used in the discretisation in one particular direction, V_i is the exact solution of the Black-Scholes equation given in [21], u_i is the numerical approximation to the exact solution of the Black-Scholes equation. Note that u_i and V_i denote entries from particular rows (columns) of the approximated matrices u and V .

To determine the rate of convergence of the discretisation schemes, we define

$$R_2 = \frac{L_2^N}{L_2^{2N}} \quad \text{and} \quad R_\infty = \frac{L_\infty^N}{L_\infty^{2N}}, \quad (2.5.3)$$

where L_2^m and L_∞^m are respectively L_2 and L_∞ norms of the errors with m discretisation points.

2.5.1 Valuation of European call options

The Analytic solution of the Black-Scholes equation (2.2.2) for European call options is known [21, 140] and is expressed as

$$V(S, t) = Se^{-\delta t} \mathcal{N}(d_1) - Ee^{-rt} \mathcal{N}(d_2), \quad (2.5.4)$$

where

$$d_1 = \frac{\ln\left(\frac{S}{E}\right) + \left(r - \delta + \frac{\sigma^2}{2}\right)t}{\sigma\sqrt{t}}, \quad d_2 = d_1 - \sigma\sqrt{t}, \quad (2.5.5)$$

and $\mathcal{N}(\cdot)$ is the cumulative probability distribution function for a standardised normal variable

$$\mathcal{N}(y) = \frac{1}{\sqrt{2\pi}} \int_{-\infty}^y e^{-\frac{x^2}{2}} dx. \quad (2.5.6)$$

The convergence of our numerical approach is investigated in both time and space directions. We start by investigating the convergence of the Sinc methods used for time discretisation based on the SE and DE transformations. For the SE and DE transformations we employ

$$t = \frac{Te^x}{1 - e^x}, \quad x_j = j\Delta t, \quad -M \leq j \leq M \quad (2.5.7)$$

and

$$t = \frac{T}{2} \tanh\left(\frac{\pi}{2} \sinh x\right) + \frac{T}{2}, \quad x_j = j\Delta t, \quad -M \leq j \leq M \quad (2.5.8)$$

respectively.

For each $M = 8, 16, 24$ and 32 , we choose the time step-size Δt as

$$\Delta t = \frac{1}{M} \log\left(\frac{\pi d M}{\alpha}\right), \quad \alpha = \frac{\pi}{2}, \quad d = \frac{\pi}{12}, \quad (2.5.9)$$

for the DE transformation and

$$\Delta t = \left(\frac{\pi d}{\alpha M} \right)^{\frac{1}{2}}, \quad \alpha = \frac{1}{2}, \quad d = \frac{\pi}{2}, \quad (2.5.10)$$

for the SE transformation. For space discretisation we employ the rational spectral method (1.2.1), where the transformation g is chosen as in (1.2.31). The effect of the transformation (1.2.1) is to increase the number of points in the region around the strike price $S = E$, influenced by the parameter $\beta = 5 \times 10^{-5}$. For spatial direction, we choose $N = 80$. The option is valued with the parameters $\sigma = 0.20$, $\delta = 0.00$ and $r = 0.05$ at maturity time $T = 0.5$. Tables 2.5.1 and 2.5.2 represent the convergence of the SE and DE Sinc methods, respectively. We observe a rapid convergence pattern

Table 2.5.1: Convergence of the SE Sinc method for European call option.

| M | Δt | L_{∞} |
|----|------------|--------------|
| 8 | 1.1107 | 1.7422E-3 |
| 16 | 0.7854 | 4.2141E-5 |
| 24 | 0.6413 | 1.6926E-6 |
| 32 | 0.5554 | 3.8831E-7 |

Table 2.5.2: Convergence of the DE Sinc method for European call option.

| M | Δt | L_{∞} |
|----|------------|--------------|
| 8 | 0.1791 | 5.7402E-3 |
| 16 | 0.1328 | 7.3120E-6 |
| 24 | 0.1055 | 6.3053E-7 |
| 32 | 0.0881 | 8.8289E-8 |

in both Sinc methods. However the DE Sinc method has a better convergence than the SE Sinc method as predicted theoretically in theorems 2.4.5 and 2.4.8. In view of this observation, in the remaining of this chapter, we will only present the results by using DE Sinc method. Note also that the problem for the European call option is solved efficiently irrespective of the stiffness of this problem.

The second experiment consists of investigating the convergence of our rational collocation method. We first evaluate the value of the European option by means of

our rational collocation method at Chebyshev-Gauss-Lobatto (CGL) points for various option parameters. The results are compared with those of finite difference (FD) using uniform grids. The results are displayed in Table 2.5.3.

Table 2.5.3: Comparison of European call option valuation by using the rational collocation (RC) method on CGL grid and the finite difference (FD) method on uniform grid.

| Schemes | T=0.5 | | T=1 | | T=2 | |
|--|-----------|------------|-----------|------------|-----------|------------|
| | L_2 | L_∞ | L_2 | L_∞ | L_2 | L_∞ |
| Parameters: $r = 0.05$, $\sigma = 0.2$, $\delta = 0.00$ | | | | | | |
| FD | 3.1909E-3 | 1.4634E-2 | 2.6060E-3 | 1.0087E-2 | 2.1086E-3 | 7.1023E-3 |
| RC | 3.1423E-3 | 1.5311E-2 | 2.5106E-3 | 1.0234E-2 | 1.9721E-3 | 6.7198E-3 |
| Parameters: $r = 0.07$, $\sigma = 0.04$, $\delta = 0.03$ | | | | | | |
| FD | 2.1539E-2 | 1.4692E-1 | 2.2936E-2 | 1.7246E-1 | 2.3767E-2 | 1.3650E-1 |
| RC | 1.4655E-2 | 1.0806E-1 | 1.0366E-2 | 7.9185E-2 | 5.3656E-3 | 4.1259E-2 |
| Parameters: $r = 0.1$, $\sigma = 0.3$, $\delta = 0.05$ | | | | | | |
| FD | 2.5533E-3 | 9.6791E-3 | 2.0822E-3 | 6.8373E-3 | 1.6691E-3 | 4.7612E-3 |
| RC | 2.4546E-3 | 9.4655E-3 | 1.9491E-3 | 6.2932E-3 | 1.5066E-3 | 4.0023E-3 |

In theory and for a range of practical problems, it has been shown and observed that spectral methods display exponential accuracy and have higher convergence than finite difference methods [25, 59, 60]. However, one can observe from Table 2.5.3 that the RC have a moderately smaller error than that of the FD. Numerically, higher order methods, in particular RC methods have difficulty in accurately approximating the solution in the region of singularity, i.e., the region of dramatic change. In the present case, the first derivative of the initial condition is discontinuous at the strike price E . As a result, the convergence of RC methods cannot be significantly superior to that of FD.

In order to overcome this, we use a high resolution grids in the region of dramatic change. This improves the accuracy of the RC methods significantly as it can be seen from Table 2.5.4. Note that several ideas have been proposed in order to improve the accuracy of the SC in the region of singularity. Here we confine our study to use coordinate transformations (1.2.31) that can potentially cluster the grid points at strike price E and then compare the result with FD with coordinate transformations (1.2.31) and the domain decomposition of Tangman *et al.* [127].

Table 2.5.4: Comparison of European call option valuation by using the rational collocation (RC), finite difference (FD) and the TGB ([127]) methods using adaptive grid.

| Schemes | T=0.5 | | T=1 | | T=2 | |
|--|-----------|------------|-----------|------------|-----------|------------|
| | L_2 | L_∞ | L_2 | L_∞ | L_2 | L_∞ |
| Parameters: $r = 0.05$, $\sigma = 0.2$, $\delta = 0.00$ | | | | | | |
| FD | 3.6137E-3 | 1.6267E-2 | 3.1758E-3 | 1.1812E-2 | 2.9222E-3 | 9.3376E-3 |
| TGB | 5.5826E-6 | 1.3075E-5 | 4.0249E-6 | 8.5471E-6 | 3.8488E-6 | 7.0143E-6 |
| RC | 1.7896E-7 | 9.2828E-7 | 4.1763E-7 | 2.5196E-7 | 3.1782E-7 | 6.7099E-7 |
| Parameters: $r = 0.07$, $\sigma = 0.04$, $\delta = 0.03$ | | | | | | |
| FD | 4.1853E-3 | 2.2697E-2 | 4.7541E-3 | 2.1273E-2 | 5.7885E-3 | 1.9339E-2 |
| TGB | 4.7227E-5 | 1.6525E-4 | 1.9620E-5 | 6.8969E-5 | 1.0234E-5 | 4.1836E-5 |
| RC | 3.6521E-7 | 1.5600E-6 | 8.6172E-7 | 2.2703E-6 | 1.6615E-6 | 6.4259E-6 |
| Parameters: $r = 0.1$, $\sigma = 0.3$, $\delta = 0.05$ | | | | | | |
| FD | 2.1539E-2 | 1.4692E-1 | 2.2936E-2 | 1.7246E-1 | 2.3767E-2 | 1.3650E-1 |
| TGB | 4.7233E-5 | 1.6528E-4 | 1.9636E-5 | 6.9032E-5 | 1.0276E-5 | 4.1954E-5 |
| RC | 3.6007E-7 | 1.5257E-6 | 8.5859E-7 | 2.2162E-7 | 1.6590E-7 | 6.5573E-7 |

From Table 2.5.4, we observe the significant improvement of RC methods while concentrating the grid points at strike price E either by grid transformations or by domain decomposition, while for FD method a moderate improvement is observed for the same set of parameters as used in Table 2.5.3. This is because high resolution grids in the region of singularity E allows the RC to capture the rapid change of option price, while in the region of low change of the option price. Our RC method displays the best accuracy compare with the TGB and the FD methods. For example, for the first set of parameters given in Table 2.5.4, at maturity time $T = 0.5$, the RC is 62 times more accurate than the TGB method and 9222 more accurate than the FD methods.

Figure 2.5.1 illustrates the convergence of the finite difference (FD), the rational collocation (RC) and the domain decomposition method of Tangman *et al.* [127] (TGB). We observe that the RC approximation yields very good results which is in line with what we see in Theorem 1.2.1. For comparison, we observe that the TGB method is less accurate than our RC method, whereas FD method displays a very poor convergence.

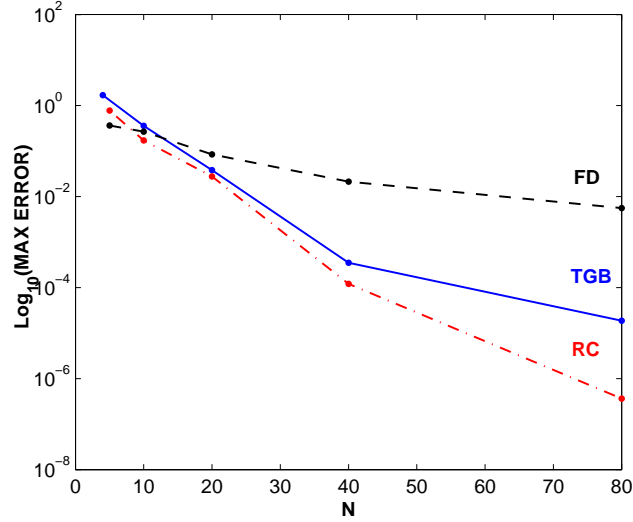


Figure 2.5.1: Convergence of the rational collocation (RC), finite difference (FD) and the TGB ([127]) methods using adaptive grid with $M = 32$, $N = 80$, $\beta = 10^4$, $S_{\min} = 0$, $S_{\max} = 200$, $r = 0.05$, $\sigma = 0.2$, $\delta = 0.00$, $E = 45$ at $T = 0.5$.

2.5.2 Valuation of European put options

Given a value of a call options, it is possible to compute the value of the corresponding put options via the call-put-parity formula [89]. Yet, puts and calls do not always share the same properties. Therefore, it is worth valuing European put options separately. The benchmark solution used to validate our numerical scheme is the analytic solution of the Black-Scholes equation (2.2.2) given by

$$Ee^{-rt}N(-d_2) - Se^{-\delta t}N(d_1), \quad (2.5.11)$$

where d_1 , d_2 are defined in (2.5.5) and N is the cumulative normal distribution defined in (2.5.6).

The value of a European put can be computed numerically by solving the PDE (2.2.3). The procedure is similar to what has been use to evaluate the European call with appropriate boundary conditions (2.3.3).

We use the same parameters as those used for valuing European calls. The results

Table 2.5.5: Comparison of European put option valuation by using the rational collocation (RC), the finite difference (FD) and ([127]) methods using adaptive grid.

| Schemes | T=0.5 | | T=1 | | T=2 | |
|--|------------|------------|-----------|------------|-----------|------------|
| | L_2 | L_∞ | L_2 | L_∞ | L_2 | L_∞ |
| Parameters: $r = 0.05$, $\sigma = 0.2$, $\delta = 0.00$ | | | | | | |
| FD | 1.1549E-3 | 2.0367E-3 | 1.7639E-3 | 3.0902E-3 | 1.0325E-3 | 5.3406E-3 |
| TGB | 7.7184E-6 | 1.8715E-5 | 5.7626E-6 | 1.2825E-5 | 4.1115E-6 | 8.8364E-6 |
| RC | 1.2523E-7 | 3.6384E-7 | 1.7647E-7 | 8.7883E-7 | 3.6925E-7 | 4.2126E-7 |
| Parameters: $r = 0.07$, $\sigma = 0.04$, $\delta = 0.03$ | | | | | | |
| FD | 4.1853E-3 | 2.2697E-2 | 4.7541E-3 | 2.1273E-2 | 5.7885E-3 | 1.9339E-2 |
| TGB | 14.7227E-5 | 1.6525E-4 | 1.9620E-5 | 6.8969E-5 | 1.0234E-5 | 4.1836E-5 |
| RC | 3.6521E-7 | 1.5600E-6 | 8.6172E-7 | 2.2703E-6 | 1.6615E-6 | 6.4259E-6 |
| Parameters: $r = 0.1$, $\sigma = 0.3$, $\delta = 0.05$ | | | | | | |
| FD | 1.1092E-3 | 6.5442E-3 | 1.3985E-3 | 2.3658E-3 | 1.0175E-3 | 3.0650E-3 |
| TGB | 5.5608E-6 | 1.3036E-5 | 3.9793E-6 | 8.4730E-6 | 1.8480E-6 | 7.0118E-5 |
| RC | 1.8831E-7 | 9.6659E-7 | 4.2101E-7 | 2.5927E-7 | 1.1776E-7 | 6.7076E-7 |

can be found in Table 2.5.5. Even in this case, we have similar observations and thus our approach is consistent. Now we would like to investigate the accuracy of our RC method for pricing exotic options, in particular digital and supershare options.

2.5.3 Valuation of European digital call options

These options belong to the so-called class of exotic options. They are not traded at exchanges. Such contracts are traded between a bank and a customer. A digital call option, also known as cash-or-nothing call or binary option, is an option with payoff 0 before the strike price and 1 (or any fixed amount Q) after the strike price. The analytic solution for the digital option is

$$V(S, t) = Qe^{-rt}\mathcal{N}(d_2), \quad (2.5.12)$$

where d_2 is defined in (2.5.5).

The discontinuous initial conditions for digital options, are susceptible to cause numerical oscillations of the Greeks with classical time integration methods such as Crank Nicolson. Our approach produces non-oscillatory behaviour of the Greeks. It

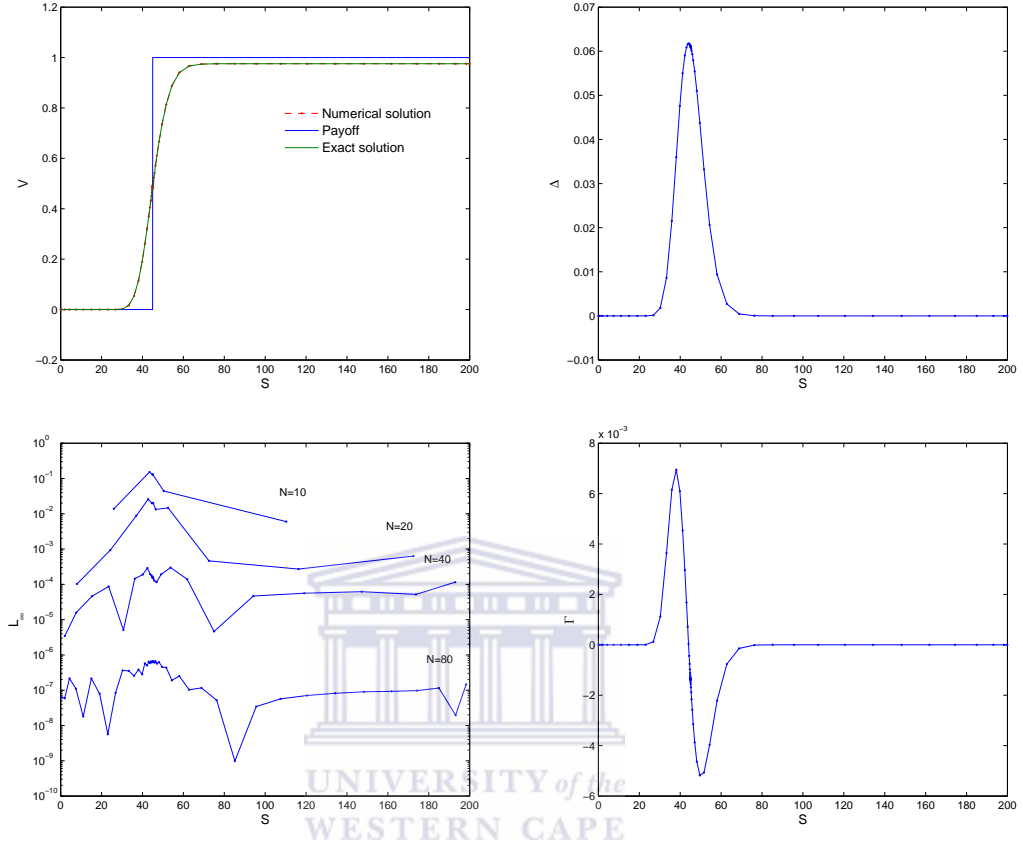


Figure 2.5.2: Valuation of Digital call options (top left figure); approximation errors (bottom left figure); and Δ (top right figure) and Γ (bottom right figure) using the rational collocation (RC) method with $M = 32$, $N = 80$, $\beta = 10^6$, $S_{\min} = 0$, $S_{\max} = 200$, $r = 0.05$, $\sigma = 0.2$, $\delta = 0.03$, $E = 45$, $T = 0.5$.

can be seen from Figure 2.5.2, where we present numerical solutions of digital call options together with their Δ , Γ and numerical errors. All results are satisfactory and free of oscillations.

We next investigate the convergence of our RC method via the maximum error and the root mean square error at maturity time $T = 0.5$ for a fixed set of parameters as given in Table 2.5.6. For comparison, we also investigate the convergence of the FD and the TGB methods. From the test experiments in Table 2.5.6, it follows that the equidistant grid FD method converges in first order. The TGB method has a second order convergence which is unexpected since it has been observed [127] that

the TGB is fourth order accurate for pricing plain vanilla options. The main reason for the convergence reduction is the discontinuous payoff encountered in the case of digital options. The convergence of the RC method is influenced by the stretching grid parameter β . For β large enough, for instance $\beta = 10^6$ in this experiment, we recover a very rapid convergence which is in line with the exponential convergence of spectral methods. This result is in good agreement with Theorem 1.2.1.

Table 2.5.6: Numerical results for valuing digital call options using the rational collocation (RC), finite difference (FD) and TGB [127] methods on adaptive grid, using parameters: $E = 45$, $T = 0.5$, $r = 0.05$, $\sigma = 0.2$, $\delta = 0.03$, $\beta = 10^6$, $M = 32$.

| N | L_2 | R_2 | L_∞ | R_∞ |
|-----|-----------|----------|------------|------------|
| FD | | | | |
| 10 | 1.3064E-1 | - | 4.0830E-1 | - |
| 20 | 3.9864E-2 | 3.2772 | 1.7503E-1 | 2.3328 |
| 40 | 2.1721E-2 | 1.8353 | 1.0756E-1 | 1.6272 |
| 80 | 1.0227E-2 | 2.1239 | 4.4625E-2 | 2.4104 |
| TGB | | | | |
| 10 | 8.8329E-2 | - | 2.2564E-1 | - |
| 20 | 1.8585E-2 | 4.7526 | 4.5051E-2 | 5.0085 |
| 40 | 4.2353E-3 | 4.3882 | 1.0453E-2 | 4.3098 |
| 80 | 1.0632E-3 | 3.9837 | 2.6072E-3 | 4.0093 |
| RC | | | | |
| 10 | 9.5957E-2 | - | 1.5190E-1 | - |
| 20 | 1.5473E-2 | 6.2014 | 2.5902E-2 | 5.8643 |
| 40 | 1.4451E-4 | 107.0782 | 2.9838E-4 | 86.8097 |
| 80 | 4.9406E-7 | 292.4868 | 6.5762E-7 | 453.7202 |

All the results are accurate, although less accurate as in the case of European call and puts. This is mainly due to non-smooth initial conditions. While the European call and put have discontinuity in the first derivative of the payoff, the digital options have discontinuity in the payoff itself.

Our approach using the grid refinement at strike price is found to perform significantly better than lower order FD method in term of accuracy for valuating European option pricing problems.

2.5.4 Valuation of supershare options

A supershare option is a combination of a long position cash-or-nothing call with amount Q/d and exercise price E and a short position cash-or-nothing call with amount Q/d and exercise price $E + d$. Supershare options present two discontinuities or regions

Table 2.5.7: Numerical results for valuing supershare options using the rational collocation (RC), finite difference (FD) and TGB [127] methods on adaptive grid using parameters: $E = 45$, $T = 0.5$, $r = 0.05$, $\sigma = 0.2$, $\delta = 0.03$, $\beta = 10^6$, $M = 32$, $S_{\max} = 200$, $S_{\min} = 0$.

| N | L_2 | R_2 | L_∞ | R_∞ |
|-----|-----------|----------|------------|------------|
| FD | | | | |
| 10 | 2.1665E-1 | - | 4.5002E-1 | - |
| 20 | 5.9147E-2 | 3.6629 | 1.7595E-1 | 2.5577 |
| 40 | 2.3717E-2 | 2.4939 | 1.0377E-1 | 1.6956 |
| 80 | 1.0892E-2 | 2.1774 | 4.3352E-2 | 2.3937 |
| TGB | | | | |
| 10 | 6.8764E-2 | - | 1.5649E-1 | - |
| 20 | 2.5056E-2 | 2.7445 | 5.0108E-2 | 3.1230 |
| 40 | 5.2340E-3 | 4.7871 | 9.0879E-3 | 5.5137 |
| 80 | 1.3097E-3 | 3.9962 | 2.2920E-3 | 3.9650 |
| RC | | | | |
| 10 | 2.2531E-1 | - | 3.1240E-1 | - |
| 20 | 6.1944E-2 | 3.6373 | 1.1113E-1 | 2.8113 |
| 40 | 5.2682E-3 | 11.7582 | 1.1464E-2 | 9.6938 |
| 80 | 1.9050E-5 | 276.5405 | 1.0088E-4 | 113.6306 |

of rapid change in the payoff function. We need to capture these regions of rapid change with high grid refinement via the grid transformation (1.2.35). In this experiment we choose $\alpha_1 = \alpha_2 = \frac{1}{2}$ and the grid stretching parameters $\beta_1 = \beta_2 = \beta = 10^5$. From Table 2.5.7, we observe that the FD and TGB methods are respectively first and second order convergent whereas the RC method displays exponential convergence. Once again, our approach produces non-oscillatory behaviour of the Greeks as it can be seen from Figure 2.5.3 where we present numerical solution for the supershare options together with their Δ , Γ and numerical errors. All the results are very good and free of oscillations.

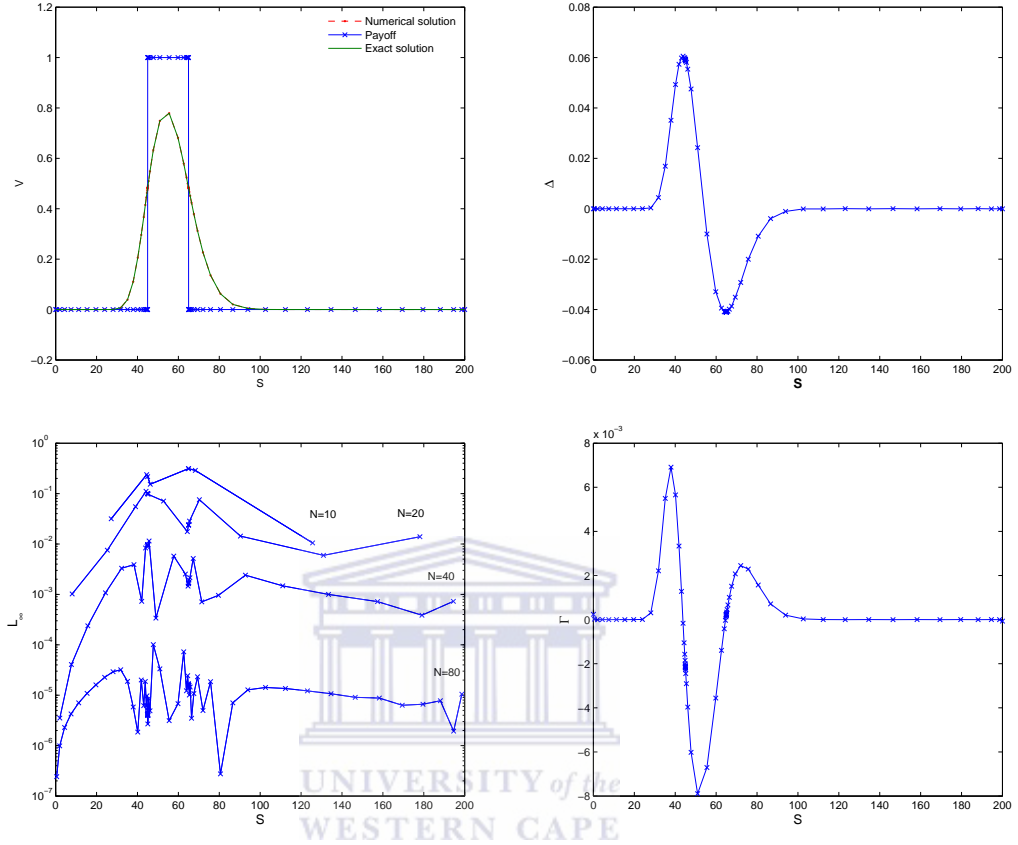


Figure 2.5.3: Valuation of supershare options (top left figure); approximation errors (bottom left figure); and Δ (top right figure) and Γ (bottom right figure) using the rational collocation (RC) method with $M = 32$, $N = 80$, $\beta = 10^6$, $S_{\min} = 0$, $S_{\max} = 200$, $Q = 20$, $d = 20$, $r = 0.05$, $\sigma = 0.2$, $\delta = 0.03$, $E = 45$, $T = 0.5$.

2.6 Summary and discussions

We have proposed a rational collocation method in space in combination with Sinc collocation time marching method for pricing European vanilla and exotic options. Extensive comparisons are carried out with standard finite difference (FD) method and the TGB approach (Tangman *et al.* [127]). In all experiments our rational collocation (RC) approach displays an exponential convergence. Also the convergence of the TGB method ([127]) is fourth order for valuing European vanilla options and further reduced to order two when the method is used to price exotic options. We achieved very good results with a very few mesh points, for instance in the case of digital options, we

achieved an error of 2.98×10^{-4} with only 40 grid points which indicate that our method is superior to other existing methods in term of accuracy.

We note that, the amount of computations involved in the fully spectral method is significantly more as compared to that of the semi-discrete spectral approach, since it involves the use of the tensor product in its computation. In view of this observation, we will use the semi-discrete type of spectral methods for the rest of the problems considered in this thesis. To this end, in the next chapter, we explore the use of implicit-explicit predictor-corrector schemes for integration in time-direction.



Chapter 3

Implicit-explicit predictor-corrector methods combined with rational spectral methods for pricing European options



In this chapter, we propose a semi-discrete spectral method for pricing European, digital and butterfly spread options in the context reaction-diffusion-advection partial differential equation (PDE). The method is based on a pseudo-spectral formulation of the PDE discretised by the means of an improved Lagrange formula. Implicit-Explicit (IMEX) Predictor-Corrector (PC) schemes are used for time integration; with the diffusion term integrated implicitly, while the reaction and advection terms are integrated explicitly. Numerical experiments illustrate that our approach is highly accurate and efficient for pricing financial options.

3.1 Introduction

In this chapter, we explore the spectral methods to discretise the option pricing problems in the asset (spatial) direction. To discretise the problem in time direction, we use a class of implicit-explicit (IMEX) methods. These methods have been used in conjunction with spectral methods [35] to solve problems involving different types of PDEs. Asher *et al.* [6] constructed families of first, second, third and fourth order IMEX multi-step methods to solve convection-diffusion equations. Ruuth [115] used multi-step IMEX and efficiently solved reaction-diffusion problems in pattern formation. Recently, Hundsdorfer and Ruuth [78] extended the construction of IMEX multi-step methods with general monotonicity and boundedness properties for hyperbolic systems with stiff source or relaxation term.

IMEX multi-step methods are used earlier in the field of option pricing. In particular, for jump-diffusion PIDE, Almendral and Oosteele [4] proposed a second-order backward differentiation formula (BDF). Feng and Linetsky [58] proposed an extrapolation approach in combination with the first-order accurate IMEX-Euler scheme and their experiments show that the extrapolation method improved significantly over the first-order IMEX-Euler scheme in solving the jump-diffusion PIDE. Another family of IMEX schemes is based on Runge-Kutta methods. Asher *et al.* [7] constructed IMEX Runge-Kutta methods for solving convection-reaction-diffusion problems. De Frutos [50, 51] introduced IMEX-RK methods as an alternative to other existing time integration methods for pricing options. We refer the interested readers to [7, 24, 32, 33, 50, 34] for recent developments on IMEX-RK methods.

One class of IMEX methods that we will be using belongs to the family of IMEX-PC schemes. These are successfully applied to solve stiff PDEs. The main idea is to split the basic multi-step IMEX into PC schemes. Cash [38] used this idea to construct a new class of multi-step methods. By splitting the BDF, he obtained a new BDF which has considerably better stability than the standard BDF while maintaining the same accuracy. Voss and Casper [134] used a split version of Adams-Moulton formulas

as a novel family of PC schemes for stiff ODEs. Voss and Khaliq [135] considered the θ -methods in a linearly implicit form as the predictor and derived an implicit second-order PC scheme for reaction-diffusion problems. Recently, Li *et. al* [95] adopted the strategy found in [6] to construct a family of higher order IMEX-PC schemes for nonlinear parabolic differential equations. Their numerical results show that these IMEX-PCs have a significant better stability than those found in [6]. More recently, Grooms and Julien [67] derived a fourth order IMEX-PC. Their method used the fourth order total variation IMEX found in [78] as a predictor and the fourth order BDF scheme as a corrector. To the best of our knowledge, IMEX-PC have not been used to price financing options, except in [83] where a second order IMEX-PC is used to price American options.

In this chapter, we present a spectral method based on the Improved Lagrange formula to compute European, digital and butterfly spread options. Our method is coupled with the third order IMEX-PC for time integration. The reason of using higher order IMEX-PC is that we expect our spectral method to provide exponential accuracy which is normally affected due to lower order time integration schemes.

The rest of this chapter is organised as follows. In section 3.2, we describe option pricing formulation in the Black-Scholes framework. Section 3.3 proposes a spatial approximation of the pricing equations using rational spectral method. In Section 3.4, we review IMEX-PC methods for solving the semi-discrete system resulting from the spatial discretisation. The overall method is analysed in Section 3.5. Numerical experiments are conducted in Section 3.6, whereas in Section 3.7 we present a summary and some discussions.

3.2 The mathematical model

Consider the financial market model $\mathcal{M} = (\Omega, \mathcal{F}, \mathbb{P}, (\mathcal{F}_\tau)_{\tau \geq 0}, (S_\tau)_{\tau \geq 0})$ where Ω is the set of all possible outcomes of the experiment known as the sample space, \mathcal{F} is the set of all events, i.e. permissible combinations of outcomes, \mathbb{P} is a map $\mathcal{F} \longrightarrow [0, 1]$ which

assigns a probability to each event, \mathcal{F}_τ is a natural filtration, S_τ a risky underlying asset price process. The triplet $(\Omega, \mathcal{F}, \mathbb{P})$ is defined as a probability space. Let B_τ a \mathbb{P} -Brownian motion, $\sigma > 0$ the volatility of the underlying asset, $r > 0$ a risk-free interest rate and $\delta \geq 0$ a continuous dividend yield. Without loss of generality, we assume that both the risk-free interest rate and the dividend yield are constants. Then under the equivalent martingale measure \mathbb{Q} , the dynamics of the Black-Scholes model satisfies the stochastic differential equation

$$dS_\tau = (r - \delta)S_\tau d\tau + \sigma S_\tau dB_\tau. \quad (3.2.1)$$

Using the Ito's formula, we derive the following Black-Scholes PDE from the above equation

$$\frac{\partial V}{\partial t} = \frac{1}{2}\sigma^2 S^2 \frac{\partial^2 V}{\partial S^2} + (r - \delta)S \frac{\partial V}{\partial S} - rV, \quad (3.2.2)$$

where $t = T - \tau$. The boundary and the final conditions make the difference between American and European style options as well as between put and call and other types of options. In this chapter, we consider European vanilla, binary and spread options whose final and boundary conditions are given in section 3.6 where we provide numerical results.

3.3 Spectral space discretisation of the PDE

Using (1.2.6) and (1.2.7), the semi-discrete version of the Black-Scholes PDE (3.2.2) is given as

$$\frac{du}{dt} = Au + g(t, u), \quad u(0) = u_0. \quad (3.3.1)$$

where $t = T - \tau$, $u = V_{ii}$, $i = 2, \dots, N-1$, $u(t) = (u_1(t), \dots, u_N(t))^T$. The matrix $A = P_{ii}D_{ii}^{(2)}$ represents the stiff part of the Black-Scholes PDE and the function $g(u, t) = (Q_{ii}D_{ii}^{(1)} - rI_{ii})u + f(t)$ is the non-stiff part together with the boundary conditions f that depend on the underlying problem. Furthermore $P = \frac{1}{2}\sigma^2 \text{diag}(S^2)$ and $Q =$

$(r - \delta)\text{diag}(S)$ are $N \times N$ diagonal matrices.

For European call options, f is given by

$$f(t) = \left(P_{ii}D_{iN}^{(2)} + Q_{ii}D_{iN}^{(1)} - rI_{iN} \right) (S_{max}e^{-\delta t} - Ee^{-rt}), \quad (3.3.2)$$

whereas for European put option f , is as follows

$$f(t) = \left(P_{ii}D_{i1}^{(2)} + Q_{ii}D_{i1}^{(1)} - rI_{i1} \right) (Ee^{-rt}). \quad (3.3.3)$$

Note that for digital we have

$$f(t) = \left(P_{ii}D_{iN}^{(2)} + Q_{ii}D_{iN}^{(1)} - rI_{iN} \right) (\tilde{Q}e^{-rt}), \quad (3.3.4)$$

whereas for butterfly spread options, we have $f(t) = 0$.

3.4 Implicit-explicit predictor-corrector time discretisation

The system of ODEs (3.3.1) can be solved by means of standard ODE time integrators. The main challenge when dealing with this type of problems is that the explicit time integrators are inadequate because the diffusion term is typically stiff and necessitates excessively small time steps. On the other hand, the use of stiffly accurate implicit time integrators which are unconditionally stable are practically time consuming. In order to avoid these problems, it could be interesting to separate non-stiff and stiff terms. The non-stiff term has to be solved explicitly whereas the stiff term has to be integrated implicitly. Such time integrators are known as implicit-explicit (IMEX) time integrators and have been used for time integration of spatially discretised PDEs of reaction-diffusion type [115]. In this article, we use IMEX-PC methods to integrate the system of ODEs obtained after spatial discretisation of the PDE (3.2.2) mentioned

above.

Let us consider the system of ODEs (3.3.1) and let k be the time step-size and u_n the approximation of the solution at $t_n = kn$. Following the strategy of [6], we may write the general s -step IMEX method when applied to the system of ODEs (3.3.1) as

$$\sum_{j=0}^s a_j u_{n+j} = k \sum_{j=0}^s b_j A u_{n+j} + k \sum_{j=0}^{s-1} c_j g(t_{n+j}, u_{n+j}), \quad (3.4.1)$$

where $a_s \neq 0$. Following [95], the split form of (3.4.1) yields the following IMEX-PC:

The Predictor:

$$(a_s I - b_s A) \tilde{u}_{n+s} = \sum_{j=0}^{s-1} (-a_j u_{n+j} + k b_j A u_{n-j} + k c_j g(t_{n+j}, u_{n+j})). \quad (3.4.2)$$

The Corrector:

$$\begin{aligned} (a_s I - b_s A) u_{n+s} = & \sum_{j=0}^{s-1} (-a_j u_{n+j} + k b_j A u_{n-j} + k b_j g(t_{n+j}, u_{n+j})) \\ & + k b_s g(t_{n+s}, \tilde{u}_{n+s}). \end{aligned} \quad (3.4.3)$$

The above IMEX-PC uses the IMEX of [6] as the predictor and implicit schemes as the corrector. Only the nonlinear term is corrected; the corrector treats the linear term implicitly. This significantly reduces the computational cost compared with the general implicit methods. As compared to the PC method used in [83, 134], the present strategy does not require the use of iterative solvers.

We denote by $\text{IMEX-PC}(s, m)$ the s -step implicit-explicit predictor-corrector of order m . We also use some IMEX-PC schemes from [95] for nonlinear stiff differential equations.

IMEX-PC(1, m): The $\text{IMEX-PC}(1, m)$, a is family of 1-step, one parameter γ IMEX-PC schemes of order m and can be written as:

The Predictor:

$$(I - \gamma kA) \tilde{u}_{n+1} = [I + (1 - \gamma)A] u_n + kg(t_n, u_n). \quad (3.4.4)$$

The Corrector:

$$(I - \gamma kA) u_{n+1} = [I + (1 - \gamma)A] u_n + (1 - \gamma)kg(t_n, u_n) + \gamma kg(t_{n+1}, \tilde{u}_{n+1}), \quad (3.4.5)$$

where the parameter $0 \leq \gamma \leq 1$ prevents large truncation errors. The choice $\gamma = \frac{1}{2}$ yields a IMEX-PC(1,2) scheme.

IMEX-PC(2, m): The IMEX-PC(2, m), a family of 2-step, two parameter (γ, c) IMEX-PC IMEX schemes of order m can be written as:

The Predictor:

$$\begin{aligned} \left[\left(\gamma + \frac{1}{2} \right) I - \left(\gamma + \frac{c}{2} \right) kA \right] \tilde{u}_{n+1} = & [2\gamma I + (1 - \gamma - c)kA] u_n \\ & + \left[\left(\frac{1}{2} - \gamma \right) I + \frac{c}{2} kA \right] u_{n-1} \\ & + (\gamma + 1)kg(t_n, u_n) \\ & - \gamma kg(t_{n-1}, u_{n-1}). \end{aligned} \quad (3.4.6)$$

The Corrector:

$$\begin{aligned} \left[\left(\gamma + \frac{1}{2} \right) I - \left(\gamma + \frac{c}{2} \right) kA \right] \tilde{u}_{n+1} = & [2\gamma I + (1 - \gamma - c)kA] u_n \\ & + \left[\left(\frac{1}{2} - \gamma \right) I + \frac{c}{2} kA \right] u_{n-1} \\ & + \left(\gamma + \frac{c}{2} \right) kg(t_{n+1}, \tilde{u}_{n+1}) \\ & + (1 - \gamma - c)kg(t_n, u_n) \\ & + \frac{c}{2} kg(t_{n-1}, u_{n-1}). \end{aligned} \quad (3.4.7)$$

Choosing $(\gamma, c) = (0, 1)$ we obtain PC(2,3).

IMEX-PC(3, m): The IMEX-PC(3, m), a family of 3-step, two parameter (γ, θ, c) IMEX-PC of order m can be written as:

The Predictor:

$$\begin{aligned}
 \left[\left(\frac{1}{2} \gamma^2 + \gamma + \theta \right) I - \frac{k}{6} A \right] \tilde{u}_{n+1} = & \left[\left(\frac{3}{2} \gamma^2 + 2\gamma - \frac{1}{2} + \theta \right) I \right. \\
 & + \left(1 - \gamma^2 - 3c + \frac{23}{12} \theta \right) kA \Big] u_n \\
 & + \left[\left(-\frac{3}{2} \gamma^2 - \gamma + 1 \right) I \right. \\
 & + \left(\frac{\gamma^2 - \gamma}{2} + 3c - \frac{4}{3} \theta \right) kA \Big] u_{n-1} \\
 & + \left[\left(\frac{1}{2} \gamma^2 - \frac{1}{6} \right) I + \left(\frac{5}{12} \theta - c \right) kA \right] u_{n-2} \\
 & + \left(\frac{\gamma^2 + 3\gamma}{2} + 1 + \frac{23}{12} \theta \right) kg(t_n, u_n) \\
 & + \left(\gamma^2 + 2\gamma + \frac{4}{3} \theta \right) kg(t_{n-1}, u_{n-1}) \\
 & + \left(\frac{\gamma^2 + \gamma}{2} + \frac{5}{12} \theta \right) kg(t_{n-2}, u_{n-2}). \quad (3.4.8)
 \end{aligned}$$

The Corrector:

$$\begin{aligned}
 \left[\left(\frac{1}{2}\gamma^2 + \gamma + \theta \right) I - \frac{k}{6}A \right] \tilde{u}_{n+1} = & \left[\left(\frac{3}{2}\gamma^2 + 2\gamma - \frac{1}{2} + \theta \right) I \right. \\
 & + \left(1 - \gamma^2 - 3c + \frac{23}{12}\theta \right) kA \Big] u_n \\
 & + \left[\left(-\frac{3}{2}\gamma^2 - \gamma + 1 \right) I \right. \\
 & + \left(\frac{\gamma^2 - \gamma}{2} + 3c - \frac{4}{3}\theta \right) kA \Big] u_{n-1} \\
 & + \left[\left(\frac{1}{2}\gamma^2 - \frac{1}{6} \right) I + \left(\frac{5}{12}\theta - c \right) kA \right] u_{n-2} \\
 & + \left(\frac{\gamma^2 + \gamma}{2} + c \right) kg(t_{n+1}, \tilde{u}_{n+1}) \\
 & + \left(1 - \gamma^2 - 3c + \frac{23}{12}\theta \right) kg(t_n, u_n) \\
 & - \left(\frac{\gamma^2 - \gamma}{2} + 3c - \frac{4}{3}\theta \right) kg(t_{n-1}, u_{n-1}) \\
 & + \left(\frac{5}{12}\theta - c \right) kg(t_{n-2}, u_{n-2}). \tag{3.4.9}
 \end{aligned}$$

The choice $(\gamma, \theta, c) = (1, 0, 0)$ yields a IMEX-PC(3, 3) scheme.

3.5 Convergence and stability results for the implicit-explicit predictor-corrector methods

In [95], Li *et al.* gave the stability and convergence results for the IMEX-PC methods for solving stiff problems. We briefly recall those results for option pricing problems.

The order of accuracy of the present IMEX-PC is given by the following theorem.

Theorem 3.5.1 ([95]). *Let us suppose that the s -step IMEX predictor schemes (3.4.2) are of order p and that the corrector schemes (3.4.3) have order q . Therefore the resulting IMEX-PC is of order $\min\{p + 1, q\}$*

Proof see [95].

We would like to analyse the stability of IMEX-PC schemes (3.4.2) and (3.4.3) when applied to the PDE problem (3.2.2). It is beneficial to transform this PDE into a constant coefficient PDE by considering the transformation $x = \log(S/E)$, where E is the strike price. Therefore the PDE problem (3.2.2) becomes

$$\frac{\partial V}{\partial t} = b \frac{\partial^2 V}{\partial x^2} - a \frac{\partial V}{\partial x} - cV, \quad -\infty \leq x \leq \infty, \quad 0 \leq t \leq T, \quad (3.5.1)$$

where $b = \frac{1}{2}\sigma^2$, $a = -(r - \delta - \frac{1}{2}\sigma^2)$, $c = r$, V denotes the value of the European options, $t = T - \tau$ is the time to expiry and T is the expiration (maturity) time.

The first step is to find a spectral representation of this problem. To this end, we consider the following change of variable:

$$V(x, t) = e^{i\xi x} u(t). \quad (3.5.2)$$

The substitution of (3.5.2) into (3.5.1) yields the scalar test equation

$$u' = H(\xi)u(t) + G(\xi)u(t), \quad (3.5.3)$$

where $H(\xi) = -b\xi^2$ and $G(\xi) = -ia\xi - c$. Applying IMEX-PC methods (3.4.2) and (3.4.3) to the scalar test equation (3.5.3) with step size k we obtain

$$(a_s - kH(\xi)b_s)\tilde{u}_{n+s} = \sum_{j=0}^{s-1} [-a_j + kH(\xi)b_j + kG(\xi)c_j] u_{s+j}, \quad (3.5.4)$$

and

$$(a_s - kH(\xi)b_s)u_{n+s} = \sum_{j=0}^{s-1} [-a_j + kH(\xi)b_j + kG(\xi)b_j] u_{s+j} + kG(\xi)b_s\tilde{u}_{n+s}. \quad (3.5.5)$$

Substituting the variables $z = kH(\xi)$, $w = kG(\xi)$ and $R^n = u_n$, into the equations (3.5.4) and (3.5.5) and plugging (3.5.4) into (3.5.5) yields the following characteristic

equation

$$\varphi(R; z, w) = R^s - \sum_{j=0}^{s-1} \left[\frac{-a_j + zb_j + wb_j}{(a_s - zb_s)} + \frac{wb_s}{(a_s - zb_s)^2} (-a_j + zb_j + wc_j) \right] R^j. \quad (3.5.6)$$

Note that the IMEX-PC is linearly stable when all the roots of the characteristic polynomial (3.5.6) have modulus less than or equal to one. In other words, let $R_i(z, w)$, for $i = 1, 2, \dots, s$ be the roots of the characteristic polynomial, then we define the stability region S of the method as

$$S = \{(z, w) \in \mathbb{C}^2 : |R_i(z, w)| \leq 1, \forall i\}. \quad (3.5.7)$$

The root of the characteristic polynomial of the IMEX-PC(1,2) is given as

$$R(z, w) = \frac{1 - \gamma z + z + \gamma^2 z^2 - \gamma z^2 + w + \gamma w^2}{(1 - \gamma z)^2}. \quad (3.5.8)$$

For higher order PC methods, we do not provide general expressions of their characteristic polynomials. We rather confine our study to special cases. The choice $(\gamma, c) = (1, 0)$ gives the following characteristic polynomial

$$\left[z - \frac{3}{2} \right] R^2 + \left[2 + \frac{4w + wz + 4w^2}{3 - 2z} \right] R - \left[\frac{1}{2} + \frac{w + 2w^2}{3 - 2z} \right] = 0. \quad (3.5.9)$$

Similarly, the choice $(\gamma, \theta, c) = (1, 0, 0)$ for 3-steps PC gives

$$\left[\frac{11}{6} - z \right] R^3 - \left[3 + \frac{6w(3 + 3w)}{11 - 6z} \right] R^2 - \left[-\frac{3}{2} + \frac{6\mu(-3 - 6\mu)}{22 - 12\lambda} \right] R - \left[\frac{1}{3} + \frac{6\mu(2 + 6\mu)}{11 - 6\lambda} \right] = 0. \quad (3.5.10)$$

Figure 3.5.1 represents the stability region (3.5.7) for the schemes (3.4.2) and (3.4.3) in the $z - \omega$ plane.

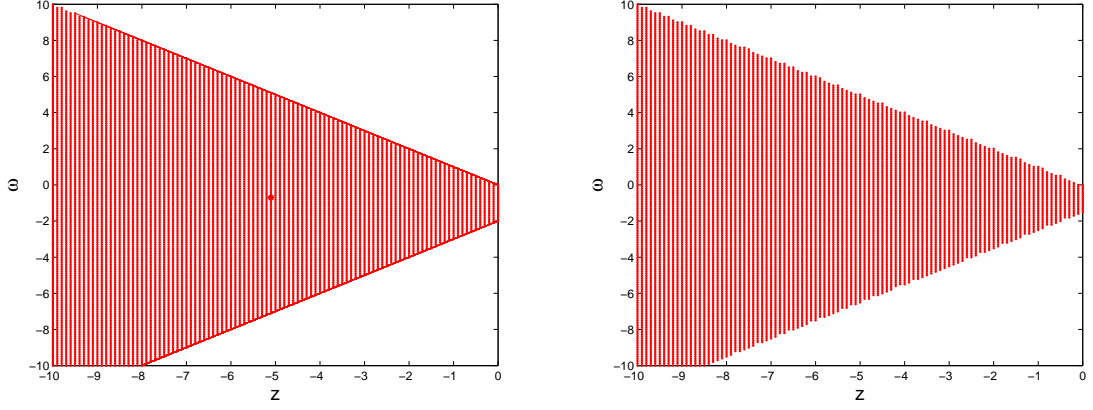


Figure 3.5.1: Stability regions of schemes (3.5.9) (left figure) and (3.5.10) (right figure)

3.6 Numerical results

In this section, we present some numerical results that we obtained by using the proposed approach. We consider European call, put, digital call and butterfly spread options.

3.6.1 Valuation of European call options

A European call option gives the holder the right to exercise the option at maturity time, T . To buy the underlying asset at maturity time T makes sense if the asset price is higher than the exercise price ($S > E$). One can buy the asset for E and sell it immediately on the market for S . If this is not the case, then the option is worthless. The value of a European call option can be determined by solving Equation (3.2.2) subject to the initial condition

$$V(S, 0) = \max(S - E, 0), \quad (3.6.1)$$

and the boundary conditions

$$\begin{aligned} V(0, t) &= 0, \\ V(S, t) &= Se^{-\delta t} - Ee^{-rt}, \quad \text{as } S \rightarrow \infty. \end{aligned} \quad (3.6.2)$$

The analytical solution of the Black-Scholes equation (3.2.2) for European call option is known [21, 140], and expressed as

$$V(S, t) = Se^{-\delta t} \mathcal{N}(d_1) - Ee^{-rt} \mathcal{N}(d_2), \quad (3.6.3)$$

where

$$d_1 = \frac{\ln\left(\frac{S}{E}\right) + \left(r - \delta + \frac{\sigma^2}{2}\right)t}{\sigma\sqrt{t}}, \quad d_2 = d_1 - \sigma\sqrt{t}, \quad (3.6.4)$$

and $\mathcal{N}(\cdot)$ is the cumulative probability distribution function for a standardised normal variable

$$\mathcal{N}(y) = \frac{1}{\sqrt{2\pi}} \int_{-\infty}^y e^{-\frac{x^2}{2}} dx. \quad (3.6.5)$$

Numerical results are obtained with $T = 0.5, 1$ and 2 years as maturity time with $S_{\min} = 0$ and $S_{\max} = 200$ with strike price $E = 45$. The number of space mesh points is $N = 80$ and the other parameters are as indicated in the Table 3.6.1 to 3.6.5 . The accuracy of the present method was measured by means of the maximum error

$$L_{\infty} = \max_{i=1, \dots, N} |u_i - V_i|, \quad (3.6.6)$$

and the root mean square error

$$L_2 = \sqrt{\frac{1}{N} \sum_{i=1}^N (u_i - V_i)^2}, \quad (3.6.7)$$

where N is the number of points used in the discretisation in one particular direction, V_i is the exact solution of the Black-Scholes equation (3.6.3), u_i is the numerical ap-

proximation to the exact solution of the Black-Scholes equation. We evaluate the value of the European option by finite difference (FD) using uniform grids, and barycentric Lagrange collocation (BLC) using the Chebyshev-Gauss-Lobatto (CGL) points for various option parameters. The results are displayed in Table 3.6.1.

Table 3.6.1: Comparison of European call option valuation using barycentric Lagrange collocation (BLC) with Chebyshev Gauss Labatto (CGL) points and finite difference method (FD) with uniform grid points.

| Schemes | T=0.5 | | T=1 | | T=2 | |
|--|------------|------------|------------|------------|------------|------------|
| | L_2 | L_∞ | L_2 | L_∞ | L_2 | L_∞ |
| Parameters: $r = 0.05$, $\sigma = 0.2$, $\delta = 0.00$ | | | | | | |
| FD | 1.9265(-3) | 7.5269(-3) | 1.7084(-3) | 6.2297(-3) | 1.5913(-3) | 5.4520(-3) |
| BLC | 1.8753(-3) | 9.3260(-3) | 1.5087(-3) | 6.3006(-3) | 1.1892(-3) | 4.1491(-3) |
| Parameters: $r = 0.07$, $\sigma = 0.04$, $\delta = 0.03$ | | | | | | |
| FD | 7.2924(-3) | 6.1838(-2) | 1.1283(-2) | 7.2901(-2) | 1.3508(-2) | 8.5026(-2) |
| BLC | 8.2255(-3) | 6.1964(-2) | 4.8242(-3) | 4.4339(-2) | 3.0501(-3) | 2.2628(-2) |
| Parameters: $r = 0.1$, $\sigma = 0.3$, $\delta = 0.05$ | | | | | | |
| FD | 1.4858(-3) | 4.5463(-3) | 1.2127(-3) | 3.2754(-3) | 9.7763(-4) | 2.3725(-3) |
| BLC | 1.4758(-3) | 5.8705(-3) | 1.1751(-3) | 3.9176(-3) | 9.3080(-4) | 2.4952(-3) |

Table 3.6.2: Comparison of European call option valuation using barycentric Lagrange collocation (BLC) with transformed Chebyshev Gauss Labatto (CGL) points and finite difference method (FD) with non-uniform grid points.

| Schemes | T=0.5 | | T=1 | | T=2 | |
|--|------------|------------|------------|------------|------------|------------|
| | L_2 | L_∞ | L_2 | L_∞ | L_2 | L_∞ |
| Parameters: $r = 0.05$, $\sigma = 0.2$, $\delta = 0.00$ | | | | | | |
| FD | 6.8107(-4) | 1.4774(-3) | 1.2556(-3) | 2.6516(-3) | 2.3119(-3) | 4.5751(-3) |
| BLC | 3.0696(-9) | 8.8089(-9) | 4.6061(-9) | 1.3591(-8) | 1.0053(-8) | 3.6679(-8) |
| Parameters: $r = 0.07$, $\sigma = 0.04$, $\delta = 0.03$ | | | | | | |
| FD | 1.9240(-3) | 8.2068(-3) | 2.3690(-3) | 7.6678(-3) | 3.3822(-3) | 7.1610(-3) |
| BLC | 4.0924(-8) | 1.7177(-7) | 6.9650(-8) | 3.2579(-7) | 1.5729(-7) | 6.5362(-7) |
| Parameters: $r = 0.1$, $\sigma = 0.3$, $\delta = 0.05$ | | | | | | |
| FD | 4.2991(-4) | 8.1881(-4) | 7.2360(-4) | 1.3072(-3) | 1.1133(-3) | 1.8128(-3) |
| BLC | 2.8688(-9) | 1.1267(-8) | 6.1628(-9) | 2.5323(-8) | 8.1796(-9) | 3.8962(-8) |

Although in theory and for a range of practical problems, it has been shown and observed that in general spectral methods have higher accuracy than finite difference methods [25, 59, 60], one can observe from Table 3.6.1 that the BLC has a moderately

Table 3.6.3: Comparison of European put option valuation using barycentric Lagrange collocation (BLC) with transformed Chebyshev Gauss Labatto (CGL) points and finite difference method (FD) with uniform grid points.

| Schemes | T=0.5 | | T=1 | | T=2 | |
|--|------------|------------|------------|------------|------------|------------|
| | L_2 | L_∞ | L_2 | L_∞ | L_2 | L_∞ |
| <i>Parameters: $r = 0.05$, $\sigma = 0.2$, $\delta = 0.00$</i> | | | | | | |
| FD | 1.8853(-4) | 3.9139(-4) | 3.6984(-4) | 9.5309(-4) | 7.8517(-4) | 2.1599(-3) |
| BLC | 3.4402(-9) | 9.4734(-9) | 2.8691(-9) | 1.0938(-8) | 6.7411(-9) | 3.6676(-8) |
| <i>Parameters: $r = 0.07$, $\sigma = 0.04$, $\delta = 0.03$</i> | | | | | | |
| FD | 1.7707(-3) | 7.7987(-3) | 1.8909(-3) | 7.4343(-3) | 2.0736(-3) | 7.4714(-3) |
| BLC | 4.0791(-8) | 1.7180(-7) | 6.9573(-8) | 3.2570(-7) | 1.5726(-7) | 6.5359(-7) |
| <i>Parameters: $r = 0.1$, $\sigma = 0.3$, $\delta = 0.05$</i> | | | | | | |
| FD | 2.8525(-4) | 5.9174(-4) | 5.0501(-4) | 1.3007(-3) | 8.1141(-4) | 2.2758(-3) |
| BLC | 2.6238(-9) | 8.3153(-9) | 6.0125(-9) | 1.1213(-8) | 6.1796(-9) | 1.4678(-8) |

smaller error than that of the FD. Numerically, higher order methods, in particular spectral methods have difficulty in approximating accurately the solution in the region of singularity, i.e., the region of dramatic change. In the present case, the first derivative of the initial condition is discontinuous at the strike price E . As a result, the BLC method cannot be significantly superior to FD as far as the accuracy is concerned.

In order to improve the accuracy of the BLC methods, we use resolution grids in the region of dramatic change. We use the transformation (1.2.31) to increase the number of points in the region around the strike price $S = E$. Therefore, from Table 3.6.2, we observe a significant improvement of BLC method when concentrating more grid points near strike price, while with FD method, the improvement is moderate. This is because high resolution grids in the region of singularity E allows the BLC to capture the rapid change in option price, while in the region of low change of the option price, the BLC method gives very accurate results for a small number of grid points.

In Figure 3.6.1, we illustrate the convergence of the IMEX-PC(1,m) with the choice $\gamma = 1/2$, IMEX-PC(2,m) with the choice $(\gamma, c) = (1, 0)$, and IMEX-PC(3,m) with the choice $(\gamma, \theta, c) = (1, 0, 0)$ at time $T = 0.5$, using the following parameters $S_{\min} = 0$, $S_{\max} = 200$, $r = 0.2$, $\sigma = 0.3$, $\delta = 0.0$ and $E = 45$, $N = 200$ and $\alpha = 2 \times 10^4$. One observes that the IMEX-PC(3,3) has the best convergence compared to the IMEX-

Table 3.6.4: Comparison of European digital call option valuation using barycentric Lagrange collocation (BLC) with transformed Chebyshev Gauss Labatto (CGL) points and finite difference method (FD) with uniform grid points.

| Schemes | T=0.5 | | T=1 | | T=2 | |
|--|------------|------------|------------|------------|------------|------------|
| | L_2 | L_∞ | L_2 | L_∞ | L_2 | L_∞ |
| <i>Parameters: $r = 0.05$, $\sigma = 0.2$, $\delta = 0.00$</i> | | | | | | |
| FD | 6.6648(-3) | 2.9135(-2) | 5.4136(-3) | 1.9930(-2) | 4.2782(-3) | 1.3269(-2) |
| BLC | 9.6328(-6) | 1.3466(-5) | 8.0988(-6) | 1.1035(-5) | 4.9873(-6) | 6.6544(-6) |
| <i>Parameters: $r = 0.07$, $\sigma = 0.04$, $\delta = 0.03$</i> | | | | | | |
| FD | 2.5120(-2) | 2.4646(-1) | 1.9574(-2) | 1.5775(-1) | 1.4467(-2) | 1.1473(-1) |
| BLC | 3.2479(-5) | 6.2697(-5) | 1.9218(-5) | 4.2730(-5) | 9.6899(-6) | 2.7942(-5) |
| <i>Parameters: $r = 0.1$, $\sigma = 0.3$, $\delta = 0.05$</i> | | | | | | |
| FD | 5.2655(-3) | 1.8233(-2) | 4.2214(-3) | 1.2180(-2) | 3.2368(-3) | 7.7694(-3) |
| BLC | 6.0569(-6) | 8.1388(-6) | 1.9365(-6) | 2.5231(-6) | 3.2007(-6) | 1.6415(-5) |

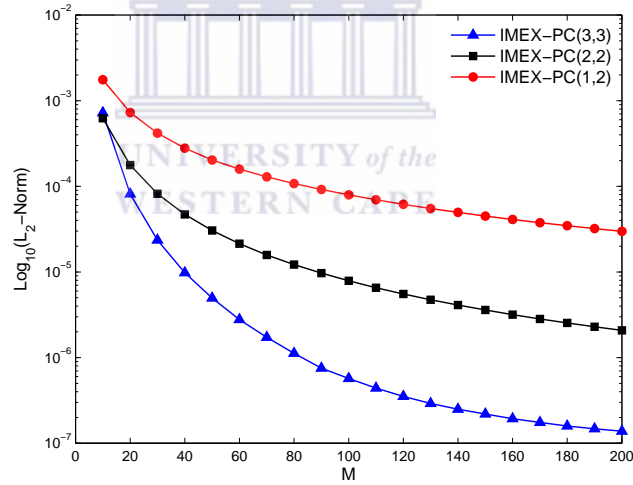


Figure 3.6.1: Performance of different IMEX-PC method for pricing European call options with $N = 200$, $r = 0.1$, $\sigma = 0.2$, $\delta = 0.0$, $E = 45$ and $\alpha = 2 \times 10^5$ at $T = 0.5$.

PC(1,2) and the IMEX-PC(2,2). It converges with order 3, while the other two methods are only second order accurate. Therefore in the remaining of this chapter, we use the IMEX-PC(3,3) as time integrating method.

Figure 3.6.2 illustrates the convergence of the mapped BLC method for different values of α . It can be seen that the mapped BLC converges much better than the FD method. Different values of the parameter α leads to different accuracy. The choice

Table 3.6.5: Comparison of European butterfly spread option valuation using barycentric Lagrange collocation (BLC) with transformed Chebyshev Gauss Labatto (CGL) points and finite difference method (FD) with uniform grid points.

| Schemes | T=0.5 | | T=1 | | T=2 | |
|--|------------|------------|------------|------------|------------|------------|
| | L_2 | L_∞ | L_2 | L_∞ | L_2 | L_∞ |
| <i>Parameters: $r = 0.05$, $\sigma = 0.2$, $\delta = 0.00$</i> | | | | | | |
| FD | 1.0574(-2) | 4.3091(-2) | 8.6844(-3) | 3.1513(-2) | 6.4097(-3) | 1.9811(-2) |
| BLC | 2.3652(-6) | 5.2302(-6) | 2.0773(-6) | 3.8961(-6) | 2.5712(-5) | 1.3077(-4) |
| <i>Parameters: $r = 0.07$, $\sigma = 0.04$, $\delta = 0.03$</i> | | | | | | |
| FD | 3.2409(-2) | 2.8985(-1) | 3.1689(-2) | 2.1213(-1) | 3.3502(-2) | 1.7927(-1) |
| BLC | 1.0341(-6) | 3.4514(-6) | 7.1643(-6) | 3.9076(-6) | 6.2304(-5) | 2.4926(-4) |
| <i>Parameters: $r = 0.1$, $\sigma = 0.3$, $\delta = 0.05$</i> | | | | | | |
| FD | 8.0303(-3) | 2.8515(-2) | 6.0627(-3) | 1.7545(-2) | 2.5792(-2) | 9.2620(-2) |
| BLC | 4.6265(-6) | 2.4136(-5) | 1.1158(-6) | 5.6118(-6) | 2.1265(-5) | 9.2620(-5) |

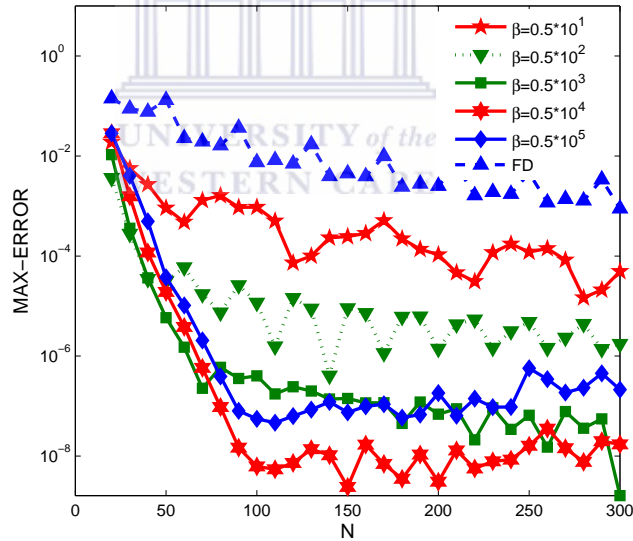


Figure 3.6.2: Convergence of the mapped BLC method for European call options with $M = 1000$, $S_{\min} = 0$, $S_{\max} = 200$, $r = 0.1$, $\sigma = 0.2$, $\delta = 0.0$, $E = 45$, $T = 0.5$

$\alpha = 2 \times 10^1$ displays the worst accuracy, but still very satisfactory results as compared to FD method. The smaller the α is, the better is the accuracy, because then more points are clustered near the strike price E . However, we find that $\alpha = 2 \times 10^4$ gives better accuracy than $\alpha = 2 \times 10^5$. The main reason is that there are not enough points left away from the region of regularity and therefore $\alpha = 2 \times 10^4$ seems to be the

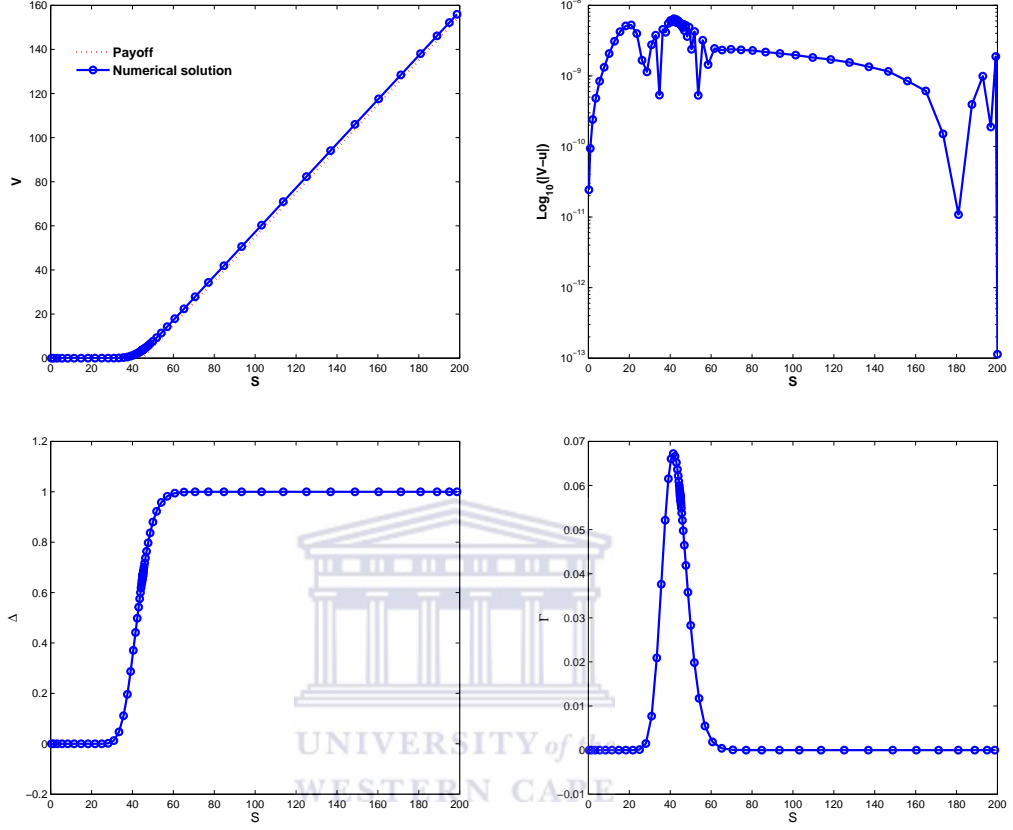


Figure 3.6.3: Valuation of the European call options (top left), its Error (top right), Δ (bottom left) and Γ (bottom right) using the the barycentric Lagrange collocation (BLC) method with $M = 1000$, $N = 80$, $S_{\min} = 0$, $S_{\max} = 200$, $r = 0.1$, $\sigma = 0.2$, $\delta = 0.0$, $E = 45$, $T = 0.5$.

optimal choice for valuing European call and put options. In the experiments below, we chose $\alpha = 2 \times 10^4$.

3.6.2 Valuation of European put options

Given the value of a call option, it is possible to compute the value of the corresponding put option via the put-call-parity [89]. However, puts and calls do not always share the same properties. Therefore, we also need to evaluate European put options by our approach.

The value of an European put can be computed numerically by solving the PDE

(3.2.2) subject to the initial condition

$$V(S, 0) = \max(E - S, 0), \quad (3.6.8)$$

and the boundary conditions

$$\begin{aligned} V(0, t) &= Ee^{-rt}, \\ V(S, t) &= 0 \quad \text{as } S \rightarrow \infty. \end{aligned} \quad (3.6.9)$$

The benchmark solution used to validate our numerical scheme is the analytic solution of the Black-Scholes equation (3.2.2) given by

$$Ee^{-rt}\mathcal{N}(-d_2) - Se^{-\delta t}\mathcal{N}(d_1) \quad (3.6.10)$$

where d_1, d_2 are defined in (3.6.4) and N is the cumulative normal distribution defined in (3.6.5).

The procedure of discretisation is similar to what has been used to evaluate the European call except that the function V_0 and the boundary f of equation (3.3.1) are given by

$$V_0 = \max(S_i - E, 0) \quad (3.6.11)$$

$$f = \left(P_{ii}D_{i1}^{(2)} + Q_{ii}D_{i1}^{(1)} - rI_{i1} \right) (Ee^{-rt}) \quad (3.6.12)$$

where $i = 2, \dots, N - 1$, the matrices $P, Q, I, D^{(1)}$ and $D^{(2)}$ are as those previously defined in the case of European call.

We use the same set of parameters as in the valuation European call options. The results are presented in Table 3.6.3. It can be seen that the conclusions are similar to those of European call options. Therefore, our approach is consistent, i.e., the approach using the grid refinement at strike price is found to perform significantly better than

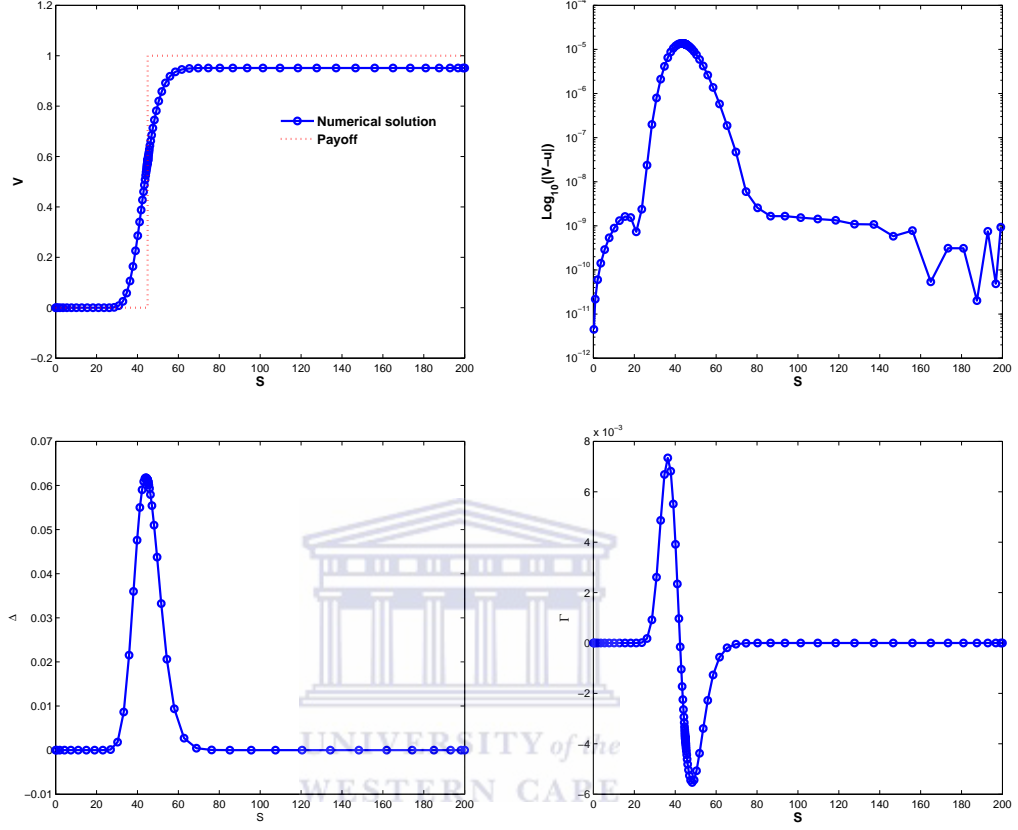


Figure 3.6.4: Valuation of the European digital call options (top left), its Error (top right), Δ (bottom left) and Γ using the the barycentric Lagrange collocation (BLC) method with $M = 1000$, $S_{\min} = 0$, $S_{\max} = 200$, $r = 0.1$, $\sigma = 0.2$, $\delta = 0.0$, $E = 45$, $T = 0.5$.

FD method in term of accuracy for valuating European option pricing problems.

Now, we investigate the utility of our approach to price exotic options, namely European binary and spread options.

3.6.3 Valuation of European digital call options

Another type of option that we are dealing within this chapter is the digital call option. This option belongs to the class of exotic options. Such contracts are traded between a financial institution (say, bank) and a customer and not at exchanges. A digital call option, also known as cash-or-nothing call or binary option, is an option with payoff

zero before the strike price and one (or any fixed amount) after the strike price. As an example of these options, we solve the Black-Scholes PDE (3.2.2) model with the payoff function given as

$$V(S, 0) = \begin{cases} 1, & \text{for } S \geq E \\ 0, & \text{for } S \leq E \end{cases} \quad (3.6.13)$$

with the following boundary conditions

$$\begin{aligned} V(0, t) &= 0, \\ V(S, t) &= e^{-rt} \text{ as } S \rightarrow \infty. \end{aligned} \quad (3.6.14)$$

The analytic solution for the digital option is

$$V(S, t) = e^{-rt} \mathcal{N}(d_2) \quad (3.6.15)$$

where d_2 is defined in (3.6.4). The discontinuous initial conditions for digital options are susceptible to cause numerical oscillations of the Greeks when time integrators such as Crank Nicolson methods are used. However, our approach produces non oscillatory behaviour of the Greeks. Figure 3.6.4 represents the numerical solution for the digital call option together with its Δ , Γ and numerical error. All these results are very satisfactory and free of oscillations. We also investigate the maximum error and the root mean square error for different maturity times and different parameters as chosen in the previous experiments. All the results are very good.

3.6.4 Valuation of Butterfly spread options

The Butterfly Spread is a combination of four options. Two long position calls with exercise price E_1 and E_3 and two short position calls with exercise price $E_2 = (E_1 + E_3)/2$. The value of a European butterfly spread call option can be determined by

solving Equation (3.2.2) subject to the initial condition

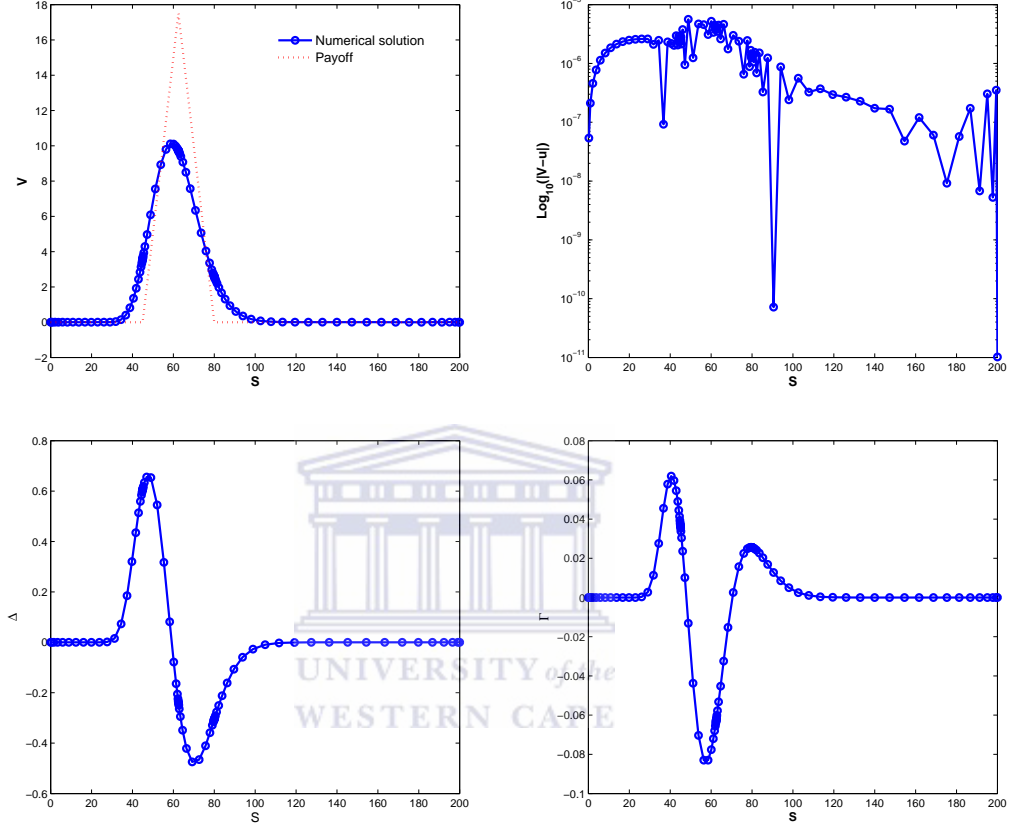


Figure 3.6.5: Valuation of butterfly spread option by the barycentric Lagrange collocation (BLC) method with $M = 1000$, $S_{\min} = 0$, $S_{\max} = 200$, $r = 0.1$, $\sigma = 0.2$, $\delta = 0.0$, $E_1 = 45$, $E_3 = 80$, $T = 0.5$.

$$V(S, 0) = \max(S - E_1) - 2 \max(S - E_2) + \max(S - E_3), \quad (3.6.16)$$

and the boundary conditions

$$V(S, t) = 0 \text{ as } S \rightarrow 0; \quad V(S, t) = 0 \text{ as } S \rightarrow \infty. \quad (3.6.17)$$

In this particular case, we need to stretch grid points at three different strike prices in order to improve the accuracy of the BLC method. The suitable map is chosen from (1.2.35) with the grid stretching parameters are $\alpha_1 = \alpha_2 = \alpha_3 = 2 \times 10^3$.

Very accurate results are obtained for different values of option parameters for different expiry times. Figure 3.6.5 displays numerical values of the butterfly spread option, together with its Δ , Γ and its error with $N = 100$, $S_{\min} = 0$, $S_{\max} = 200$, $r = 0.1$, $\sigma = 0.2$, $\delta = 0.0$, $E_1 = 45$, $E_3 = 80$ at $T = 0.5$. To ensure that the error is dominated by the spatial discretisation, we choose $M = 1000$. All the results are satisfactory and free of oscillations. To further investigate the accuracy of the mapped BLC method for pricing butterfly spread options, we compare the results with those obtained by using the FD method. The results are presented in Table 3.6.5.

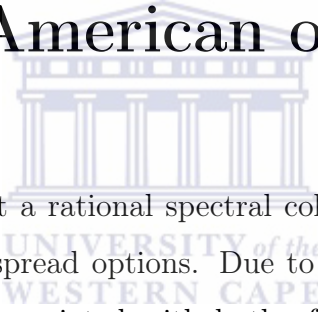
3.7 Summary and discussions

We have considered a barycentric Lagrange discretisation in space in combination with the third order IMEX-PC time marching method for pricing European vanilla, digital and butterfly spread options. Extensive comparisons are carried out with standard finite difference (FD) scheme. The error using the barycentric Lagrange discretisation appears to be very small as compared to the standard finite difference (FD) scheme. Furthermore, we achieve significantly higher order accuracy using coordinate transformations that stretch points around the strike price. Results show that our method is very accurate and reliable in pricing the class of options indicated in this chapter.

In the next chapter, we extend our rational spectral method to solve a class of American style options.

Chapter 4

Rational spectral collocation method for pricing American options



In this chapter, we present a rational spectral collocation method for pricing American vanilla and butterfly spread options. Due to the early exercise possibilities, free boundary conditions are associated with both of these PDEs. The problem is first reformulated as a variational inequality. Then, by adding a penalty term, the resulting variational inequality is transformed into a nonlinear advection-diffusion-reaction equation on fixed boundaries. This nonlinear PDE is discretised in asset (space) direction by means of rational interpolation using suitable barycentric weights and transformed Chebyshev points. This gives a system of stiff nonlinear ODEs which is then integrated using the implicit forth-order Lobatto time integration method. We carry out extensive comparisons with other results obtained by using some existing methods found in literature.

4.1 Introduction

Among a huge variety of financial derivative securities traded in exchange markets such as call or put on dividend paying stocks, foreign currency options, callable bonds and others, American options are the most traded [140]. American options give their holder

the right but not the obligation to exercise or exit the contract by the expiration date mentioned in the contract. This added freedom makes American options the most attractive to investors as compared to other derivatives of similar types. However they are more difficult to price than the European options which can only be exercised at expiration. In fact, analytical solutions of American Black-Scholes PDE models are rarely found in acceptable form, and therefore one has to resort to numerical methods in order to solve such problems.

American option pricing problems can be reformulated as a differential linear complementary problem (LCP)[140]. The main challenge with the LCP resides in tracking the location of the early exercise boundary. There are two main ways to track the location of the early exercise boundary. One simple approach in addressing the early exercise condition is to advance the discrete solution in time step ignoring the constraint, and then to apply the constraint explicitly as described in Brennan and Schwartz [27]. The drawback of this approach is that the solution is in an inconsistent state at the beginning of each of the time steps and thus affects the convergence of the method. Another approach is to track the early exercise boundary explicitly, for example, the LCP of Borici and Luthi [22, 23], the LCP of Dempster *et al.* [52] and the methods based on front-fixing transformations [105, 145]. The problem with this second approach is that the early exercise boundary moves with an infinite speed at maturity, making estimations difficult.

Recently, Forsyth and Vetzal [61] proposed a penalty method to solve American options. The main idea is to alter the set of variational inequalities into a set of nonlinear partial differential equations through the penalisation. The major benefit of the penalty method is that it can be generalised to a variety of financial contracts including multi-dimensional problems. In this paper, we will use this approach and discretise the nonlinear PDE in space using rational spectral collocation method.

In this chapter, we present a rational spectral collocation method using the penalty approach for pricing American vanilla and butterfly spread options.

The rest of this chapter is organised as follows. In Section 4.2, we describe option

pricing formulation in the Black-Scholes framework. Section 4.3 considers the spatial approximations of the pricing equations using the rational spectral collocation method. Numerical experiments are presented in Section 4.4, and in Section 4.5 we present the summary and discussions.

4.2 The mathematical model

Consider a financial market model $\mathcal{M} = (\Omega, \mathcal{F}, \mathbb{P}, (\mathcal{F}_\tau)_{\tau \geq 0}, (S_\tau)_{\tau \geq 0})$ where Ω is the set of all possible outcomes of the experiment known as the sample space, \mathcal{F} is the set of all events, i.e., permissible combinations of outcomes, \mathbb{P} is a map $\mathcal{F} \rightarrow [0, 1]$ which assigns a probability to each event, \mathcal{F}_τ is a natural filtration and S_τ a risky underlying asset price process. The triplet $(\Omega, \mathcal{F}, \mathbb{P})$ is defined as a probability space.

Let B_τ be a \mathbb{P} -Brownian motion, $\sigma > 0$ the volatility of the underlying asset, $r > 0$ a risk-free interest rate and $\delta \geq 0$ a continuous dividend yield. Without loss of generality, we assume that both the risk-free interest rate and the dividend yield are constants. Then under the equivalent martingale measure \mathbb{Q} , the dynamics of the Black-Scholes model satisfies the stochastic differential equation

$$dS_\tau = (r - \delta)S_\tau d\tau + \sigma S_\tau dB_\tau. \quad (4.2.1)$$

Using Ito's formula the above equation leads to the following Black-Scholes PDE

$$\frac{\partial V}{\partial t} = \frac{1}{2}\sigma^2 S^2 \frac{\partial^2 V}{\partial S^2} + (r - \delta)S \frac{\partial V}{\partial S} - rV, \quad (4.2.2)$$

where $t = T - \tau$. The boundary and the final conditions make the difference between American and European style options as well as between put and call and other types of options. Note also that American options represent its European counterparts adding the early exercise premium as shown by Wilmott *et al.* [54]. In view of all these facts,

for American put options, one obtains the following free boundary-values problem

$$\left. \begin{aligned} V_t &= L_{BS}V, \quad S_f(t) \leq S < \infty, \quad 0 \leq t \leq T, \\ V(S, 0) &= \max(E - S, 0), \\ \lim_{S \rightarrow \infty} V(S, t) &= 0, \\ V(S, 0) &= \max(E - S, 0), \\ V(S_f(t), t) &= E - S_f(t), \\ \frac{\partial V}{\partial S}(S_f(t), t) &= -1, \end{aligned} \right\} \quad (4.2.3)$$

where T the expiry time, and

$$L_{BS} \equiv \frac{1}{2} \sigma^2 S^2 \frac{\partial^2}{\partial S^2} + (r - \delta) S \frac{\partial}{\partial S} - r.$$

The problem (4.2.3) can be formulated as a linear complementarity problem (LCP)[148]:

$$\left. \begin{aligned} V_t - L_{BS}V &\geq 0, \\ V(S, t) - V^*(S) &\geq 0, \\ (V_t - L_{BS}V)(V(S, t) - V^*(S)) &= 0, \\ V(S, 0) &= \max(E - S, 0), \\ \lim_{S \rightarrow \infty} V(S, t) &= 0, \end{aligned} \right\} \quad (4.2.4)$$

where V is the value of the option and V^* denotes its exercise value. In next section, we proposed a spectral discretisation based on a penalty approach to solve the American vanilla and butterfly spread option problems.

4.3 Spectral space discretisation of the nonlinear PDE

We first transform the variational inequality (4.2.4) into a nonlinear partial differential equation on a fixed domain by adding a penalty term. We follow the approach in [61] and construct a penalty method to approximate the American option problem on a

single asset in terms of a nonlinear PDE as

$$\left. \begin{aligned} \frac{\partial V_\epsilon}{\partial \tau} &= L_{BS} V_\epsilon + \frac{1}{\epsilon} [V_\epsilon(S, t) - V_\epsilon^*(S)]^+, \quad S_m \leq S \leq S_M, \quad 0 \leq t \leq T, \\ V_\epsilon(S, 0) &= V_\epsilon^*(S) = \max(E - S, 0), \\ (V_t - L_{BS} V)(V(S, t) - V^*(S)) &= 0, \\ V_\epsilon(S_m, t) &= E, \\ V_\epsilon(S_M, t) &= 0, \end{aligned} \right\} \quad (4.3.1)$$

where $0 < \epsilon \ll 1$ is the penalty constant and $[V_\epsilon(S, t) - V_\epsilon^*(S)]^+ = \max(V_\epsilon(S, t) - V_\epsilon^*(S), 0)$ is the penalty term. To the best of our knowledge, most of the schemes used to value American options using the penalty term are finite difference, finite element and finite volume methods. However, our method in this chapter is based on a rational spectral collocation method which is partly described in Chapter 1.

We apply the method of lines and discretise the problem first in space and then in time. One of the advantages of this methodology is that the underlying PDE is transformed into a system of ODEs which can easily be solved using efficient ODEs solvers. We discretise the asset value by means of rational Chebyshev collocation method. Let $x = g(y_j)$ be the transformed Chebyshev points, chosen from (1.2.18) and (1.2.22) for American vanilla and butterfly spread options, respectively. The first step is to transform $x \in [-1, 1]$ into $S \in [S_m, S_M]$ that better suits the option problems at hand as $x = (2S - (S_M + S_m))/(S_M - S_m)$. Now writing $V_\epsilon(S, t) = u(x, t)$, the PDE (4.3.1) together with its initial and boundary conditions yields

$$\left. \begin{aligned} u_t &= \frac{1}{2} \sigma^2 S^2 \left(\frac{2}{S_M - S_m} \right)^2 u_{xx} + (r - \delta) S \left(\frac{2}{S_M - S_m} \right) u_x + ru + \frac{1}{\epsilon} [u - u^0]^+, \\ u(x, 0) &= \max(E - S, 0), \quad -1 \leq x \leq 1, \quad S_m \leq S \leq S_M, \\ u(-1, t) &= E - S_m, \quad u(1, t) = 0, \quad 0 \leq t \leq T. \end{aligned} \right\} \quad (4.3.2)$$

The rational collocation method can be obtained by replacing the solution u into (4.3.2)

with

$$\tilde{u}(x) = \sum_{j=0}^N \tilde{u}_j L_j^{(\omega)}(x), \quad (4.3.3)$$

and collocating at $N - 1$ points x_1, \dots, x_{N-1} . This yields the following system of nonlinear ODEs for \tilde{u}_i

$$\begin{aligned} \tilde{u}_{i,t} &= p(x_i) \sum_{j=0}^N \tilde{u}_j L_j^{(\omega)''}(x_i) + q(x_i) \sum_{j=0}^N \tilde{u}_j L_j^{(\omega)'}(x_i) + r\tilde{u}_i + f(\tilde{u}_i), \\ \tilde{u}_0 &= \tilde{u}(-1, t), \quad \tilde{u}_N = \tilde{u}(1, t), \end{aligned} \quad (4.3.4)$$

where

$$p(x_i) = \frac{1}{2} \sigma^2 S_i^2 \left(\frac{2}{S_M - S_m} \right)^2, \quad q(x_i) = (r - \delta) S_i \left(\frac{2}{S_M - S_m} \right), \quad f(\tilde{u}_i) = \frac{1}{\epsilon} [\tilde{u}_i - \tilde{u}_i^0]^+.$$

In order to write the expression (4.3.4) in matrix form, we introduce the following matrix and vector notations

$$\begin{aligned} \tilde{\mathbf{u}} &= [\tilde{u}_1, \tilde{u}_2, \dots, \tilde{u}_{N-1}]^T, \\ D^{(1)} &= \left(D_{ij}^{(1)} \right), \quad D_{ij}^{(1)} = L_j^{(\omega)'}(x_i); \quad i, j = 1, 2, \dots, N-1, \\ D^{(2)} &= \left(D_{ij}^{(2)} \right), \quad D_{ij}^{(2)} = L_j^{(\omega)''}(x_i); \quad i, j = 1, 2, \dots, N-1, \\ P &= \text{diag}(p(x_i)), \quad Q = \text{diag}(q(x_i)); \quad i = 1, 2, \dots, N-1, \\ \mathbf{g} &= \left[f(u_i) + \left(p(x_i) D_{i0}^{(2)} + q(x_i) D_{i0}^{(1)} + r I_{i0} \right) \tilde{u}_0 + \left(p(x_i) D_{iN}^{(2)} + q(x_i) D_{iN}^{(1)} + r I_{iN} \right) \tilde{u}_N \right]^T, \end{aligned} \quad (4.3.5)$$

where $i = 1, 2, \dots, N-1$ and I is a $(N+1) \times (N+1)$ identity matrix.

Consequently, (4.3.4) can be expressed as a nonlinear initial value problem of the form

$$\frac{d\tilde{\mathbf{u}}}{dt} = A\tilde{\mathbf{u}} + \mathbf{g}, \quad (4.3.6)$$

with $A = PD^{(2)} + QD^{(1)} - rI$. The main difficulty when dealing with the system of the kind (4.3.6) is that the use of explicit time integrators is not efficient because the system

suffers from stiffness as the mesh in the asset direction is refined. Consequently, the time step must be significantly smaller in order to fulfill the drastic stability condition present in explicit time integrators. As a remedy, we employ implicit time integrators which are more stable. We use forth-order Lobatto method [68] for time integration with adaptive time stepping.

4.4 Numerical results

In this section, we present numerical results of the rational collocation method to price American vanilla put and butterfly spread options. We have tested the method for several sets of realistic parameters. Here, we present the results obtained for particular values given in Table 4.4.1 and 4.4.4. Note that similar conclusions are reported for other sets of parameters. In all numerical experiments, unless otherwise indicated, we choose the grid stretching parameter as $\alpha = 20$ and truncate the computational domain in such a way that $S_m = 0$ and $S_M = 200$.

4.4.1 Valuation of American put options

As a first example, we consider the case of an American put option. Table 4.4.1 presents the data used for this example. In order to illustrate the utility of our rational spectral collocation method based on the penalty approach, two experiments are performed. As a benchmark solution, we take the value of the options obtained by using the penalty method in [61] with 50000 time and space grid points. The first experiment checks the behaviour of the method with respect to the penalty parameter ϵ . In this experiment, we take an absolute and relative error tolerances of the implicit forth-order Lobatto method to be 10^{-5} .

Table 4.4.1: Data used to value American put options.

| Parameters | r | σ | δ | E | T |
|------------|------|----------|----------|-----|-----|
| Values | 0.05 | 0.20 | 0.00 | 100 | 0.5 |

Table 4.4.2 shows the results of American put options obtained by using the set of parameters from Table 4.4.1. We vary the value of the penalty parameter ϵ , and for each fixed number of spatial nodes we then compute the error of the American put options, the ratio between two consecutive errors and evaluate the number of time steps of the adaptive Lobatto time integrator.

We observe that the error is nearly independent of the spatial mesh points and is of order $\mathcal{O}(\epsilon)$. Furthermore, we notice that the number of time steps depends on the

Table 4.4.2: Results of the rational spectral collocation (RSC) method with respect to the penalty term for valuing American put options with the set of parameters given in Table 4.4.1.

| ϵ | Nodes | Error | Ratio | Time steps |
|------------|-------|---------|--------|------------|
| 10^{-2} | 50 | 1.15E-2 | *** | 59 |
| 10^{-3} | 50 | 1.61E-3 | 7.1200 | 64 |
| 10^{-4} | 50 | 5.88E-4 | 2.7395 | 190 |
| 10^{-5} | 50 | 4.79E-4 | 1.2285 | 627 |
| 10^{-2} | 100 | 1.14E-2 | *** | 59 |
| 10^{-3} | 100 | 1.20E-3 | 9.5250 | 100 |
| 10^{-4} | 100 | 1.36E-4 | 8.8438 | 209 |
| 10^{-5} | 100 | 3.09E-5 | 4.4014 | 706 |
| 10^{-2} | 200 | 1.15E-2 | *** | 59 |
| 10^{-3} | 200 | 1.19E-3 | 9.6912 | 102 |
| 10^{-4} | 200 | 1.46E-4 | 8.1322 | 215 |
| 10^{-5} | 200 | 4.28E-5 | 3.4092 | 713 |

penalisation parameter in order to ensure the stability constraint, i.e, as the penalty term $\epsilon \rightarrow 0$, the number of time steps increases moderately. We obtain very satisfactory results for a small number of grid points. For instance, for $\epsilon = 10^{-5}$ and $N = 50$ an error of order 10^{-4} is obtained. Similar results were obtained in [50, 83] but they required to use a larger number of mesh points.

In the second example, we would like to investigate the spatial convergence of the rational spectral collocation (RSC) method and compare with the convergence of some existing methods which we recompute in order to use the same set of parameters. To ensure that errors in numerical results are dominated by spatial rather than temporal errors we impose an absolute, relative error tolerances of the implicit forth-order

Lobatto method and the penalty term to be 10^{-8} .

Table 4.4.3: Comparison of the rational spectral collocation (RSC) method with other existing methods for valuing American put options with the set of parameters given in Table 4.4.1.

| | Method A | | Method B | | Method C | | RSC | |
|-----|----------|---------|----------|---------|----------|---------|----------|---------|
| N | $V(E)$ | Error | $V(E)$ | Error | $V(E)$ | Error | $V(E)$ | Error |
| 20 | 2.953828 | 1.70E-0 | 4.215878 | 4.39E-1 | 4.222097 | 4.34E-1 | 4.651765 | 3.92E-3 |
| 40 | 4.221527 | 4.34E-1 | 4.550680 | 1.05E-1 | 4.555841 | 9.98E-2 | 4.654778 | 9.05E-4 |
| 80 | 4.555846 | 9.98E-2 | 4.627469 | 2.82E-2 | 4.630338 | 2.53E-2 | 4.655634 | 4.92E-5 |
| 160 | 4.630491 | 2.52E-2 | 4.647740 | 7.91E-3 | 4.649266 | 6.38E-3 | 4.655679 | 4.80E-6 |
| 320 | 4.649285 | 6.36E-3 | 4.653227 | 2.42E-3 | 4.654034 | 1.61E-3 | 4.655684 | 4.96E-7 |

In tables 4.4.3, 4.4.5, 4.4.6 and 4.4.7, columns with headings Method A, Method B and Method C denote the results obtained from our computation for the penalty method of Forsyth and Vetzal [61], the Crank-Nicolson method based on the Brennan and Schwartz approach [27] and the projected successive overrelaxation (PSOR) method of Cryer [48], respectively. From Table 4.4.3, we observe that our RSC has higher order of convergence compared to the existing methods. Our method produces a satisfactory error of order 10^{-3} with only 20 grid points, whereas other methods require almost 16 times more points, to obtain a similar error.

Figure 4.4.1 (top) displays the value of the option with respect to value of the underlying asset. By clustering more grids points around the strike price we managed to recover high accuracy of the RSC method as stated in Theorem 1.2.1.

Furthermore, we compute the value of $\Delta (= \partial V / \partial S)$ and $\Gamma (= \partial^2 V / \partial S^2)$. The Δ of the put is always negative, see Figure 4.4.1 (bottom left). Therefore, the value of a put decreases if the asset price increases, see Figure 4.4.1 (top). This is in good agreement with the theory [77].

The Γ measures how Δ changes with respect to the asset price. It becomes zero when it is away from the strike price, but at the strike it becomes more and more peaked as represented in Figure 4.4.1 (bottom right). We see that Γ is small and has the largest value at strike price. We observe that Γ put is always positive and increases to a maximum with an asset price close to the exercise price. Furthermore, we observe that the numerical values of the American put options and their Greeks are free of

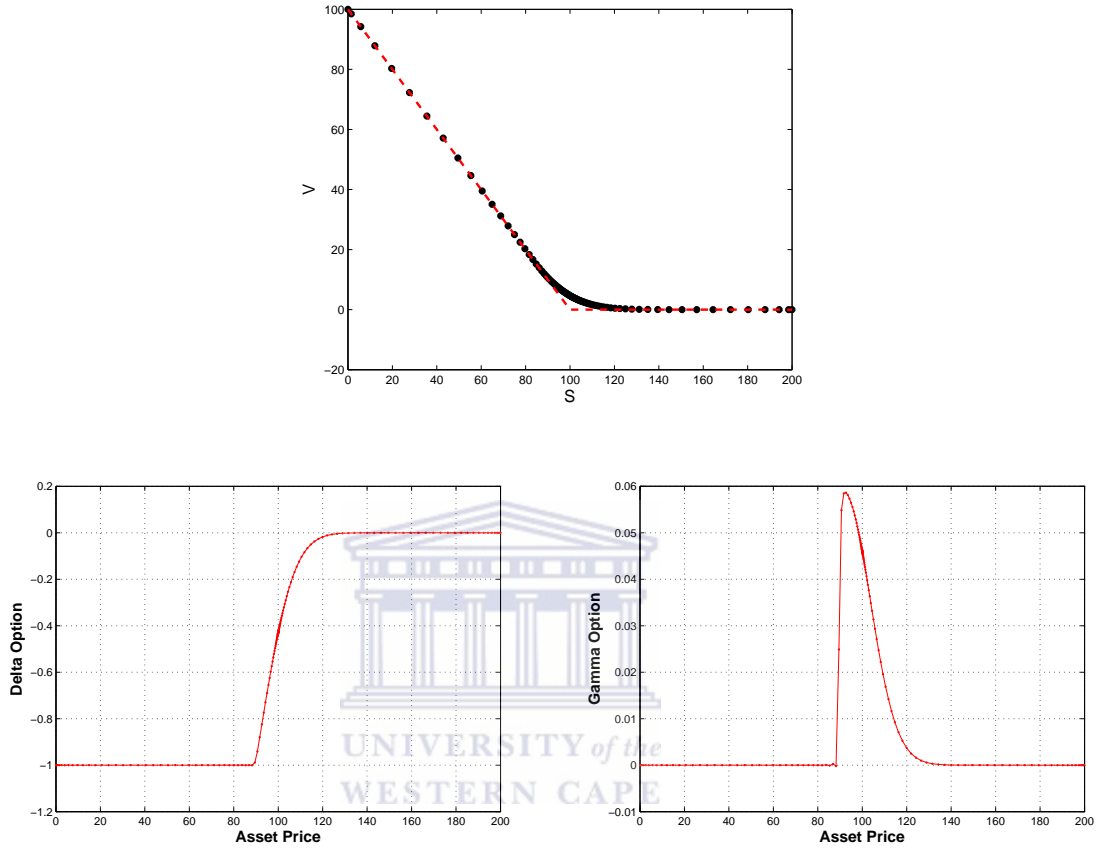


Figure 4.4.1: Values of the American put option (top figure), Δ (left bottom figure) and Γ (right bottom figure) using parameters given in Table 4.4.1. The other parameters are $S_m = 0$, $S_M = 200$ and $\beta = 20$.

spurious oscillations around the strike price E that are typically present in numerical solution of the American option type contracts, in particular while computing Γ , due to the discontinuity of the second order derivative in the optimal exercise price.

4.4.2 Valuation of American butterfly spread options

A more challenging problem is the valuation of the American butterfly options. A butterfly option has the payoff

$$V(S, 0) = \max(S - E_1, 0) - 2 \max(S - E_2, 0) + \max(S - E_3, 0), \quad E_2 = (E_1 + E_3)/2, \quad (4.4.1)$$

and the boundary conditions

$$V(S, t) = 0 \quad \text{as } S \rightarrow 0; \quad V(S, t) = 0 \quad \text{as } S \rightarrow \infty. \quad (4.4.2)$$

Table 4.4.4 presents the data used for simulating this model. We first investigate the convergence of the RSC method and compare the results with those obtained by other existing methods. As a benchmark solution, we use the value of the options obtained

Table 4.4.4: Data used to value American butterfly spread options

| Parameters | r | σ | δ | E_1 | E_2 | E_3 | T |
|------------|------|----------|----------|-------|-------|-------|-----|
| Values | 0.05 | 0.20 | 0.00 | 90 | 100 | 110 | 0.5 |

by using the penalty method presented in [61] with 50000 time and space grid points. As in the previous case, to ensure that errors in numerical results are dominated by spatial rather than temporal errors, we impose an absolute, relative error tolerances of the implicit forth-order Lobatto method to be 10^{-8} . The grid stretching parameter is taken to be $\alpha = 50$. The convergence is explored at three different strike prices E_1 , E_2 and E_3 . Clearly, the numerical results for this experiment illustrate the advantage of using our rational spectral collocation method with the grid stretching strategy over the existing methods. Rapid convergence of the RSC is observed while valuing the American butterfly options at strike prices E_1 , E_2 and E_3 as illustrated in tables 4.4.5, 4.4.6 and 4.4.7, respectively. Our RSC approach shows very accurate results obtained with few grid points. For example, at the strike price E_2 an accuracy of order 10^{-2} attained with only 20 points in the case of RSC method which cannot be achieved in

Table 4.4.5: Comparison of the convergence of the rational spectral collocation (RSC) method with other existing methods for valuing American butterfly spread options at strike price E_1 with the set of parameters given in Table 4.4.4.

| | Method A | | Method B | | Method C | | RSC | |
|-----|----------|---------|----------|---------|----------|---------|----------|---------|
| N | $V(E_1)$ | Error | $V(E_1)$ | Error | $V(E_1)$ | Error | $V(E_1)$ | Error |
| 20 | 3.850580 | 1.40E-0 | 4.644988 | 6.08E-1 | 4.800868 | 4.52E-1 | 5.212192 | 4.09E-2 |
| 40 | 4.219791 | 1.03E-0 | 5.000685 | 2.52E-1 | 5.161263 | 9.19E-2 | 5.255192 | 2.05E-3 |
| 80 | 4.743739 | 5.09E-1 | 5.077096 | 1.76E-1 | 5.233733 | 1.94E-2 | 5.253491 | 3.55E-4 |
| 160 | 5.166896 | 8.62E-2 | 5.105809 | 1.47E-1 | 5.255290 | 2.15E-3 | 5.253196 | 5.49E-5 |
| 320 | 5.169988 | 8.32E-2 | 5.134745 | 1.18E-1 | 5.251017 | 2.12E-3 | 5.253147 | 4.90E-6 |

 Table 4.4.6: Comparison of the convergence of the rational spectral collocation (RSC) method with other existing methods for valuing American butterfly spread options at strike price E_2 with the set of parameters given in Table 4.4.4.

| | Method A | | Method B | | Method C | | RSC | |
|-----|----------|---------|----------|---------|----------|---------|----------|---------|
| N | $V(E_2)$ | Error | $V(E_2)$ | Error | $V(E_2)$ | Error | $V(E_2)$ | Error |
| 20 | 3.977636 | 6.01E-0 | 9.302053 | 6.89E-1 | 9.871566 | 1.19E-1 | 9.955600 | 3.55E-2 |
| 40 | 8.653698 | 1.34E-0 | 9.512456 | 4.78E-1 | 9.913464 | 7.76E-2 | 9.994326 | 3.26E-3 |
| 80 | 8.679782 | 1.31E-0 | 9.822351 | 1.69E-1 | 9.957679 | 3.34E-2 | 9.991326 | 2.59E-4 |
| 160 | 9.478241 | 5.13E-1 | 9.875372 | 1.16E-1 | 9.976355 | 1.47E-2 | 9.991026 | 4.06E-5 |
| 320 | 9.648192 | 3.43E-1 | 9.967679 | 2.34E-2 | 9.997890 | 6.82E-3 | 9.991062 | 4.64E-6 |

 Table 4.4.7: Comparison of the convergence of the rational spectral collocation (RSC) method with other existing methods for valuing American butterfly spread options at strike price E_3 with the set of parameters given in Table 4.4.4.

| | Method A | | Method B | | Method C | | RSC | |
|-----|----------|---------|----------|---------|----------|---------|----------|---------|
| N | $V(E_3)$ | Error | $V(E_3)$ | Error | $V(E_3)$ | Error | $V(E_3)$ | Error |
| 20 | 1.758169 | 3.14E-0 | 4.454015 | 4.45E-1 | 4.600968 | 2.98E-1 | 4.811230 | 8.73E-2 |
| 40 | 4.535713 | 3.63E-1 | 4.686623 | 2.12E-1 | 4.832751 | 6.58E-2 | 4.897053 | 1.51E-3 |
| 80 | 4.722869 | 1.76E-1 | 4.745747 | 1.52E-1 | 4.882757 | 1.58E-2 | 4.898053 | 5.05E-4 |
| 160 | 4.715394 | 1.83E-1 | 4.771779 | 1.27E-1 | 4.890226 | 8.33E-3 | 4.898503 | 5.51E-5 |
| 320 | 4.848402 | 5.02E-2 | 4.806425 | 9.21E-2 | 4.893375 | 5.18E-3 | 4.898553 | 5.10E-6 |

the case of the penalty method of Forsyth [61] with even 320 points.

Figure 4.4.2 (top) displays the value of the option value with respect to the underlying asset. The Δ of the butterfly spread option is positive on $[S_m, E_2]$ and negative on the interval $[E_2, S_M]$, see Figure 4.4.2 (bottom left). Therefore, the value of an American butterfly spread options increases and decreases if the asset price increases, on $[S_m, E_2]$ and $[E_2, S_M]$ respectively, see Figure 4.4.2 (top). This is again consistent with the results found in [147]. From Figure 4.4.2 (bottom left), we see that Γ is small and has the largest absolute value at the strike price E_2 . We observe that the numerical values of the American butterfly spread options and their Greeks are free of spurious

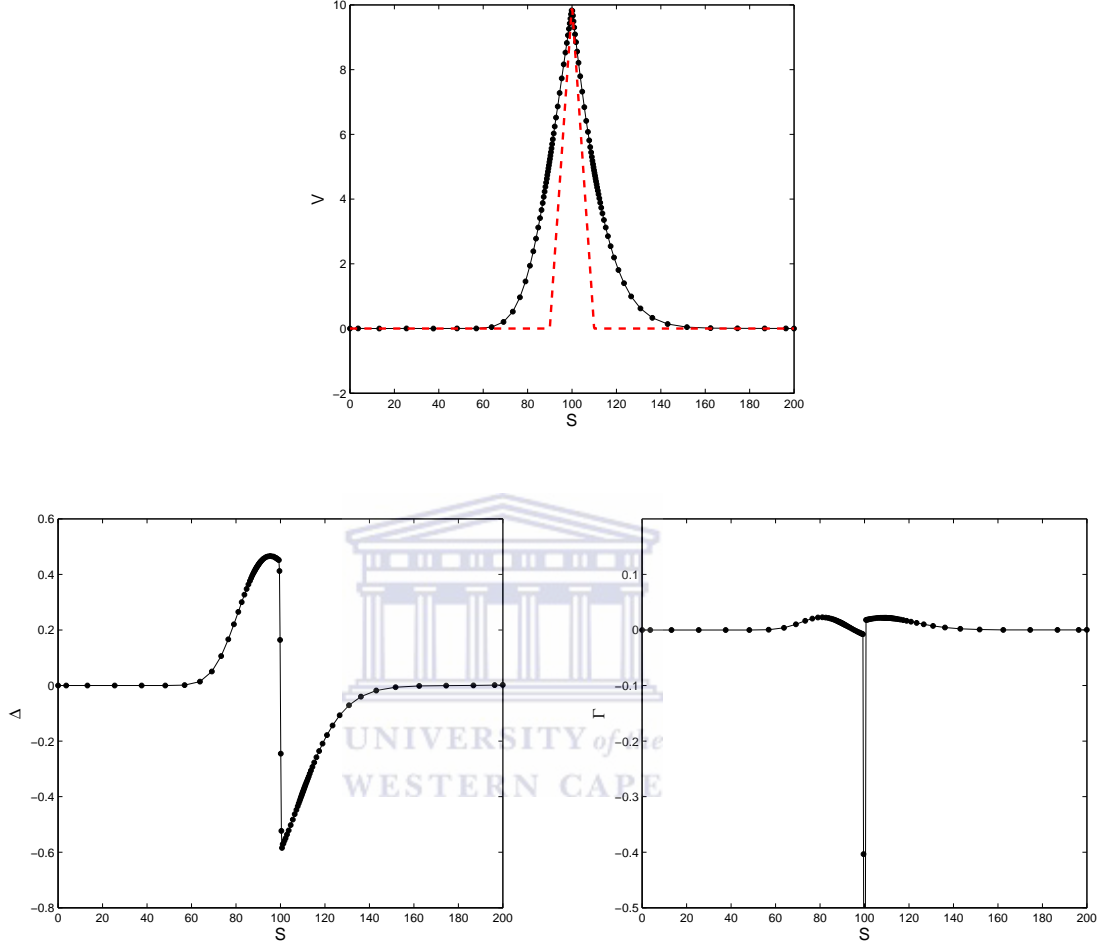


Figure 4.4.2: Values of the American butterfly spread option (top figure), Δ (left bottom figure) and Γ (right bottom figure) using parameters given in Table 4.4.4. The other parameters are $S_m = 0$, $S_M = 200$ and $\beta = 50$.

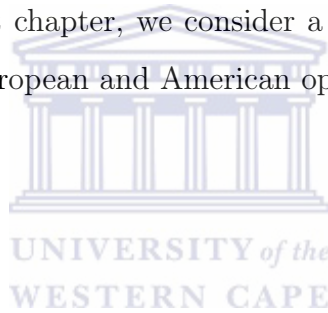
oscillations around the strike prices E_1 , E_2 and E_3 . In view of the above mentioned, our method is robust and reliable for valuing American vanilla and butterfly spread options and is therefore an alternative method for valuing this class of financial derivatives.

4.5 Summary and discussions

We have presented a rational spectral collocation (RSC) method based on the penalty approach for pricing American vanilla and butterfly spread options. The method is cou-

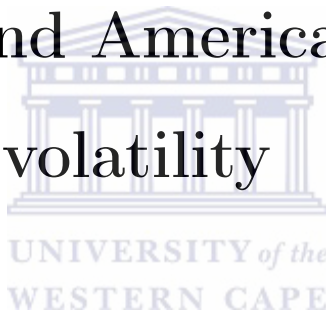
pled with implicit forth-order Lobatto time integration method [68] for time marching. Extensive comparisons were carried out with the existing methods seen in the literature. We found that the error using our RSC method appeared to be less compared with those obtained by some existing methods. We achieved significant higher order accuracy using conformal mappings with Chebyshev discretisation. The computed Greeks were free of spurious oscillations which occurs when methods such as Crank-Nicolson are used. Our approach is found to be very accurate, efficient, reliable and hence can be a possible alternative to other approaches for pricing American options.

So far we have found very satisfactory results for some basic standard and non-standard options. In next chapter, we consider a more challenging problem, namely, the problem of pricing European and American options ‘under local volatility’.



Chapter 5

Spectral methods for pricing European and American options under local volatility



In this chapter, we present a spectral method for solving a partial differential equation arising from pricing the European options under local volatility. We then extend this approach to solve a partial differential complementary problem associated with the American options under local volatility. We consider these options on both dividend and non-dividend paying assets. In the case of European options, the PDE is discretised directly in space, while a penalty approach is used to solve the partial differential complementary problem that arises from American options. The free boundary problem arising from American options is first reformulated as a variational inequality. The variational inequality is transformed into a nonlinear partial differential equation on fixed boundaries by adding a penalty term. Then, the resulting nonlinear partial differential equation is discretised in asset direction by means of a rational spectral collocation approximation, which uses the “sinh” transformation in order to accommodate more grids at a desired region. The application of this rational spectral collocation method leads to a system of ordinary differential equations that we solve using the

implicit fifth-order RADAU [68] time integration method.

5.1 Introduction

Numerous mathematical models are developed in the classical Black-Scholes framework to help the investors in their decision making process. However, some of these models have severe shortcomings, for example, they did not include volatility skew or smile, encountered in the Black-Scholes model. To this end, a number of models have been proposed in order to encompass these shortcomings; in particular, stochastic volatility models [73, 76], deterministic local volatility functions [43, 56], jump-diffusion models [86, 102], Lévy models [99, 112] amongst others.

In this chapter, we consider the local volatility function approach to value European and American options. This approach was pioneered by Dupire [56], Derman and Kani [53] and Rubinstein [114]; and has subsequently been improved by many other researchers, see, e.g., [5, 90]. The local volatility function approach has become popular with practitioners, because of its simplicity and the fact that it conveniently retains the market completeness of the Black-Scholes model. Moreover, the existence of a forward equation that describes the evolution of call option prices as functions of maturity time and strike price makes it possible to express the unknown volatility function directly in terms of known option prices.

In this chapter, we present a spectral collocation method for valuing European and American options under local volatility. Our method is based on the rational collocation method using the “sinh” transformation. In the case of American options, the partial differential complementary (PDC) problem is first transformed into a nonlinear PDE by adding a penalty term.

The rest of this chapter is organised as follows. In Section 5.2, we describe the formulation of the mathematical models with local volatility in terms of a PDE and PDC problem. Section 5.3 considers the spatial approximations of these models using rational spectral method. Numerical experiments are reported in Section 5.4, whereas

in Section 5.5 we present summary and conclusions.

5.2 The mathematical model

Unlike the traditional Black-Scholes model, where the volatility is assumed to be constant, it is assumed that under the local volatility model the volatility depends on the underlying stock price and time. The main idea with the model is to calibrate it to fit the market prices of liquid European options so that the model fits the actual market prices for all maturity times and strike prices for the option. When the calibration is done, it is possible to reproduce all the option prices in the market for every maturity and strike.

Now, let S_t denotes a risky underlying asset price process at time t , $0 \leq t \leq T$. Suppose that $r_t > 0$ is a risk-free interest rate, $\delta_t \geq 0$ a continuous dividend yield. The risk neutral diffusion process for the evolution of the stock price under the local volatility model is given by the following stochastic differential equation

$$dS = (r_t - \delta_t)S_t dt + \sigma_L(S_t, t)S_t dB_t, \quad (5.2.1)$$

where B_t is a standard Brownian motion and $\sigma(S, t)$ is the local volatility function. Standard applications of Ito's formula on (5.2.1) give that the value of the European option $V(S, t)$ at the time t satisfies the following backward partial differential equation

$$\frac{\partial V}{\partial t} = \frac{1}{2}\sigma_L^2(S, t)S^2 \frac{\partial^2 V}{\partial S^2} + (r(t) - \delta(t))S \frac{\partial V}{\partial S} - r(t)V. \quad (5.2.2)$$

Nevertheless, empirical evidences suggest that the volatility implied by the price of traded options varies with the maturity time T and the strike price E . The boundary and the initial conditions make the difference between American and European style options as well as between put and call and other types of options.

In the case when $r(t)$ and $\delta(t)$ are constant, the solution of the European vanilla

call option under local volatility is uniquely determined by

$$\left. \begin{aligned} V_t &= \frac{1}{2}\sigma_L^2(S, t)S^2V_{SS} + (r - \delta)SV_S - rV, \\ V(S, 0) &= \max(S - E, 0), \\ V(0, t) &= 0, \\ V(S, t) &= Se^{-\delta t} - Ee^{-rt}, \text{ as } S \rightarrow \infty. \end{aligned} \right\} \quad (5.2.3)$$

In practice, American option pricing problems can be reformulated as a differential linear complementary problem (LCP):

$$\left. \begin{aligned} V_t - L_{BS}V &\geq 0, \\ V - V^* &\geq 0, \\ (V_t - L_{BS}V)(V - V^*) &= 0, \end{aligned} \right\} \quad (5.2.4)$$

where V is the value of the option, V^* denotes its exercise value and L_{BS} denotes the Black-Scholes operator

$$L_{BS} \equiv \frac{1}{2}\sigma^2 S^2 \frac{\partial^2}{\partial S^2} + (r - \delta)S \frac{\partial}{\partial S} - r. \quad (5.2.5)$$

We approximate the linear complementarity problem (5.2.4) by a nonlinear PDE on fixed boundary by applying the penalty method developed in [61]. This gives

$$\left. \begin{aligned} V_t &= L_{BS}V + \frac{1}{\epsilon} [V - V^*]^+, \quad 0 \leq S < \infty, \quad 0 \leq t \leq T, \\ V^*(S) &= V(S, 0) = \max(E - S, 0), \\ V(S, t) &= E, \quad S \rightarrow 0, \\ V(S, t) &= 0, \quad S \rightarrow +\infty, \end{aligned} \right\} \quad (5.2.6)$$

where $0 < \epsilon \ll 1$ is the penalty constant and $[V - V^*]^+ = \max(V - V^*, 0)$ is the penalty term.

To solve the above problems, we need to know the local volatility surface (function) $\sigma_L(S, t)$. The following theorems suggest how to choose the local volatility function.

Theorem 5.2.1 (Dupire local volatility formula [56]). *Given that the underlier price follows the stochastic differential equation (SDE) (5.2.1), the local volatility function, $\sigma_L(S, t)$, is given by*

$$\sigma_L(S, t) = \frac{\frac{\partial V}{\partial t} + (r(t) - \delta(t))S \frac{\partial V}{\partial S} + r(t)V}{\frac{1}{2}S^2 \frac{\partial^2 V}{\partial S^2}} \quad (5.2.7)$$

where $V = V(S, t)$ is the value of the European call option.

Proof. See [56].

In practice, the local volatility function in term of the market implied volatility is given as in the following theorem.

Theorem 5.2.2 ([142]). *We assume that the implied volatility function, $\tilde{\sigma}(S, t)$, is differentiable once with respect to t and twice with respect to S . The local volatility function, $\sigma_L(S, t)$, in the PDE (5.2.2) in term of the implied volatility is given by*

$$\sigma_L^2(S, t) = \frac{\tilde{\sigma}^2 + 2t\tilde{\sigma} \frac{\partial \tilde{\sigma}}{\partial t} + 2(r(t) - \delta(t))St\tilde{\sigma} \frac{\partial \tilde{\sigma}}{\partial S}}{\left[1 + Sd_1\sqrt{t} \frac{\partial \tilde{\sigma}}{\partial S}\right]^2 + S^2t\tilde{\sigma} \left[\frac{\partial^2 \tilde{\sigma}}{\partial S^2} - d_1\sqrt{t} \left(\frac{\partial \tilde{\sigma}}{\partial S}\right)^2\right]}, \quad (5.2.8)$$

where

$$d_1 = \frac{\ln(S/E) + (r(t) - \delta(t) + \tilde{\sigma}^2/2)t}{\tilde{\sigma}\sqrt{t}}, \quad d_2 = d_1 - \tilde{\sigma}\sqrt{t}. \quad (5.2.9)$$

Proof. See [142].

In the next section, we propose spatial discretisations of the PDEs involved in pricing European and American options under local volatility. Our method is based on the rational spectral collocation approximations as described below.

5.3 Spectral space discretisation of the PDEs

We discretise the PDEs (5.2.3) and (5.2.6) in asset (space) direction by means of rational spectral collocation method. Let $x = g(y_j)$ be the transformed Chebyshev points are chosen from (1.2.31), the first step is to transform $x \in [-1, 1]$ into $S \in [S_m, S_M]$ that better suits the option at hand as $x = (2S - (S_M - S_m))/(S_M + S_m)$. Now writing $V(S, t) = u(x, t)$, the PDE (5.2.6) together with its initial and boundary conditions yields

$$\left. \begin{aligned} u_t &= p(x, t)u_{xx} + q(x, t)u_x + r(t)u + f(u), \\ u(x, 0) &= \max(E - S, 0), \quad -1 \leq x \leq 1, \quad S_m \leq S \leq S_M, \\ u(-1, t) &= E - S_m, \quad u(1, t) = 0, \quad 0 \leq t \leq T, \end{aligned} \right\} \quad (5.3.1)$$

where

$$\begin{aligned} p(x, t) &= \frac{1}{2} \sigma_L^2(S, t) S^2 \left(\frac{2}{S_M - S_m} \right)^2, \quad q(x, t) = (r(t) - \delta(t)) S \left(\frac{2}{S_M - S_m} \right), \\ f(u) &= \frac{1}{\epsilon} [u - u^0]^+. \end{aligned}$$

A rational spectral collocation method can be obtained by replacing the solution u in (5.3.1) with an unknown linear rational polynomial

$$\tilde{u}(x) = \sum_{j=0}^N \tilde{u}_j L_j^{(\omega)}(x), \quad (5.3.2)$$

and collocating at $N - 1$ points x_1, \dots, x_{N-1} . This yields the following system of nonlinear ODEs for \tilde{u}_i

$$\left. \begin{aligned} \tilde{u}_{i,t} &= p(x_i) \sum_{j=0}^N \tilde{u}_j L_j^{(\omega)''}(x_i) + q(x_i) \sum_{j=0}^N \tilde{u}_j L_j^{(\omega)'}(x_i) + r \tilde{u}_i + f(\tilde{u}_i), \\ \tilde{u}_0 &= \tilde{u}(-1, t), \quad \tilde{u}_N = \tilde{u}(1, t). \end{aligned} \right\} \quad (5.3.3)$$

In order to write (5.3.3) in matrix form, we introduce the following matrix and vector notations

$$\begin{aligned}
 \tilde{\mathbf{u}} &= [\tilde{u}_1, \tilde{u}_2, \dots, \tilde{u}_{N-1}]^T, \\
 D^{(1)} &= \left(D_{ij}^{(1)} \right), \quad D_{ij}^{(1)} = L_j^{(\omega)'}(x_i), \quad i, j = 1, \dots, N-1, \\
 D^{(2)} &= \left(D_{ij}^{(2)} \right), \quad D_{ij}^{(2)} = L_j^{(\omega)''}(x_i), \quad i, j = 1, \dots, N-1, \\
 P &= \text{diag}(p(x_i)), \quad Q = \text{diag}(q(x_i)), \quad i = 1, \dots, N-1, \\
 \mathbf{g} &= \left[f(u_i) + \left(p(x_i)D_{i0}^{(2)} + q(x_i)D_{ij}^{(1)} + rI_{i0} \right) \tilde{u}_0 + \left(p(x_i)D_{iN}^{(2)} + q(x_i)D_{ij}^{(1)} + rI_{iN} \right) \tilde{u}_N \right]^T,
 \end{aligned} \tag{5.3.4}$$

where I is a $(N+1) \times (N+1)$ identity matrix.

Consequently, (5.3.3) can be expressed as a nonlinear initial value problem of the form

$$\frac{d\tilde{\mathbf{u}}}{dt} = A\tilde{\mathbf{u}} + \mathbf{g}. \tag{5.3.5}$$

with $A = PD^{(2)} + QD^{(1)} - rI$.

In the case of the European options, $f(\tilde{u}_i) = 0$. The main difficulty when dealing with the system of type (5.3.5) is that the use of explicit time integrators is not efficient because the system suffers from stiffness as the mesh in the asset direction is refined. Consequently, the time step-size must be significantly smaller in order to fulfill the drastic stability condition present in explicit time integrators. As a remedy, we employ implicit time integrators which are more stable. We use fifth-order RADAU method [68] for time integration with adaptive time stepping.

5.4 Numerical results

In this section, we present several numerical experiments to illustrate the performance and the convergence of our spectral method. We consider both European call and American put options under local volatility ([132]), where the local volatility function

is chosen to be

$$\sigma_L(S, t) = 0.15 + 0.15(0.5 + 2t) \frac{(S/100 - 1/2)^2}{(S/100)^2 + 1.44}. \quad (5.4.1)$$

It is plotted in Figure 5.4.1. We have tested the method for several sets of realistic parameters. Here, we set the following benchmark parameters throughout the implementations $T = 0.5$, $E = 100$, $r = 0.1$, $\delta = 0.0$, for non-dividend paying assets, and $T = 0.5$, $E = 100$, $r = 0.1$, $\delta = 0.07$ when a continuous dividend of 7% is paid. For both models, we set the computational domain in a such way that $S_m = 0$ and $S_M = 200$. The grid stretching parameter is chosen as $\alpha = 10^4$. Note that the conclusions for other sets of parameters are similar to the ones reported here, which indicate that the method is robust.

To determine numerically the order of convergence of the discretisation scheme, we define the ‘Ratio’ of the differences between numerical and benchmark solutions at strike price using N and $2N$ grid points, respectively.

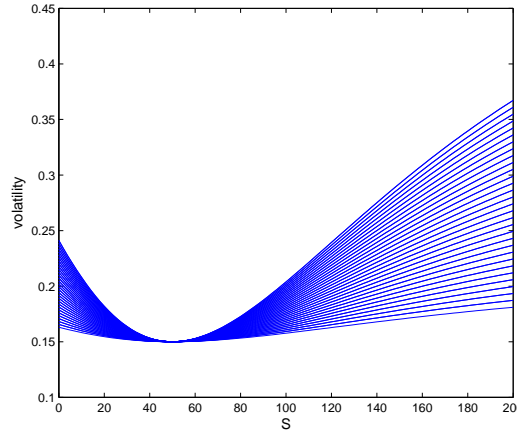


Figure 5.4.1: Local volatility function at different times

5.4.1 Valuation European options under local volatility

As a first model, we consider the case of European call options under local volatility. In order to illustrate the utility of our spectral collocation method, we perform two experiments with two sets of parameters. In the first experiment, we investigate the behaviour of the time integrator with respect to the tolerance and the number of degrees of freedom N . All the results are reported in tables 5.4.1-5.4.2, where the time integrator tolerance (TOL) varies from 10^{-5} to 10^{-9} . The number of spatial grid points are taken as $N = 40, 80$ and 160 . We denote by ERROR the absolute errors between numerical solutions and the benchmark value which is the numerical value of our spectral method obtained with 640 spatial grid points with TOL= 10^{-10} , ITER is the number of total time iterations and ‘Time’ the computational time in second.

Table 5.4.1: Results for the fully discrete numerical method for solving European options under local volatility using the set of parameters $T = 0.5$, $E = 100$, $r = 0.1$, $\delta = 0.0$. Benchmark solution: 7.39883446.

| TOL | N | ERROR | ITER | Time |
|-----------|-----|---------|------|------|
| 10^{-5} | 40 | 2.03E-5 | 10 | 0.05 |
| 10^{-6} | 40 | 1.74E-5 | 12 | 0.06 |
| 10^{-7} | 40 | 2.36E-5 | 16 | 0.09 |
| 10^{-8} | 40 | 2.94E-5 | 21 | 0.11 |
| 10^{-9} | 40 | 2.98E-5 | 31 | 0.17 |
| 10^{-5} | 80 | 5.03E-5 | 10 | 0.20 |
| 10^{-6} | 80 | 1.29E-5 | 12 | 0.21 |
| 10^{-7} | 80 | 5.72E-6 | 16 | 0.37 |
| 10^{-8} | 80 | 4.36E-7 | 21 | 0.55 |
| 10^{-9} | 80 | 6.64E-8 | 31 | 0.77 |
| 10^{-5} | 160 | 5.03E-5 | 10 | 1.33 |
| 10^{-6} | 160 | 1.29E-5 | 12 | 2.04 |
| 10^{-7} | 160 | 5.39E-6 | 16 | 2.53 |
| 10^{-8} | 160 | 4.63E-7 | 21 | 2.95 |
| 10^{-9} | 160 | 7.97E-8 | 31 | 3.40 |

From Table 5.4.1, we observe that the number of total iterations required by the code is independent of the number of grid points N but depends only on the tolerance of the time integrator. This is usually the case when using stiff time integrators. For the

Table 5.4.2: Results for the fully discrete numerical method for solving European options under local volatility using the set of parameters $T = 0.5$, $E = 100$, $r = 0.1$, $\delta = 0.07$. Benchmark solution: 5.2274224.

| TOL | N | ERROR | ITER | Time |
|-----------|-----|---------|------|------|
| 10^{-5} | 40 | 2.05E-5 | 10 | 0.06 |
| 10^{-6} | 40 | 1.70E-5 | 12 | 0.07 |
| 10^{-7} | 40 | 2.31E-5 | 15 | 0.12 |
| 10^{-8} | 40 | 2.93E-5 | 21 | 0.11 |
| 10^{-9} | 40 | 2.97E-5 | 31 | 0.15 |
| 10^{-5} | 80 | 5.10E-5 | 10 | 0.16 |
| 10^{-6} | 80 | 1.31E-5 | 12 | 0.27 |
| 10^{-7} | 80 | 5.79E-6 | 16 | 0.28 |
| 10^{-8} | 80 | 4.41E-7 | 21 | 0.35 |
| 10^{-9} | 80 | 5.50E-8 | 31 | 0.51 |
| 10^{-5} | 160 | 5.10E-5 | 10 | 0.99 |
| 10^{-6} | 160 | 1.31E-5 | 12 | 1.12 |
| 10^{-7} | 160 | 5.89E-6 | 16 | 1.62 |
| 10^{-8} | 160 | 4.55E-7 | 21 | 2.29 |
| 10^{-9} | 160 | 6.87E-8 | 31 | 3.09 |

same number of grid points N , we observe a moderate increase of the number of time steps and hence a moderate increase of the computational time. When the number of grid points is large enough, e.g., $N = 80$ and $N = 160$ we observe that the errors are proportional to the tolerance. The results presented in tables 5.4.1-5.4.2 show the order of convergence and the robustness of the RADAU time integrator.

We next investigate the convergence of our spectral method. To ensure that the exponential accuracy of our rational spectral collocation method is not polluted by the time integrator, we choose the time integration tolerance to be 10^{-10} . In tables 5.4.3-5.4.4, we keep the tolerance fixed, vary the number of grid points, and report the value of the European option at the strike price E , the error, the ratio and the number iterations required to obtained the desired accuracy. We observe a very rapid decrease of the error as the number of grid points N increases. Note that the last three approximations of order 10^{-8} , 10^{-9} and 10^{-10} in Table 5.4.3 are in general difficult to attain with standard finite difference, finite element and finite volume methods

Table 5.4.3: Errors in spectral discretisation method for solving European options under local volatility using the set of parameters $T = 0.5$, $E = 100$, $r = 0.1$, $\delta = 0.0$. TOL = 10^{-10} , Benchmark solution: 7.39883446.

| N | $V(E)$ | Error | Ratio | ITER |
|-----|------------|----------|--------|------|
| 20 | 7.42342535 | 2.45E-2 | | 46 |
| 40 | 7.39886440 | 2.99E-5 | 821.4 | 46 |
| 80 | 7.39883448 | 1.90E-8 | 1573.4 | 46 |
| 160 | 7.39883447 | 4.48E-9 | 4.2 | 46 |
| 320 | 7.39883446 | 8.13E-10 | 5.5 | 46 |

 Table 5.4.4: Errors in spectral discretisation method for solving European options under local volatility using the set of parameters $T = 0.5$, $E = 100$, $r = 0.1$, $\delta = 0.07$. TOL = 10^{-10} , Benchmark solution: 5.2274223.

| N | $V(E)$ | Error | Ratio | ITER |
|-----|-----------|----------|--------|------|
| 20 | 5.2528695 | 2.54E-2 | | 44 |
| 40 | 5.2274522 | 2.98E-5 | 852.8 | 46 |
| 80 | 5.2274224 | 1.93E-8 | 1545.7 | 46 |
| 160 | 5.2274223 | 3.67E-9 | 5.2 | 46 |
| 320 | 5.2274223 | 9.65E-11 | 38.1 | 46 |

Figure 5.4.2 (top) displays the value of the option with respect to the value of the underlying asset. By clustering more grids points around the strike price we managed to recover high accuracy of the proposed method as stated in Theorem 1.2.1. From these plots we can also observe the effect of dividends. More precisely, as the figure shows, when the asset pays dividend then the value of the asset can be less than that of payoff, which is in line with the theory [77].

We have also calculated Δ and Γ for the options. The Δ of the put is always negative, see Figure 5.4.3 (bottom left). Therefore, the value of a put decreases if the asset price increases, see Figure 5.4.3 (top). This is in agreement with the theory [77]. The Γ becomes zero when it is away from the strike price, but at the strike price, it becomes more and more peaked as can be seen from Figure 5.4.2 (bottom right). We see that Γ is small and has the largest value at strike price. We observe that the Γ of the put is always positive and increases to a maximum with an asset price close to the exercise price. Unlike the finite difference, where the curves of Δ and Γ possess spurious oscillations around the strike price, those obtained from our approach (see

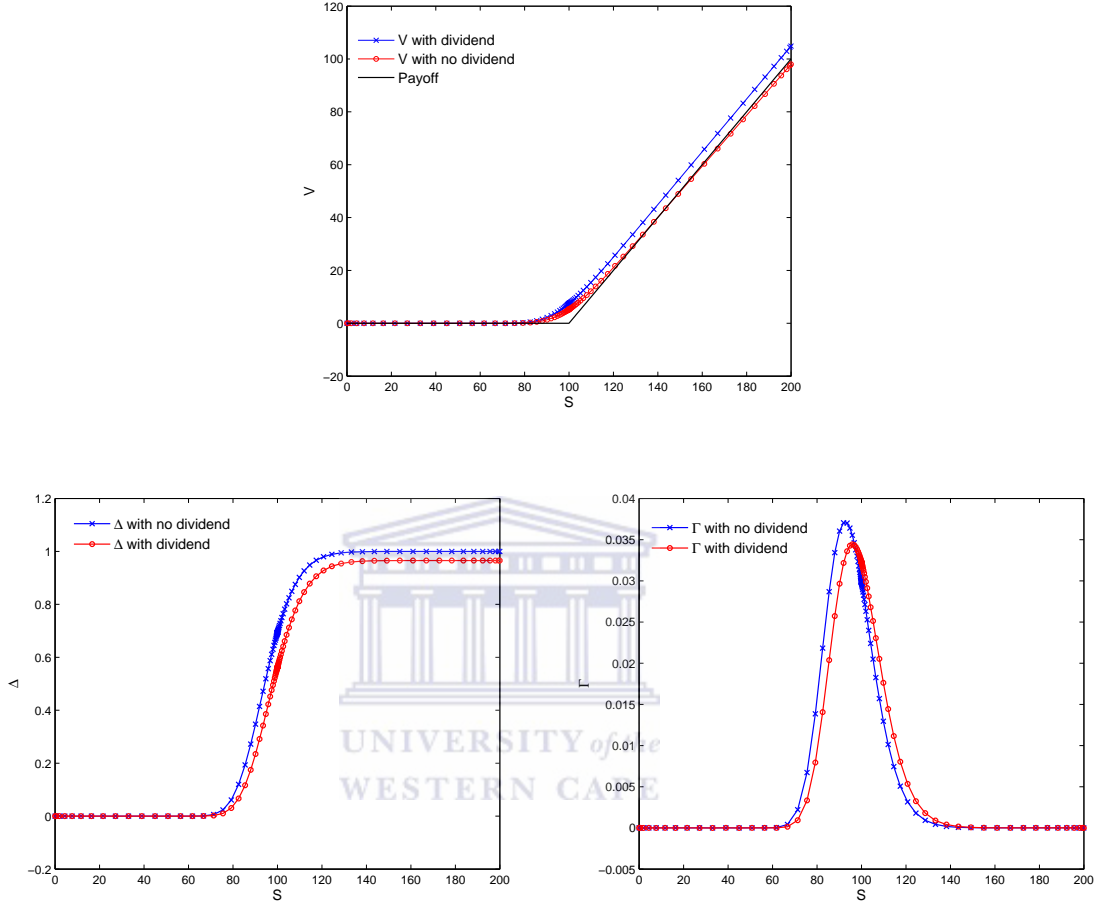


Figure 5.4.2: Values of European call options under local volatility (top figure), Δ (left bottom figure) and Γ (right bottom figure) using the parameters given as $T = 0.5$, $E = 100$, $r = 0.1$, $\delta = 0.0$ and $\delta = 0.7$. The other parameters are $S_m = 0$, $S_M = 200$ and $\beta = 10^4$.

figures 5.4.3-5.4.2) are free of these oscillations which confirm the robustness of the proposed approach.

5.4.2 Valuation of American options under local volatility

In this subsection, we investigate the performance of our spectral method for valuing American options under local volatility for the same sets of parameters that are used to price European options. In the first experiment, we check the convergence of our

method with respect to the penalty parameter ϵ . We define by ‘Change’ the difference between two numerical solutions computed with two successive penalty terms and ‘Ratio’ the ratio between two consecutive ‘Change’. Table 5.4.5 shows the results

Table 5.4.5: Convergence of the rational spectral method with respect to the penalty term for valuing American put options with the set of parameters $T = 0.5$, $E = 100$, $r = 0.1$, $\delta = 0.0$.

| ϵ | N | $V(E)$ | Change | Ratio |
|------------|-----|-----------|---------|-------|
| 10^{-2} | 80 | 3.0571563 | | |
| 10^{-3} | 80 | 3.0769181 | 1.97E-2 | |
| 10^{-4} | 80 | 3.0788449 | 1.92E-3 | 10.25 |
| 10^{-5} | 80 | 3.0790329 | 1.88E-4 | 10.24 |
| 10^{-6} | 80 | 3.0790517 | 1.87E-5 | 10.05 |
| 10^{-2} | 160 | 3.0687214 | | |
| 10^{-3} | 160 | 3.0762810 | 7.55E-3 | |
| 10^{-4} | 160 | 3.0770347 | 7.53E-4 | 10.03 |
| 10^{-5} | 160 | 3.0771094 | 7.47E-5 | 10.08 |
| 10^{-6} | 160 | 3.0771168 | 7.42E-6 | 10.06 |
| 10^{-2} | 320 | 3.0713049 | | |
| 10^{-3} | 320 | 3.0765403 | 5.23E-3 | |
| 10^{-4} | 320 | 3.0770597 | 5.19E-4 | 10.07 |
| 10^{-5} | 320 | 3.0771117 | 5.20E-5 | 9.98 |
| 10^{-6} | 320 | 3.0771171 | 5.35E-6 | 9.71 |

of American put options obtained by using the set of parameters used in the case of European options. We vary the value of the penalty parameter ϵ and check the performance of the rational spectral collocation method with respect to the penalty parameter. We observe that the error is nearly independent of the spatial mesh points and is of order $\mathcal{O}(\epsilon)$. We obtain very satisfactory results for a small number of grid points.

In the next numerical experiment, we verify the behaviour of our spectral method. We define the ‘Difference’ between two numerical solutions at strike price using N and $2N$ grid points and the ‘Ratio’ of two consecutive ‘Difference’. To avoid the pollution in the results due to the use of the time integrator, we set the tolerance as $TOL = 10^{-5}$. The results are presented in tables 5.4.6-5.4.7 which show the superior accuracy of the proposed approach.

Table 5.4.6: Results of the of the rational spectral method for valuing American put options under local volatility using $T = 0.5$, $E = 100$, $r = 0.1$, $\delta = 0.0$, $\epsilon = 10^{-5}$, $TOL = 10^{-5}$.

| N | $V(E)$ | Difference | Ratio | ITER |
|--------------------------------|-----------|------------|--------|------|
| 20 | 3.0306859 | | | 67 |
| 40 | 3.0874523 | 5.67E-2 | | 319 |
| 80 | 3.0790329 | 8.41E-3 | 6.74 | 645 |
| 160 | 3.0771094 | 1.92E-3 | 4.37 | 746 |
| 320 | 3.0771117 | 2.29E-6 | 839.96 | 856 |
| Benchmark solution: 7.39883446 | | | | |

Table 5.4.7: Results of the rational spectral method for valuing American put options using $T = 0.5$, $E = 100$, $r = 0.1$, $\delta = 0.07$, $\epsilon = 10^{-5}$, $TOL = 10^{-5}$.

| N | $V(E)$ | Difference | Ratio | ITER |
|--------------------------------|-----------|------------|-------|------|
| 20 | 4.0353575 | | | 67 |
| 40 | 3.9795348 | 5.58E-2 | | 319 |
| 80 | 3.9810469 | 1.51E-3 | 36.91 | 645 |
| 160 | 3.9812023 | 1.55E-4 | 9.73 | 746 |
| 320 | 3.9810469 | 4.51E-5 | 3.44 | 856 |
| Benchmark solution: 7.39883446 | | | | |

5.5 Summary and discussions

We have presented a spectral method for pricing European and American options under local volatility. The method is coupled with the implicit time integrator RADAU5 with adaptive time stepping. Our method produced very accurate and efficient results for these options for both non-dividend and dividend paying assets. Furthermore the computed Greeks were free of spurious oscillations with occurs when methods such Cranck Nicolson are used.

In the next chapter, we design and implement a class of efficient spectral methods to solve the partial integro-differential equations that model the jump-diffusion processes for European vanilla and butterfly spread options.

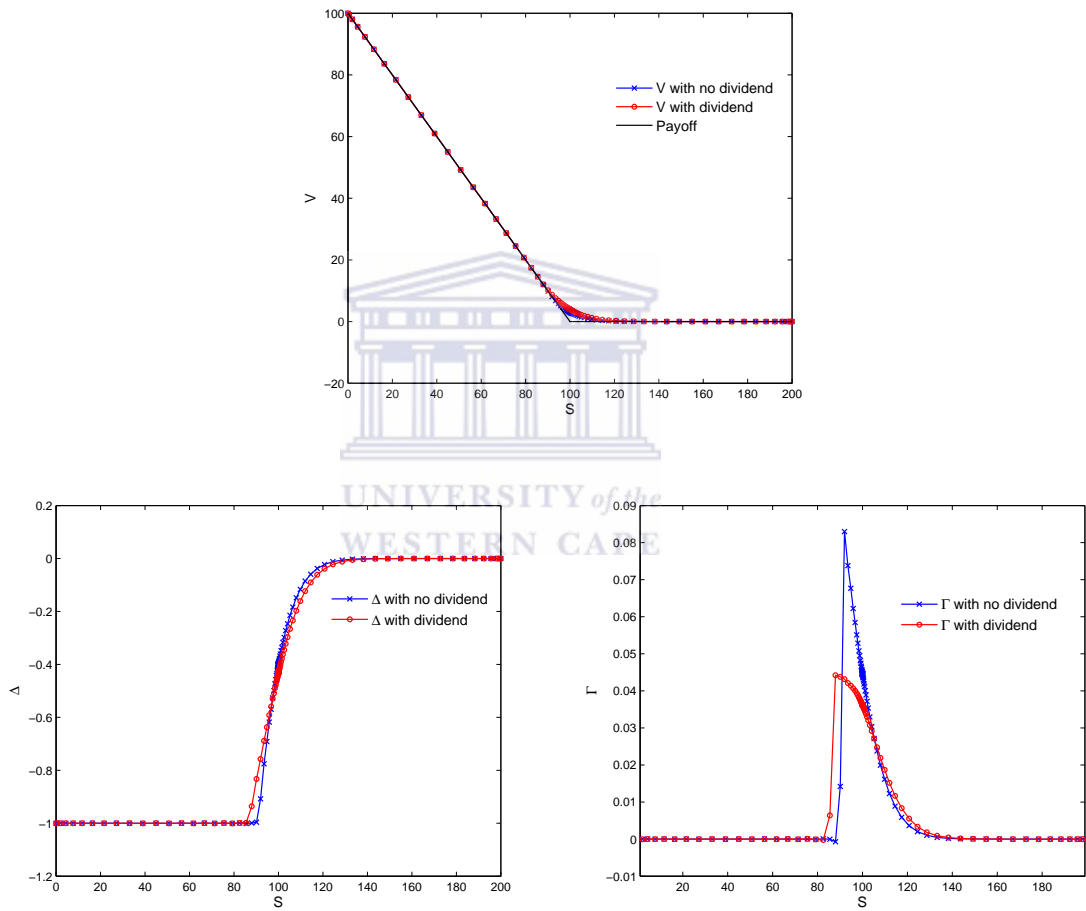


Figure 5.4.3: Values of the American put option under local volatility (top figure), Δ (left bottom figure) and Γ (right bottom figure) using the parameters given as $T = 0.5$, $E = 100$, $r = 0.1$, $\delta = 0.0$ and $\delta = 0.7$. The other parameters are $S_m = 0$, $S_M = 200$ and $\beta = 10^4$.

Chapter 6

Robust spectral method for numerical valuation of European options under Merton's jump-diffusion model



In this chapter we propose a novel numerical method based on rational spectral collocation and Clenshaw-Curtis quadrature methods together with the “sinh” transformation for pricing European vanilla and butterfly spread options under Merton’s jump-diffusion model. Under certain assumptions, such model leads to a partial integro-differential equation (PIDE). The differential and integral parts of the PIDE are approximated by the rational spectral collocation and the Clenshaw-Curtis quadrature methods, respectively. The application of spectral collocation methods to the PIDE leads to a system of ordinary differential equations which is solved using the implicit-explicit predictor-corrector (IMEX-PC) schemes in which the diffusion term is integrated implicitly whereas the convolution integral, reaction and advection terms are integrated explicitly.

6.1 Introduction

The jump-diffusion model was initially introduced by Merton [102] for pricing options for the stocks whose returns were discontinuous. As indicated in [147], the stock price in jump diffusion model is not a continuous function of time. This phenomena leads to large changes in market prices due to rare events. More importantly, the jump-diffusion model yields implied volatility curves similar to volatility smiles observed on markets [147]. Therefore, pricing of options under jump-diffusion processes requires solving a partial integro-differential equation involving a non-local integral term.

In this chapter, we present a spectral collocation method for valuing standard European call and European butterfly spread call options under Merton's jump-diffusion process. Our method is coupled with the third order IMEX-PC time integration method. This IMEX-PC is different than IMEX-RK used in [50, 51] which was used there for solving convection-reaction-diffusion problem. We use this higher order IMEX-PC so as to maintain the exponential accuracy of the spectral methods which is usually polluted due to low order time integration methods.

The rest of this chapter is organised as follows. In Section 6.2, we describe the formulation of the Black-Scholes and jump-diffusion models. Section 6.3 considers the spatial approximations of these models using rational spectral method. In Section 6.4, we discuss IMEX-PC methods for solving the semi-discrete system resulting from the spatial discretisation. Numerical experiments are conducted in Section 6.5, whereas in Section 6.6 we present summary and discussions.

6.2 The mathematical model

Consider the financial market model $\mathcal{M} = (\Omega, \mathcal{F}, \mathbb{P}, (\mathcal{F}_\tau)_{\tau \geq 0}, (S_\tau)_{\tau \geq 0})$ where Ω is the set of all possible outcomes of the experiment known as the sample space, \mathcal{F} is the set of all events, i.e. permissible combinations of outcomes, \mathbb{P} is a map $\mathcal{F} \longrightarrow [0, 1]$ which assigns a probability to each event, \mathcal{F}_τ is a natural filtration and S_τ a risky underlying

asset price process. The triplet $(\Omega, \mathcal{F}, \mathbb{P})$ is defined as a probability space.

Let B_τ a \mathbb{P} -Brownian motion, $\sigma > 0$ the volatility of the underlying asset, $r > 0$ a risk-free interest rate and $\delta \geq 0$ a continuous dividend yield. Without loss of generality, we assume that both the risk-free interest rate and the dividend yield are constants. Then under the equivalent martingale measure \mathbb{Q} , the dynamics of the Black-Scholes model satisfies the stochastic differential equation

$$dS_\tau = (r - \delta)S_\tau d\tau + \sigma S_\tau dB_\tau. \quad (6.2.1)$$

Applying the Ito's, formula under the transformation $x = \log(S/E)$, where E is the strike price, we derive a PDE for European style derivatives

$$\frac{\partial V}{\partial t} = \frac{1}{2}\sigma^2 \frac{\partial^2 V}{\partial x^2} + \left(r - \delta - \frac{1}{2}\sigma^2\right) \frac{\partial V}{\partial x} - rV, \quad -\infty \leq x \leq \infty, \quad 0 \leq t \leq T, \quad (6.2.2)$$

where V denote the value of the European options, $t = T - \tau$ is the time to expiry and T is the expiry time.

In a jump-diffusion model, the asset price motion is given by a process of the form

$$\frac{dS_\tau}{S_\tau} = (r - \delta - \lambda\kappa)d\tau + \sigma dB_\tau + (\eta - 1)dN_\tau, \quad (6.2.3)$$

where $(N_\tau)_{\tau \geq 0}$ is a Poisson process with intensity λ and independent of $(B_\tau)_{\tau \geq 0}$; $\eta - 1$ represents the impulse function for a jump from S to ηS and $\kappa = \mathbb{E}[\eta - 1]$ is the expectation of the impulse. Therefore the Black-Scholes PDE (6.2.2) becomes a partial-integro differential equation (PIDE) of the form

$$\frac{\partial V}{\partial t} = \frac{1}{2}\sigma^2 \frac{\partial^2 V}{\partial x^2} + \left(r - \delta - \frac{1}{2}\sigma^2 - \lambda\kappa\right) \frac{\partial V}{\partial x} - (r + \lambda)V + \lambda \int_{-\infty}^{\infty} V(y, t) f(y - x) dy, \quad (6.2.4)$$

where $f(z)$ is the probability density function of the jump amplitude η .

In Merton's jump-diffusion model, the density function is a normal distribution

function with mean μ and standard deviation σ_J , i.e,

$$f(z) = \frac{1}{\sqrt{2\pi}\sigma_J} e^{-\frac{(z-\mu)^2}{2\sigma_J^2}}, \quad (6.2.5)$$

with the expected value of the jump size κ in (6.2.4) given by

$$\kappa = e^{\mu + \frac{\sigma_J^2}{2}}. \quad (6.2.6)$$

It is the feature of each option that characterises the initial and boundary conditions of the problem (6.2.4). For European call options the initial and boundary conditions are set as

$$V(x, 0) = \max(Ee^x - E, 0) \quad (6.2.7)$$

and

$$V(x, t) = 0 \text{ as } x \rightarrow -\infty; \quad V(x, t) = Ee^x - Ee^{-rt} \text{ as } x \rightarrow \infty. \quad (6.2.8)$$

On the other hand, European Butterfly spread options possess three singularities at E_1 , $E_2 = (E_1 + E_3)/2$ and E_3 . Under the transformation $x = \log(S/E_2)$ its initial and boundary conditions are given by

$$V(x, 0) = \max(E_2e^x - E_1) - 2\max(E_2e^x - E_2) + \max(E_2e^x - E_3) \quad (6.2.9)$$

and

$$V(x, \tau) = 0 \text{ as } x \rightarrow -\infty; \quad V(x, \tau) = 0 \text{ as } x \rightarrow \infty. \quad (6.2.10)$$

6.3 Spectral space discretisation of the PIDE

In this section, we describe the application of the rational spectral method combined with the Clenshaw-Curtis quadrature rule, discussed in Chapter 1, to discretise the PIDE (6.2.4) and transform it into a system of ODEs which we will solve using IMEX-

PC methods described in the next section. Let $\xi_k = g(\varepsilon_k)$, $\varepsilon_k = \cos(\pi k/N)$ be the transformed Chebyshev points, x_m and x_M the minimum and maximum values of x , respectively and $l = x_M - x_m$. Using the notation $V(x, t) = u(\xi, t)$, the PDE part of the PIDE (6.2.4) can be written as

$$\frac{\partial u}{\partial t} = \frac{1}{2}\sigma^2 \left(\frac{2}{l}\right)^2 \frac{\partial^2 u}{\partial \xi^2} + \left(r - \delta - \frac{1}{2}\sigma^2 - \lambda\kappa\right) \left(\frac{2}{l}\right) \frac{\partial u}{\partial \xi} - (r + \lambda)u, \quad 0 \leq t \leq T. \quad (6.3.1)$$

The matrix form is obtained by applying the rational spectral method

$$\dot{\mathbf{u}}(t) = D_N \mathbf{u}(t), \quad (6.3.2)$$

where

$$D_N = \frac{1}{2}\sigma^2 \left(\frac{2}{l}\right)^2 D^{(2)} + \left(r - \delta - \frac{1}{2}\sigma^2 - \lambda\kappa\right) \left(\frac{2}{l}\right) D^{(1)} - (r + \lambda)I. \quad (6.3.3)$$

Here I , $D^{(1)}$ and $D^{(2)}$ denote the identity, the first and the second differentiation matrices, respectively.

We first split the integral part into following two parts [4] and then evaluate them at inner grid points x_j for $j = 0, 1, \dots, N$, :

$$\int_{-\infty}^{\infty} V(x, t)f(y-x)dy = \int_{x_m}^{x_M} V(x, t)f(y-x)dy + \int_{\mathbb{R} \setminus [x_m, x_M]} V(x, t)f(y-x)dy. \quad (6.3.4)$$

We use the Clenshaw-Curtis quadrature rule to compute the first integral over the

interval $[x_m, x_M]$

$$\begin{aligned}
 \int_{x_m}^{x_M} V(x, t) f(y - x) dy &= \frac{1}{2} l \int_{-1}^1 V(x, t) f(y - x) d\varepsilon \\
 &= \frac{1}{2} l \int_{-1}^1 g'(\varepsilon) V(x, t) f(y - x) d\xi, \\
 &= \frac{1}{2} l \int_{-1}^1 g'(\varepsilon) f(y - x) u(\xi, t) d\xi, \\
 &= \frac{1}{2} l \sum_{k=0}^N w_k g'(\varepsilon_k) f(x_k - x_j) u(\xi_k, t). \tag{6.3.5}
 \end{aligned}$$

The sum in (6.3.5) can be computed using matrix notations, i.e.,

$$\frac{1}{2} l \sum_{k=0}^N w_k g'(\varepsilon_k) f(x_k - x_j) u(\xi_k, t) = J \mathbf{u}(t), \tag{6.3.6}$$

where J is a $(N + 1) \times (N + 1)$ matrix with entries

$$J_{jk} = \frac{1}{2} l w_k g'(\varepsilon_k) f(x_k - x_j). \tag{6.3.7}$$

The second integral over $\mathbb{R} \setminus [x_m, x_M]$ is equal to zero for European butterfly spread options. For the European call options, we can explicitly calculate the outer integral in Merton's model using the boundary conditions (6.2.8)

$$\ell(x, t) = \int_{\mathbb{R} \setminus [x_m, x_M]} V(x, t) f(y - x) dy = \int_{\mathbb{R} \setminus [x_m, x_M]} (Ee^x - Ee^{-rt}) f(y - x) dy. \tag{6.3.8}$$

Hence using the explicit value of the probability density function in the case of Merton's model, (6.3.8) yields

$$\ell(x, t) = Ee^{x+\mu+\frac{\sigma_J^2}{2}} \Phi\left(\frac{x - x_M + \mu + \sigma_J^2}{\sigma_J}\right) - Ee^{-rt} \Phi\left(\frac{x - x_M + \mu}{\sigma_J}\right), \tag{6.3.9}$$

where the cumulative normal distribution Φ is defined by

$$\Phi(z) = \frac{1}{\sqrt{2\pi}} \int_{-\infty}^z e^{-\frac{y^2}{2}} dy. \quad (6.3.10)$$

It should be noted that in either case, the unbounded integral (6.3.8) can be expressed as

$$\ell(x, t) = \ell_1(x) + \ell_2(x)e^{-rt}. \quad (6.3.11)$$

After collecting all the terms of the differential and the integral parts, a semi-discretised form of the PIDE is obtained

$$\dot{\mathbf{u}}(t) = \tilde{A}\mathbf{u}(t) + \lambda\zeta(t), \quad (6.3.12)$$

where $\tilde{A} = D_N + \lambda J$ is a $(N+1) \times (N+1)$ matrix, $\mathbf{u}(t) = [u(x_0, t), u(x_1, t) \dots u(x_N, t)]^T$ and $\zeta(t) = [\ell(x_0, t), \ell(x_1, t) \dots \ell(x_N, t)]^T$.

We solve the system (6.3.12) by using an efficient time integration method as described in the next section.

6.4 Time integration

The main challenge when dealing with problems of type (6.3.12) is that the explicit time integrators are inadequate because the diffusive term which is typically stiff, necessitates excessively small time steps. On the other hand, the use of stiffly accurate implicit time integrators which are unconditionally stable, is not practically feasible due to the non-local form of the integral term. In order to avoid these problems, it could be interesting to separate the non-stiff and the stiff terms. The non-stiff term has to be solved explicitly whereas the stiff term has to be integrated implicitly. Such time integrators are known as implicit-explicit (IMEX) time integrators and have been used for time integration of spatially discretised PDEs of reaction-diffusion type ([115]). In this chapter, we use IMEX-PC methods to integrate the system of ODEs obtained after

spatial discretisation of the European call options under jump-diffusion processes.

To begin with, let us write the system of ODEs (6.3.12) in the form

$$\frac{d\mathbf{u}}{dt} = A\mathbf{u} + \mathbf{g}(t, \mathbf{u}), \quad \mathbf{u}(t_0) = \mathbf{u}_0, \quad (6.4.1)$$

where $\mathbf{u}(t) = [u(x_0, t), u(x_1, t) \dots u(x_N, t)]^T$,

$$A = \frac{1}{2}\sigma^2 \left(\frac{2}{l}\right)^2 D^{(2)} - (r + \lambda)I$$

is a $(N + 1) \times (N + 1)$ matrix and

$$\mathbf{g}(\mathbf{u}, t) = \left(r - \delta - \frac{1}{2}\sigma^2 - \lambda\kappa\right) \left(\frac{2}{l}\right) D^{(1)}\mathbf{u} + \lambda J\mathbf{u} + \lambda\zeta(t).$$

To simulate (6.4.1) in time direction, we use the IMEX-PC method (3.4.8)-(3.4.9) discussed in previous chapter.

6.4.1 Convergence and stability results for the implicit-explicit predictor-corrector methods

The stability analysis of the IMEX-PC schemes (3.4.2)-(3.4.3) when applied to the PIDE (6.2.4) is investigated as follows. The first step is to find a spectral representation of this problem. To this end we consider the following change of variable:

$$V(x, t) = e^{i\xi x} u(t). \quad (6.4.2)$$

The substitution of (6.4.2) into PIDE (6.2.4) yields the scalar test equation

$$u' = F(\xi)u(t) + G(\xi)u(t), \quad (6.4.3)$$

where $F(\xi) = -\frac{1}{2}\sigma^2\xi^2$ and $G(\xi) = i\xi(r - \delta - \frac{\sigma^2}{2} - \kappa\lambda) + (r + \lambda) + \lambda \int_{\mathbb{R}} e^{i\xi z} f(z) dz$.

Applying IMEX-PC methods (3.4.2)-(3.4.3) to the scalar test equation (6.4.3) with

step-size k , we obtain

$$(a_s - kH(\xi)b_s)\tilde{u}_{n+s} = \sum_{j=0}^{s-1} [-a_j + kH(\xi)b_j + kG(\xi)c_j]u_{s+j}, \quad (6.4.4)$$

and

$$(a_s - kH(\xi)b_s)u_{n+s} = \sum_{j=0}^{s-1} [-a_j + kH(\xi)b_j + kG(\xi)b_j]u_{s+j} + kG(\xi)b_s\tilde{u}_{n+s}. \quad (6.4.5)$$

Substituting the following variables $z = kH(\xi)$, $w = kG(\xi)$ and $R^n = u_n$, into the equations (6.4.4) and (6.4.5) and plugging (6.4.4) into (6.4.5), we get the following characteristic equation

$$\varphi(R; z, w) = R^s - \sum_{j=0}^{s-1} \left[\frac{-a_j + zb_j + wb_j}{(a_s - zb_s)} + \frac{wb_s}{(a_s - zb_s)^2}(-a_j + zb_j + wc_j) \right] R^j. \quad (6.4.6)$$

Note that the IMEX-PC is linearly stable when all the roots of the characteristic polynomial (6.4.6) have modulus less than or equal to one. In other words, let $R_i(z, w)$, for $i = 1, 2, \dots, s$ be the roots of the characteristic polynomial. Then we define the stability region S of the method as

$$S = \{(z, w) \in \mathbb{C}^2 : |R_i(z, w)| \leq 1, \forall i\}. \quad (6.4.7)$$

The root of the characteristic polynomial of the IMEX-PC(1,2) is given as

$$R(z, w) = \frac{1 - \gamma z + z + \gamma^2 z^2 - \gamma z^2 + w + \gamma w^2}{(1 - \gamma z)^2}. \quad (6.4.8)$$

For higher steps PC methods, we will not display general expressions of their characteristic polynomials; we confine our study to specific cases. The choice $(\gamma, c) = (1, 0)$ gives the following characteristic polynomial

$$\left[z - \frac{3}{2} \right] R^2 + \left[2 + \frac{4w + wz + 4w^2}{3 - 2z} \right] R - \left[\frac{1}{2} + \frac{w + 2w^2}{3 - 2z} \right] = 0. \quad (6.4.9)$$

Similarly, the choice $(\gamma, \theta, c) = (1, 0, 0)$ for 3-steps PC gives

$$\left[\frac{11}{6} - z \right] R^3 - \left[3 + \frac{6w(3+3w)}{11-6z} \right] R^2 - \left[-\frac{3}{2} + \frac{6\mu(-3-6\mu)}{22-12\lambda} \right] R - \left[\frac{1}{3} + \frac{6\mu(2+6\mu)}{11-6\lambda} \right] = 0. \quad (6.4.10)$$

Figure 6.4.1 represents the stability region (6.4.7) for the schemes (3.4.2) and (3.4.3)

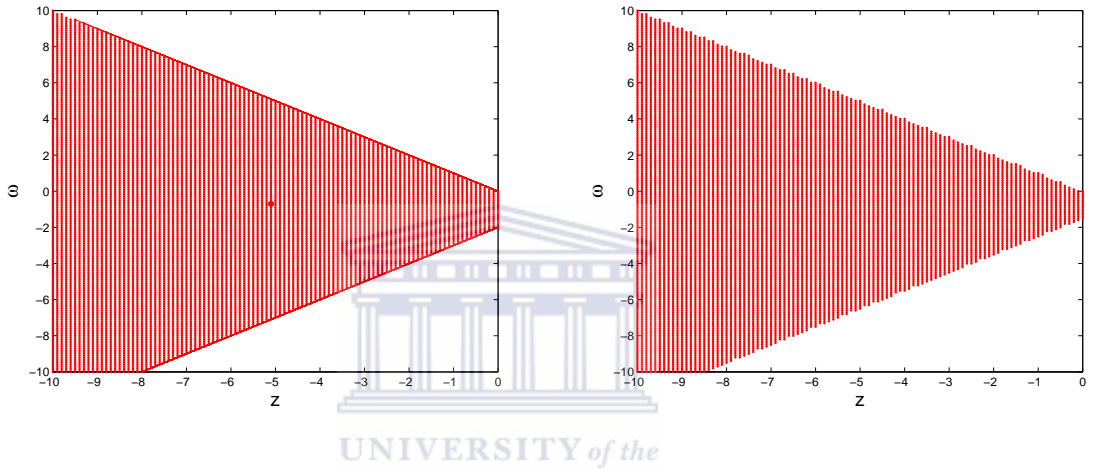


Figure 6.4.1: Stability regions of schemes (6.4.9) (left figure) and (6.4.10) (right figure)

in the $z - \omega$ plane.

6.5 Numerical results

In this section, we perform a number of numerical experiments which illustrate the performance and convergence of our method for valuing options described in Chapter 1, viz, European call and butterfly spread options under Merton's model.

6.5.1 Valuation of European call options

There exists an analytical solution for an European call option under Merton's jump-diffusion process. In particular for $\mu = 0$ the analytical solution of (6.2.4) and its Δ

and Γ are then given by

$$V(S, t) = \sum_{m=0}^{\infty} \frac{e^{-\lambda' t} (\lambda' t)^m}{m!} V_{BS}(t, S, E, r_m, \sigma_m, \delta), \quad (6.5.1)$$

$$\Delta(S, t) = \sum_{m=0}^{\infty} \frac{e^{-\lambda' t} (\lambda' t)^m}{m!} \Delta_{BS}(t, S, E, r_m, \sigma_m, \delta), \quad (6.5.2)$$

$$\Gamma(S, t) = \sum_{m=0}^{\infty} \frac{e^{-\lambda' t} (\lambda' t)^m}{m!} \Gamma_{BS}(t, S, E, r_m, \sigma_m, \delta), \quad (6.5.3)$$

where $t = T - \tau$, $\lambda' = \lambda(1 + \kappa)$, $\sigma_m^2 = \sigma^2 + m\sigma_J/t$, $r_m = r - \lambda\kappa + (m \ln(1 + \kappa))/t$, and the Black-Scholes price for a call, its Δ and Γ are given by

$$V_{BS}(t, S, E, r_m, \sigma_m, \delta) = S\Phi(d_1) - Ee^{-rt}\Phi(d_2), \quad (6.5.4)$$

$$\Delta_{BS}(t, S, E, r_m, \sigma_m, \delta) = e^{-\delta t}\Phi(d_1), \quad (6.5.5)$$

$$\Gamma_{BS}(t, S, E, r_m, \sigma_m, \delta) = e^{-\delta t} \frac{\Phi'(d_1)}{\sigma S \sqrt{t}}, \quad (6.5.6)$$

where

$$d_1 = \frac{\log(S/E) + (r - \delta + \frac{\sigma^2}{2})}{\sigma \sqrt{t}}, \quad d_2 = d_1 - \sigma \sqrt{t},$$

and the cumulative normal distribution Φ is defined by

$$\Phi(z) = \frac{1}{\sqrt{2\pi}} \int_{-\infty}^z e^{-\frac{y^2}{2}} dy. \quad (6.5.7)$$

We solve the PIDE (6.2.4) using the parameters presented in Table 6.5.1 by using our spectral collocation method. In our experiments, unless otherwise indicated, the spectral collocation method is combined with the IMEX-PC(3,3). We choose the grid stretching parameter $\alpha = 10^4$ and the computational domain between $x_{\min} = -1.5$ and $x_{\max} = 1.5$ to ensure the accuracy of the solutions. The number of space grid points $N = 80$ and the number of time grid points $M = 800$. The term ‘Ratio’ is defined as in Chapter 3 In Figure 6.5.1, we compare the numerical and analytical solutions for

Table 6.5.1: Data used to value a vanilla call option under Merton's model

| Parameters | r | ρ | δ | μ | σ_J | λ | E | T |
|------------|------|--------|----------|-------|------------|-----------|-----|-----|
| Values | 0.05 | 0.20 | 0.00 | 0.00 | 0.2 | 2 | 100 | 0.5 |

the European call option under jump-diffusion and pure diffusion ($\lambda = 0$) processes. Clearly, numerical solutions are in good agreement with analytical ones. The difference between the jump-diffusion process and the pure diffusion process is shown in Figure 6.5.1 and is quite substantial [128].

Although numerical solution appear to be in good agreement with exact solutions, their derivatives may be subject to large errors. Therefore, it is also important to look at the Greeks, in particular the first derive, Δ , and the second derivative, Γ . Greeks measure the sensitivity of the option value to variations in asset price and parameters of the model [128].

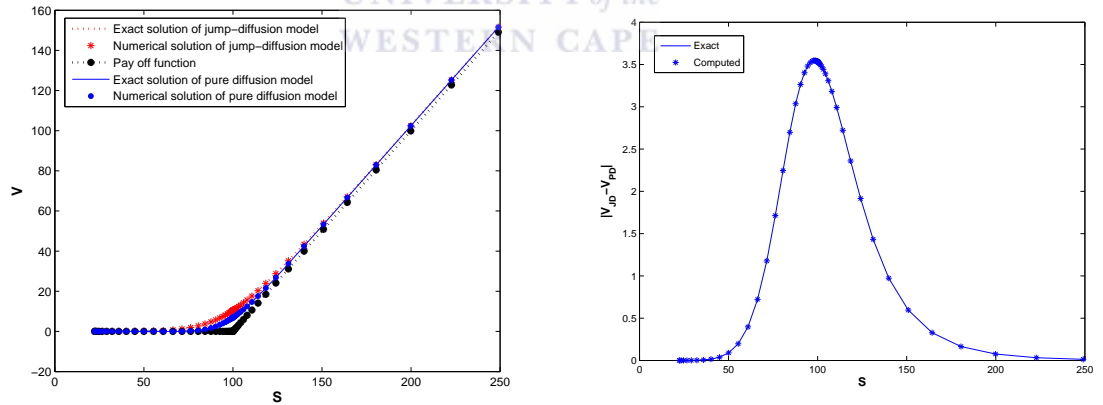


Figure 6.5.1: Numerical and analytical solutions of European call under jump and pure diffusion models (left figure) and difference between values of European call under jump and pure diffusion (right figure) with parameters given in Table 6.5.1. The other parameters $\alpha = 10^4$, $x_{\min} = -1.5$, $x_{\max} = 1.5$, $N = 80$ and $M = 800$.

Figure 6.5.2 shows that numerical values of $\Delta (= \partial V / \partial S)$ and $\Gamma (= \partial^2 V / \partial S^2)$ are in good agreement with those of their exact values.

We next investigate the convergence behaviour of our spectral collocation method for the solution of the jump-diffusion model with the parameters of Table 6.5.1. We

choose to calculate the error of our scheme for European call under Merton's model and its Greeks at the strike price which is a point of most financial interest. Figure 6.5.3 shows the convergence in V , Δ and Γ of the finite difference, spectral collocation with Chebyshev-Gauss-Lobatto (CGL) points and spectral collocation methods with mapped Chebyshev-Gauss-Lobatto points while varying the mapping parameter α . To ensure that the numerical error is dominated by the space discretisation, we choose the number of time grid points as $M = 800$.

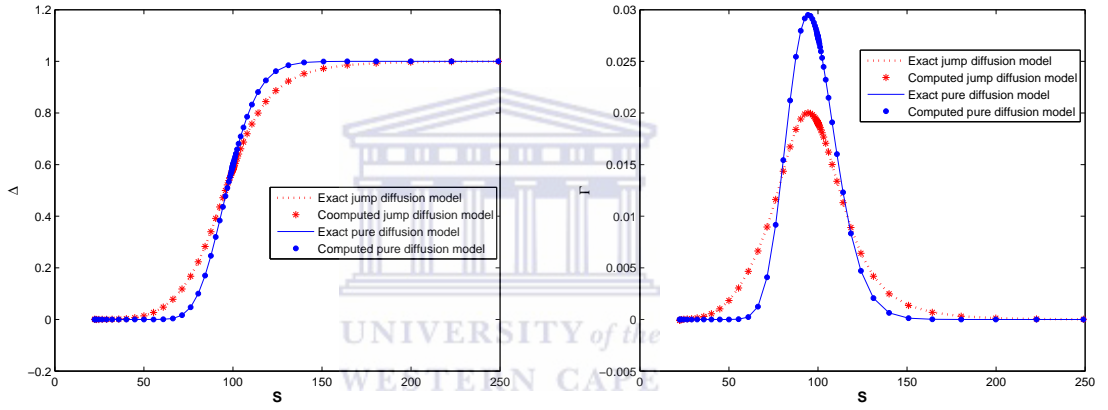


Figure 6.5.2: Numerical and analytical values of the Δ (left figure) and Γ (right figure) European call under jump-diffusion and pure diffusion model, with parameters given in Table 6.5.1. The other parameters are $\alpha = 10^4$, $x_{\min} = -1.5$, $x_{\max} = 1.5$, $N = 80$ and $M = 800$.

One can observe from Figure 6.5.3 that the spectral collocation method has a moderately smaller error than that of the finite difference method. Numerically, higher order methods, in particular spectral methods have difficulty in accurately approximating the solution in the region of singularity, i.e., the region of dramatic change. In the present case, the first derivative of the initial condition is discontinuous at the strike price E which explains the poor convergence of the spectral collocation method with CGL points. Using a high resolution grid in the region of dramatic change through the use of coordinate transformations (1.2.31), we observe a significant improvement of the convergence of spectral methods. We obtained exponential convergence of the method both for the evaluation of V and the Greeks. Once the temporal error dominates, the

Table 6.5.2: Numerical results for pricing European call options under jump-diffusion process at the spot price $S = 100$ using parameters given in Table 6.5.1. The other parameters are $\alpha = 10^4$, $x_{\min} = -1.5$, $x_{\max} = 1.5$, $N = 80$ and $M = 800$.

| N | M | T=0.5 | | | T=1 | | | T=2 | | |
|-----|-----|---------|--------|-------|---------|---------|--------|---------|---------|--------|
| | | Error | Ratio | CPU | Error | Ratio | CPU | Error | Ratio | CPU |
| 20 | 25 | 2.34E-2 | - | 0.035 | 6.34E-2 | - | 0.039 | 8.84E-2 | - | 0.039 |
| 40 | 50 | 3.23E-5 | 715.61 | 0.061 | 4.02E-5 | 1574.90 | 0.069 | 5.15E-5 | 1715.80 | 0.069 |
| 80 | 100 | 2.45E-6 | 13.30 | 0.145 | 3.24E-6 | 12.42 | 0.155 | 5.90E-6 | 8.73 | 0.164 |
| 160 | 200 | 1.23E-7 | 19.91 | 0.780 | 7.48E-7 | 4.33 | 0.808 | 1.76E-6 | 3.34 | 1.065 |
| 320 | 400 | 1.46E-8 | 8.46 | 9.665 | 3.83E-7 | 1.95 | 10.800 | 1.41E-6 | 1.25 | 10.727 |

decay becomes algebraic as expected.

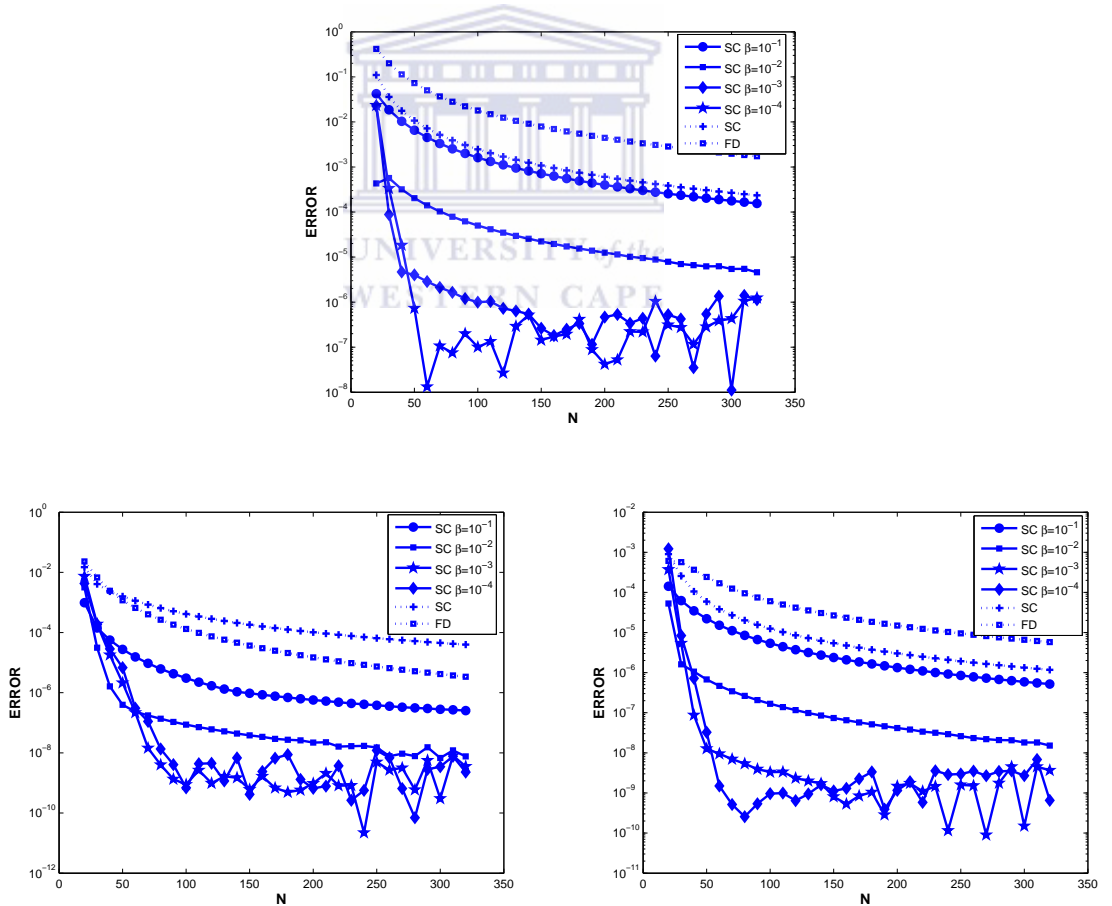


Figure 6.5.3: Error vs. N at spot price $S = 100$, for the spectral collocation (with different values of α) and the finite difference methods for pricing European call options (top figure), Δ (left bottom figure) and Γ (right bottom figure) using the parameters given in Table 6.5.1. The other parameters are $x_{\min} = -1.5$, $x_{\max} = 1.5$ and $M = 800$.

The exponential convergence of our approach is confirmed by the results presented in Table 6.5.2. We compute the European call option with jump for four levels of accuracy at three maturity times $T = 0.5$, $T = 1$ and $T = 2$. We observe that our method converges exponentially even for long maturity time options. Satisfactory results are found with a few number of grid points in a very small amount of computing time, i.e., an error of the order of 10^{-5} at the maturity time $T = 0.5$ can be obtained with a total of only 40 points and 50 time steps in 70 milliseconds. Both figures 6.5.1 and 6.5.2 show that the option values and Greeks are very stable and no spurious oscillations occur. Furthermore, Figure 6.5.3 and Table 6.5.2 show that our spectral collocation method combined with the IMEX-PC(3,3) is efficient as compared to FD method and exponentially convergent for valuing European option under Merton's jump-diffusion model.



6.5.2 Valuation of European butterfly spread options

In this subsection, we investigate performance of our proposed method for valuing European butterfly options under jump-diffusion model at the strike price E_2 using the parameters presented in Table 6.5.3. In this particular case, we need to stretch grid points at three different strike prices in order to improve the accuracy of the spectral collocation method. The suitable map is chosen from (1.2.31) where the grid stretching parameters are taken as $\alpha_1 = \alpha_2 = \alpha_3 = 10^4$. Figure 6.5.4 shows that the numerical

Table 6.5.3: Data used to value a butterfly spread option under Merton's model

| Parameters | r | ρ | δ | μ | σ_J | λ | E_1 | E_3 | T |
|------------|------|--------|----------|-------|------------|-----------|-------|-------|-----|
| Values | 0.05 | 0.20 | 0.00 | 0.00 | 0.2 | 2 | 100 | 0.5 | 0.5 |

and exact solutions are in good agreement in both cases of pure diffusion and jump-diffusion models. Once again, the difference between the jump-diffusion process and the pure diffusion process is shown in Figure 6.5.4 and it is quite substantial. From Figure 6.5.5 we observe that the numerical approximations for Δ and Γ are in a good agreement with the exact ones.

Table 6.5.4: Numerical results for pricing European butterfly spread options under jump-diffusion process at the spot price $S = 100$ using parameters given in Table 6.5.3. The other parameters are $\alpha = 10^4$, $x_{\min} = -1.5$, $x_{\max} = 1.5$, $N = 80$ and $M = 800$.

| N | M | T=0.5 | | | T=1 | | | T=2 | | |
|-----|-----|---------|---------|--------|---------|---------|--------|---------|--------|--------|
| | | Error | Ratio | CPU | Error | Ratio | CPU | Error | Ratio | CPU |
| 20 | 25 | 4.36E-2 | - | 0.071 | 3.35E-2 | - | 0.072 | 3.71E-2 | - | 0.073 |
| 40 | 50 | 3.73E-2 | 1.17 | 0.091 | 2.29E-2 | 1.46 | 0.096 | 1.43E-2 | 2.59 | 0.090 |
| 80 | 100 | 1.61E-5 | 2315.20 | 0.345 | 1.22E-5 | 1882.00 | 0.347 | 1.91E-5 | 747.37 | 0.364 |
| 160 | 200 | 2.10E-6 | 7.68 | 1.780 | 4.03E-6 | 3.03 | 1.808 | 8.53E-6 | 2.24 | 1.865 |
| 320 | 400 | 6.95E-7 | 3.02 | 11.665 | 2.33E-6 | 1.72 | 11.800 | 5.70E-6 | 1.50 | 11.727 |

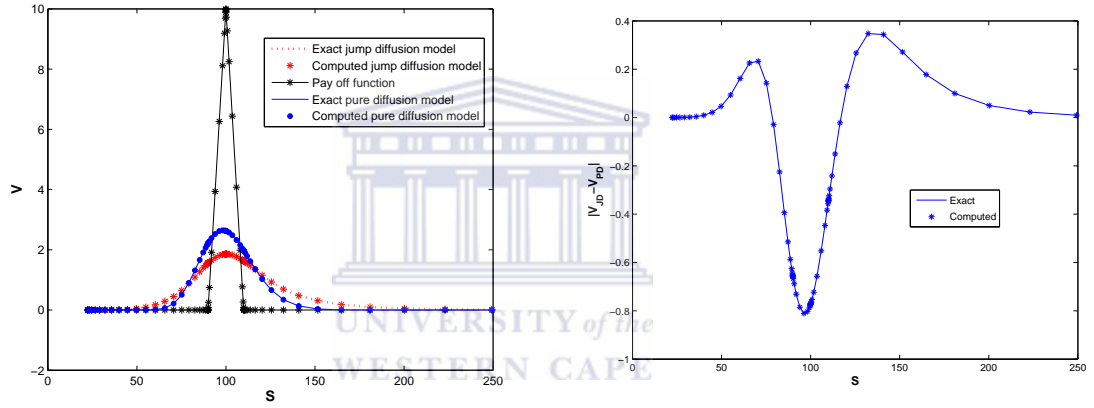


Figure 6.5.4: Numerical and analytical solutions of European butterfly spread options under jump and pure diffusion models (left figure) and difference between values of European butterfly spread options under jump and pure diffusion (right figure) using parameters given in Table 6.5.3. The other parameters are $\alpha = 10^4$, $x_{\min} = -1.5$, $x_{\max} = 1.5$, $N = 80$ and $M = 800$.

From Figure 6.5.6, we observe that very rapid convergence is achieved in the case of European butterfly spread option which has three regions of singularity. Our approach allows the use of high resolution grids around the strike prices E_1 , E_2 and E_3 which significantly improves the convergence of usual spectral collocation methods. Rapid convergence is also observe when we calculate the Δ and the Γ of the European butterfly spread options under jump-diffusion model. In this case, the convergence is slower than that in the case of European call under jump-diffusion but is still exponential.

It is interesting to compare the convergence of our method with the finite difference method with uniform grids and spectral collocation method with CGL points. We see

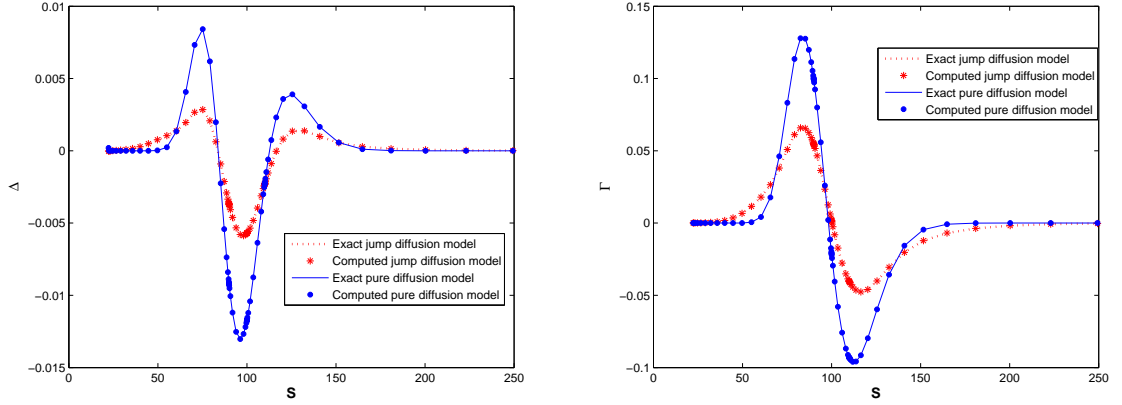


Figure 6.5.5: Numerical and analytical values of the Δ (left figure) and Γ (right figure) European butterfly spread options under jump-diffusion and pure diffusion model, using parameters given in Table 6.5.3. The other parameters are $\alpha = 10^4$, $x_{\min} = -1.5$, $x_{\max} = 1.5$, $N = 80$ and $M = 800$.

that we need very few number of spatial points for our spectral method to get the same level of accuracy. For instance, on the plot of European butterfly spread options, an error of 10^2 requires $N = 188$ for the spectral collocation method with CGL points, $N = 110$ points for the finite difference method, but requires only $N = 45$ points for our spectral collocation method. One can note from Figure 6.5.6 that a large number of points have been used in the case of finite difference and spectral collocation method based on CGL points, while only a few number of points are needed for our spectral collocation method to achieve the same accuracy.

The exponential accuracy of our method is further corroborated by the results presented in Table 6.5.4. We compute the European butterfly spread option with jump with four different spatial mesh points at three maturity times $T = 0.5$, $T = 1$ and $T = 2$. We observe that our approach is exponentially convergent even for long maturity options although the convergence is slower than in the case of European call option. Satisfactory results are found with a few number of grid points in a small amount of computing time, i.e., an error of 10^{-5} at the maturity time $T = 0.5$ can be obtained with a total 80 points and 100 time steps in 0.4 seconds. Our spectral collocation method

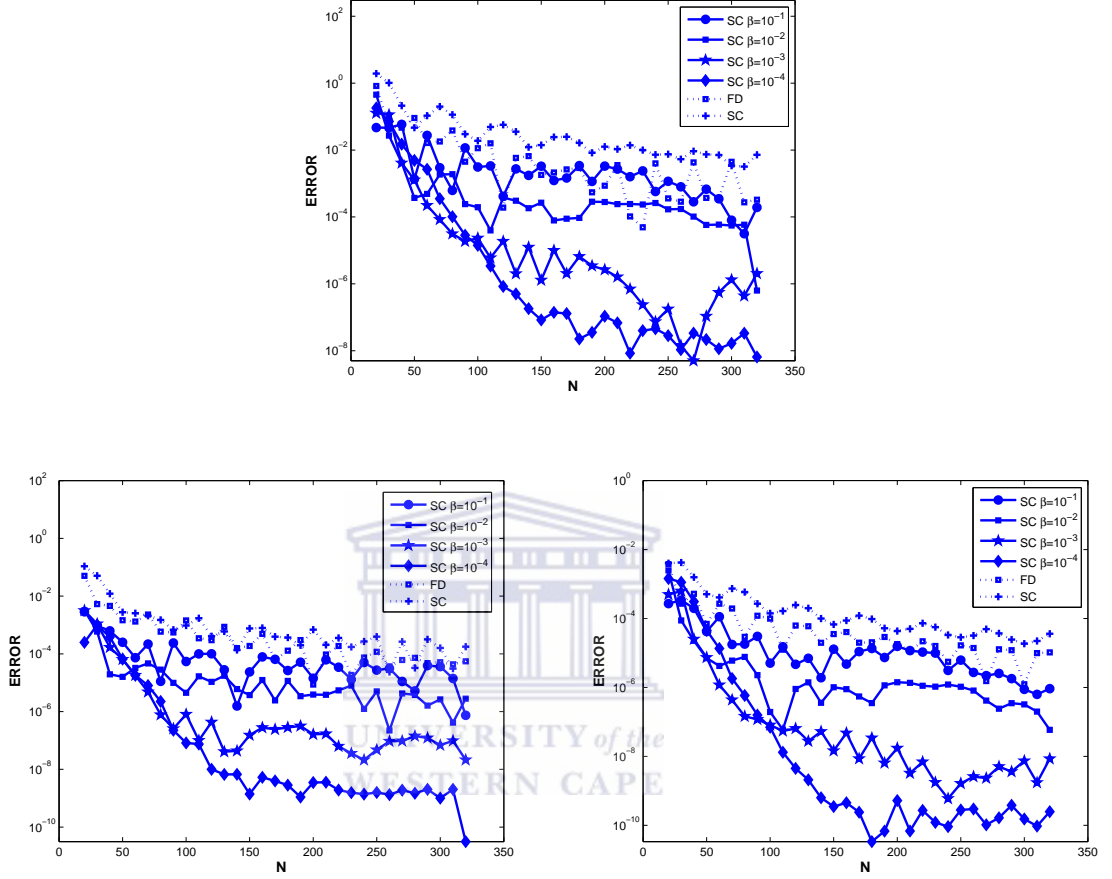


Figure 6.5.6: Error vs. N at spot price $S = 100$, for the spectral collocation (with different values of α) and the finite difference methods for pricing European butterfly spread options (top figure), Δ (left bottom figure) and Γ (right bottom figure) using parameters given in Table 6.5.1. The other parameters are $x_{\min} = -1.5$, $x_{\max} = 1.5$ and $M = 800$.

combined with the IMEX-PC(3, 3) is also efficient and exponentially convergent for valuing European butterfly spread option under Merton's jump-diffusion model.

6.6 Summary and discussions

We have proposed a spectral collocation method in space in combination with the third order IMEX-PC time marching method for pricing European vanilla and butterfly spread options under Merton's jump-diffusion model. Extensive comparisons were

carried out with the standard finite difference method and the spectral collocation with Chebyshev-Gauss-Lobatto points. In all experiments our spectral collocation method has exponential convergence when we use adaptive grid, whereas poor convergence is recorded for the finite difference method and the spectral collocation with Chebyshev-Gauss-Lobatto points. We also obtain exponential convergence in our approach for valuing the Δ and Γ for both European call and butterfly spread options.

In next chapter, we construct the numerical method for solving the partial integro-differential equations and partial integro-differential complementary problems associated with the American style jump-diffusion models.



Chapter 7

Spectral collocation methods to price American options with jump-diffusion processes



In this chapter, we present a spectral method based on a penalty approach for solving partial integro-differential complementary (PIDC) problems arising from pricing American options when the underlying assets are driven by a jump-diffusion process under constant and local volatility. The PIDC problem is first reformulated as a variational inequality. Then it is transformed into a nonlinear partial integro-differential equation (PIDE) on fixed boundaries by adding a penalty term. This nonlinear PIDE is discretised in asset (space) direction by means of a spectral method using suitable barycentric weights and transformed Chebyshev points. The differential and integral parts of the PIDE are approximated by the rational spectral collocation method and the Clenshaw-Curtis quadrature formula, respectively. The application of spectral collocation methods to the PIDE leads to a system of ordinary differential equations which is solved using the implicit forth-order Lobatto time integration method.

7.1 Introduction

One of the well known stochastic models linking the equilibrium condition between the expected return on the option, the expected return on the stock and the riskless interest rate is the Black-Scholes equation derived by Black and Scholes [21]. In recent years, many shortcomings of the Black-Scholes model are identified, and subsequently more general models for stochastic dynamics of the risky assets have been developed; in particular, stochastic volatility models [73, 76], deterministic local volatility functions [43, 56], jump-diffusion models [86, 102], Lévy models [99, 112] among others. In this chapter, we consider the jump-diffusion approach with constant and local volatility to value American options.

Pricing American options under jump-diffusion processes are more challenging than those without jumps. The reason being the presence of a non-local integral term. In literature, several classes of numerical methods have been proposed to solve such problems. Briani *et al.*[29] used the fully explicit schemes, although their approach required very restrictive conditions for stability. Cont and Volchkova [44] used implicit schemes to treat the differential part. The use of the Crank-Nicolson time stepping method for the PDE portion and evaluation of the convolution integral term explicitly were tested by Tavella and Randall [128]. However, such an asymmetric treatment of PDE and integral part introduces biases in the viscosity solution. More specifically, the second order convergence is not achieved for long dated options. d'Halluin *et al.* [55] employed the Crank-Nicolson scheme with the Rannacher time smoothing to the PIDE with a fixed point iterative procedure as the system solver and obtained second order convergence even for long dated options. Andersen and Andreasen [5] derived a forward PIDE for European call options and applied it to the calibration problem. They also used an unconditionally stable operator splitting (ADI) finite difference method and used the fast Fourier transform (FFT) to accelerate the scheme. Almendral and Oosterlee [4] proposed a matrix splitting technique to price European options under jump-diffusion processes. To avoid the wrap around effect, they embedded the resulting

Toeplitz matrix into a circulant matrix.

Towards the improvements in some of the approaches mentioned above, Feng and Linetsky [58] proposed an approach that combined extrapolation and implicit-explicit Euler (IMEX-Euler). Their approach was a significant improvement on the classical IMEX-Euler scheme and was found very competitive for short maturity options. Mayo [100] showed how to use the operator splitting of Andersen and Andreasen [5] to reduce the solution of the pricing equation in the Kou's [86] and similar models to a sequence of ODEs that can be solved efficiently. Sachs and Strauss [116] proposed an efficient second order fully implicit method. Their approach relied on transforming the PIDE to eliminate the convection term and then to use finite difference methods on uniform grids. This exhibited a structure that can be solved efficiently by a circulant preconditioned conjugate gradient method. Subsequently, Lee and Sun [93] implemented a fourth order compact boundary value method in order to achieve the fourth order accuracy in space and time.

In this chapter, we present a spectral collocation method for valuing American options with constant and local volatility under Merton's jump-diffusion process. Spectral and pseudo-spectral methods for solving partial differential equations with smooth initial conditions have been proved to have exponential accuracy [35, 60, 124]. However, the prospects of using such methods for problems with non-smooth initial conditions remain controversial. The difficulty is mainly attributed due to the presence of the Gibbs phenomenon which appears when approximating non-smooth solutions using polynomial interpolations. This has usually a detrimental effect on the stability of the computational scheme. Thus, it is often perceived that spectral methods are too sensitive to allow the modeling of complex problems which are often non-smooth. The literature is rich with ideas for overcoming this drawback of spectral methods. One approach is to use adaptive grid methods in order to concentrate more grid points and achieve high resolution around the region where the solution changes rapidly. In this regard, the standard approach in adaptive spectral methods has been to use coordinate transformations [85, 130].

In this work, we use the rational spectral collocation method and Clenshaw-Curtis quadrature formula. We use a “tan” transformation to accommodate more grid points around the strike price. The differential and integral parts of the PIDE are approximated by the rational spectral collocation method and the Clenshaw-Curtis quadrature formula, respectively. The resulting system of ODEs is then integrated using an implicit fourth-order Lobatto time integration method.

The rest of this chapter is organised as follows. In section 7.2, we describe the formulation of the mathematical models with jump-diffusion processes in terms of a partial integro-differential equation and a partial integro-differential complementary problem. Section 7.3 deals with the spatial approximations of these models using spectral collocation method. Numerical experiments are reported in Section 7.4, whereas in Section 7.5 we present summary and discussions.

7.2 The mathematical model

Consider the financial market model $\mathcal{M} = (\Omega, \mathcal{F}, \mathbb{P}, (\mathcal{F}_\tau)_{\tau \geq 0}, (S_\tau)_{\tau \geq 0})$ where Ω is the set of all possible outcomes of the experiment known as the sample space, \mathcal{F} is the set of all events, i.e., permissible combinations of outcomes, \mathbb{P} is a map $\mathcal{F} \rightarrow [0, 1]$ which assigns a probability to each event, \mathcal{F}_τ is a natural filtration and S_τ a risky underlying asset price process. Let B_τ be a \mathbb{P} -Brownian motion, $\sigma > 0$ the volatility of the underlying asset, $r > 0$ a risk-free interest rate, $\delta \geq 0$ a continuous dividend yield. Without loss of generality, we assume that both the risk-free interest rate and the dividend yield are constants, $(N_\tau)_{\tau \geq 0}$ is a Poisson process with identity λ and independent of B_τ ; $\eta - 1$ represents the impulse function for a jump from S to ηS and $\kappa = \mathbb{E}[\eta - 1]$ is the expectation of the impulse. Then under the equivalent martingale measure \mathbb{Q} , the dynamics of the jump-diffusion model satisfies the stochastic differential equation

$$\frac{dS_\tau}{S_\tau} = (r - \delta - \lambda\kappa)d\tau + \sigma dB_\tau + (\eta - 1)dN_\tau. \quad (7.2.1)$$

Let $V(S, \tau)$ denotes the value of the options with strike price E depending on the underlying asset S and the time τ . Using the arguments in [141], the following backward partial integro-differential equation (PIDE) can be derived from the above equation:

$$V_t = \frac{1}{2}\sigma^2 S^2 V_{SS} + (r - \delta - \lambda\kappa)SV_S - (r + \lambda)V + \lambda \int_0^\infty V(S\eta)g(\eta)d\eta, \quad (7.2.2)$$

where $S \in [0, +\infty)$, $t \in [0, T]$, with T the maturity time, $t = T - \tau$, $g(\eta)$ is the probability density function of the jump amplitude η and must satisfy $\int_0^\infty g(\eta)d\eta = 1$. In the case of Merton jump-diffusion model, $g(\eta)$ is given by the log-normal density

$$g(\eta) = \frac{1}{\sqrt{2\pi}\sigma_J} \eta e^{-\frac{(\ln \eta - \mu)^2}{2\sigma_J^2}}, \quad (7.2.3)$$

where μ is the mean and σ_J the standard deviation with the expected value of the jump size κ in (7.2.2) given by

$$\kappa = e^{\mu + \frac{\sigma_J^2}{2}}. \quad (7.2.4)$$

We first note that the integrals can be written as correlation integrals. That is, by making the exponential changes of variables $S = Ee^s$, $\eta = e^z$ the PIDE (7.2.2) can be rewritten as

$$V_t = \frac{1}{2}\sigma^2 V_{ss} + (r - \delta - \frac{1}{2}\sigma^2 - \lambda\kappa)V_s - (r + \lambda)V + \lambda \int_{-\infty}^\infty V(s + z, t)f(z)dz, \quad (7.2.5)$$

If we define the right hand side in the above equation by $L_{JD}V$, i.e.,

$$L_{JD}V \equiv \frac{1}{2}\sigma^2 V_{ss} + (r - \delta - \frac{1}{2}\sigma^2 - \lambda\kappa)V_s - (r + \lambda)V + \lambda \int_{-\infty}^\infty V(s + z, t)f(z)dz, \quad (7.2.6)$$

and if the $V^*(S)$ is the payoff, then the American jump-diffusion option problem can

be stated in the following partial integro-differential complementary problem (PIDC)

$$\left. \begin{aligned} V_t - L_{JD}V &\geq 0, \\ V - V^* &\geq 0, \\ (V_t - L_{JD}V)(V - V^*) &= 0. \end{aligned} \right\} \quad (7.2.7)$$

In case of American jumps diffusion models under local volatility $\sigma_L(S, t)$ a similar PIDE is given as

$$V_t = \frac{1}{2}\sigma_L^2(S, t)V_{ss} + (r - \delta - \frac{1}{2}\sigma_L^2(S, t) - \lambda\kappa)V_s - (r + \lambda)V + \lambda \int_{-\infty}^{\infty} V(x + z, t)f(z)dz. \quad (7.2.8)$$

To solve the above problems, we use the local volatility function $\sigma_L(S, t)$, given by (5.4.1).

In next section, we propose a spectral discretisation method based on a penalty approach to solve the American option problems.

7.3 Spectral space discretisation of the nonlinear PIDE

We consider the problem of pricing American options under jump-diffusion process given by (7.2.7) which involves an unknown boundary. The model is approximated by an nonlinear partial-integro differential equation on a fixed domain by adding a penalty term yielding

$$\left. \begin{aligned} V_t &= L_{JD}V + \frac{1}{\epsilon} [V - V^*]^+, \quad -\infty < S < +\infty, \quad 0 \leq t \leq T, \\ V^*(s) &= V(s, 0) = \max(E - Ee^s, 0), \\ V(S, t) &= E - Ee^s, \quad s \rightarrow -\infty, \\ V(s, t) &= 0, \quad s \rightarrow +\infty, \end{aligned} \right\} \quad (7.3.1)$$

where $0 < \epsilon \ll 1$ is the penalty constant and $[V - V^*]^+$ is the penalty term with $[V - V^*]^+ = \max(V - V^*, 0)$. We then describe the application of the rational spectral

collocation method combined with the Clenshaw-Curtis quadrature rule to discretise the PIDE (7.3.1) and transform it into a system of ODEs which is then integrated by the fourth order implicit Lobatto time integrator [68]. Let $x_j = g(y(j))$, $y(j) = \cos(\pi j/N)$ be the transformed Chebyshev points; and s_m and s_M the minimum and the maximum values of s , respectively. Writing $V(s, t) = u(x, t)$, the PDE part of the PIDE (7.3.1) can be written as

$$\frac{\partial u}{\partial t} = p(x) \frac{\partial^2 u}{\partial x^2} + q(x) \frac{\partial u}{\partial x} - (r + \lambda)u + f(u), \quad (7.3.2)$$

with

$$p(x) = \frac{1}{2} \sigma^2 \left(\frac{2}{s_M - s_m} \right)^2, \quad q(x) = \left(r - \delta - \frac{1}{2} \sigma^2 - \lambda \kappa \right) \left(\frac{2}{s_M - s_m} \right), \quad f(u) = \frac{1}{\epsilon} [u - u^0]^+.$$

In order to write the expression (7.3.2) in matrix form, we introduce the following matrix and vector notations

$$\begin{aligned} \mathbf{u} &= [u_1, u_2, \dots, u_{N-1}]^T, \\ D^{(1)} &= \left(D_{ij}^{(1)} \right), \quad D_{ij}^{(1)} = L_j^{(\omega)'}(x_i); \quad i, j = 1, \dots, N-1, \\ D^{(2)} &= \left(D_{ij}^{(2)} \right), \quad D_{ij}^{(2)} = L_j^{(\omega)''}(x_i); \quad i, j = 1, \dots, N-1, \\ P &= \text{diag}(p(x_i)), \quad Q = \text{diag}(q(x_i)); \quad i = 1, \dots, N-1, \\ \mathbf{g} &= \left[f(u_i) + \left(p(x_i) D_{i0}^{(2)} + q(x_i) D_{i0}^{(1)} + r I_{i0} \right) u_0 \right. \\ &\quad \left. + \left(p(x_i) D_{iN}^{(2)} + q(x_i) D_{iN}^{(1)} - (r + \lambda) I_{iN} \right) u_N \right]^T, \end{aligned} \quad (7.3.3)$$

where $i = 1, \dots, N-1$ and I is a $(N+1) \times (N+1)$ identity matrix. Consequently, (7.3.2) can be expressed as a nonlinear initial value problem of the form

$$\frac{d\mathbf{u}}{dt} = D_N \mathbf{u} + \mathbf{g}, \quad (7.3.4)$$

with $D_N = P D^{(2)} + Q D^{(1)} - r I$.

To approximate the integral part, first we split the integral into two parts and then evaluate them at interior grid points x_j for $j = 1, 2, \dots, N-1$ as follows:

$$\int_{-\infty}^{\infty} V(s, t) f(z - s) dz = \int_{s_m}^{s_M} V(s, t) f(z - s) dy + \int_{\mathbb{R} \setminus [s_m, s_M]} V(s, t) f(z - s) dz. \quad (7.3.5)$$

Using the Clenshaw-Curtis quadrature rule we compute the first integral over the interval $[s_m, s_M]$ as

$$\begin{aligned} \int_{s_m}^{s_M} V(s, t) f(z - s) dz &= \frac{1}{2}(s_M - s_m) \int_{-1}^1 V(s, t) f(z - s) dy \\ &= \frac{1}{2}(s_M - s_m) \int_{-1}^1 g'(y) V(s, t) f(z - s) dx \\ &= \frac{1}{2}(s_M - s_m) \int_{-1}^1 g'(y) f(z - s) u(x, t) dx \\ &= \frac{1}{2}(s_M - s_m) \sum_{j=1}^{N-1} w_j g'(y_j) f(s_j - s_i) u(x_j, t). \end{aligned} \quad (7.3.6)$$

The right hand side in (7.3.6) can be computed in a matrix form

$$\frac{1}{2}(s_M - s_m) \sum_{j=1}^{N-1} w_j g'(y_j) f(x_j - x_i) u(x_j, t) = J \mathbf{u}(t), \quad (7.3.7)$$

where J is a $(N+1) \times (N+1)$ matrix with entries

$$J_{ij} = \frac{1}{2}(s_M - s_m) w_j g'(y_j) f(x_j - x_i). \quad (7.3.8)$$

For the American put options under jumper-diffusion process, we can explicitly calculate the outer integral in Merton's model, using the boundary conditions given in (7.3.1), as

$$\begin{aligned} \ell(s, t) &= \int_{\mathbb{R} \setminus [s_m, s_M]} V(s, t) f(z - s) dy \\ &= \int_{\mathbb{R} \setminus [s_m, s_M]} E f(z - s) dz. \end{aligned} \quad (7.3.9)$$

Hence using the explicit value of the probability density function in the case of Merton's model, (7.3.9) yields

$$\ell(s, t) = (E - Ee^{s_m})\Phi\left(\frac{s_m - s - \mu}{\sigma_J}\right), \quad (7.3.10)$$

where the cumulative normal distribution Φ is defined by

$$\Phi(z) = \frac{1}{\sqrt{2\pi}} \int_{-\infty}^z e^{-\frac{y^2}{2}} dy. \quad (7.3.11)$$

After gathering all the terms of the differential and the integral parts, a semi-discretised form of the PIDE is obtained

$$\dot{\mathbf{u}} = A\mathbf{u} + \mathbf{g} + \lambda\zeta(t), \quad (7.3.12)$$

where $A = D_N + \lambda J$ is a $(N-1) \times (N-1)$ matrix. We solve this system by using a fourth order Lobatto time integrator method.

In the next section, we investigate the performance and the convergence of our spectral collocation method for valuing American options under jump-diffusion process.

7.4 Numerical results

In this section, we present several numerical experiments to illustrate the performance of our spectral method. We consider American put options under constant and local volatility jumps diffusion process ([132]), where the local volatility function is chosen as in (5.4.1). We have tested the method for several sets of realistic parameters. Here, we give the results for a set of parameters given in Table 7.4.1. For both models, we set the computational domain so that $s_m = -1$ and $s_M = 1$, which gives $S_m = Ee^{s_m}$ and $S_M = Ee^{s_M}$; the grid stretching parameter is chosen as $\alpha = 35$. Note that the conclusions for other sets of parameters are similar to the ones reported here. To determine numerically the order of convergence rate of the discretisation scheme, we

Table 7.4.1: Data used to value American options under Merton's model

| Parameters | r | ρ | δ | μ | σ_J | λ | E | T |
|------------|------|--------|----------|-------|------------|-----------|-----|-----|
| Values | 0.05 | 0.20 | 0.00 | 0.00 | 0.2 | 0.5 | 100 | 0.5 |

define the ‘Ratio’ of the differences between numerical and benchmark solutions at strike price using N and $2N$ grid points, respectively. As a benchmark solution, we choose the solutions computed with our method with $N = 500$ mesh points, $\epsilon = 10^{-9}$ the penalty parameter and $TOL = 10^{-9}$ the tolerance for the time integrator.

7.4.1 Valuation of American jump-diffusion model under constant volatility

As a first example, we consider the case of American put options with jump-diffusion under constant volatility. In order to illustrate the utility of our spectral collocation method based on the penalty approach, we perform two experiments. In the first experiment, we check the behaviour of the method with respect to the penalty parameter ϵ . We take an absolute and relative error tolerances of the implicit forth-order Lobatto method to be 10^{-5} . We vary the value of the penalty parameter ϵ , and for each fixed number of spatial nodes we then compute the error of the American put options and the ratio between two consecutive errors. All the results are presented in Table 7.4.2. We observe that the error is nearly independent of the spatial mesh points and is of order $\mathcal{O}(\epsilon)$. We obtain very satisfactory results for a small number of grid points. For instance, for $\epsilon = 10^{-5}$ and $N = 80$ an error of order 10^{-4} is obtained.

In the next numerical experiment, we verify the behaviour of our spectral method. We choose the penalty parameter to be $\epsilon = 10^{-6}$ and the time integration tolerance to be 10^{-6} . From Table 7.4.3, we keep the tolerance fixed, vary the number of grid points, and report the value of the American options at the strike price E , the ‘Error’ and the ‘Ratio’ which is obtained by dividing the difference between the numerical and benchmark solutions obtained at N and $2N$ grid points, respectively. We observe a

Table 7.4.2: Results for the fully discrete numerical method for solving jump-diffusion for American options with constant volatility using parameters given in Table 7.4.1 and $TOL=10^{-5}$. Benchmark solution: 5.5676747.

| ϵ | N | Error | Ratio |
|------------|-----|---------|-------|
| 10^{-2} | 80 | 7.93E-3 | *** |
| 10^{-3} | 80 | 9.13E-4 | 8.68 |
| 10^{-4} | 80 | 2.34E-4 | 3.90 |
| 10^{-5} | 80 | 1.66E-4 | 1.41 |
| 10^{-2} | 160 | 7.90E-3 | *** |
| 10^{-3} | 160 | 7.83E-4 | 10.08 |
| 10^{-4} | 160 | 8.58E-5 | 9.12 |
| 10^{-5} | 160 | 1.87E-5 | 4.58 |
| 10^{-2} | 320 | 7.90E-3 | *** |
| 10^{-3} | 320 | 7.71E-4 | 10.25 |
| 10^{-4} | 320 | 6.61E-5 | 11.65 |
| 10^{-5} | 320 | 1.71E-6 | 38.64 |

Table 7.4.3: Errors in spectral discretisation numerical method for solving jump-diffusion model for American options with constant volatility; and using parameters given in Table 7.4.1 and $\epsilon = 10^{-6}$, $TOL = 10^{-6}$. Benchmark solution: 5.5676747.

| N | $V(E)$ | Error | Ratio |
|-----|-----------|---------|-------|
| 20 | 5.5211304 | 4.65E-2 | *** |
| 40 | 5.5669529 | 7.21E-4 | 64.48 |
| 80 | 5.5675031 | 1.71E-4 | 4.20 |
| 160 | 5.5676454 | 2.92E-5 | 5.86 |
| 320 | 5.5676692 | 5.50E-6 | 5.30 |

very rapid decrease of the error as the number of grid points N increases.

Furthermore, we evaluate option's Δ and Γ . The Δ of the put is always negative, see Figure 7.4.1 (bottom left). Therefore, the value of a put decreases if the asset price increases, see Figure 7.4.1 (top). This is in good agreement with the theory [77]. The Γ becomes zero when it is away from the strike price, but at the strike it becomes more and more peaked as we see in Figure 7.4.1 (bottom right). We see that Γ is small and has the largest value at strike price. Furthermore, we observe that the numerical values of these options and their Greeks are free of spurious oscillations around the strike price E that are typically present in numerical solutions of American

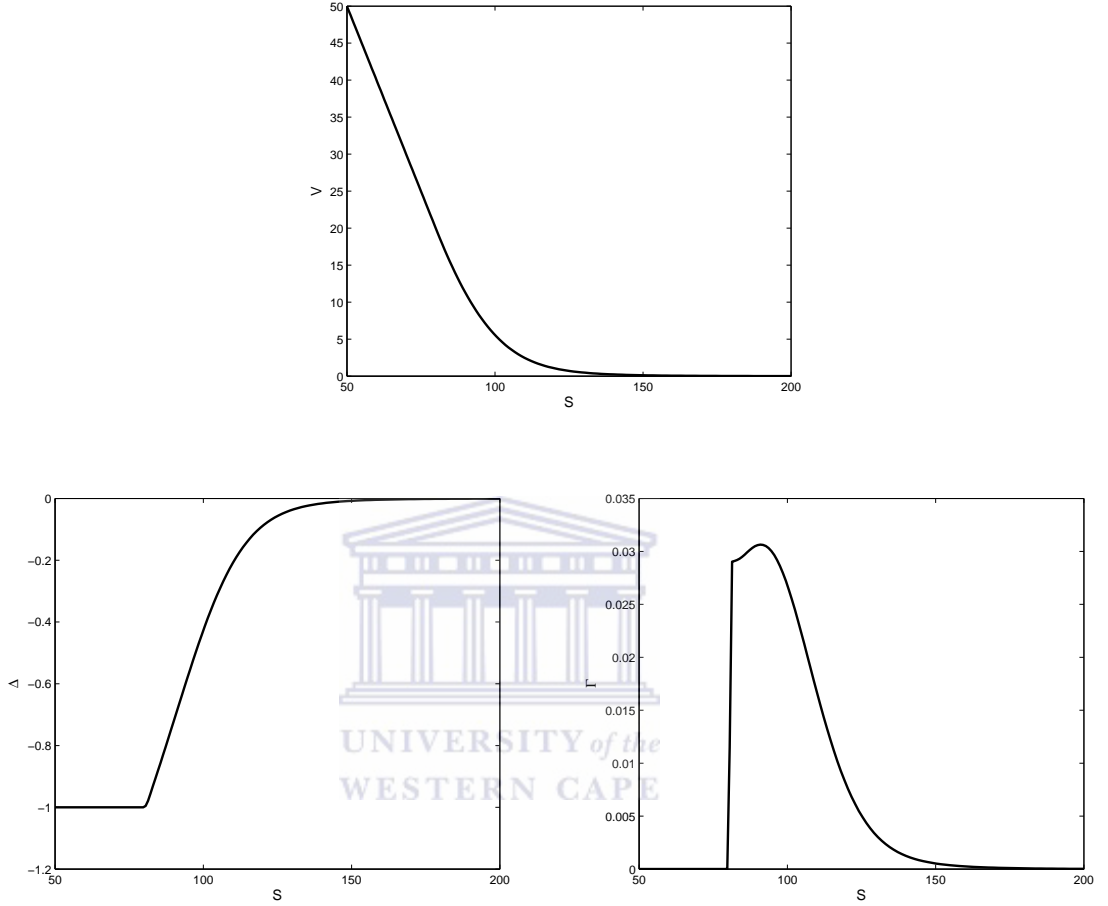


Figure 7.4.1: American put option under jump-diffusion process value (top), Δ (left bottom) and Γ (right bottom) using the data as in Table 7.4.1. The other parameters are $s_m = -1$, $s_M = 1$ and $\beta = 35$.

style contracts, in particular while computing Γ , due to the discontinuity of the second order derivative in the optimal exercise price.

7.4.2 Valuation of American jump-diffusion model under local volatility

One of the other challenging problem is the evaluation of American options under local volatility jump-diffusion process. To investigate the performance of our spectral approach for this type of problems, we perform similar experiments as in the case of

constant volatility. Firstly, we investigate the behaviour of our method with respect to the penalty parameter ϵ . All the results are reported in Table 7.4.4, where the penalty parameter varies from 10^{-2} to 10^{-5} and the number of spatial grid points are taken as $N = 80, 160$ and 320 . From Table 7.4.4, we observe that the error is of the order

Table 7.4.4: Results for the fully discrete numerical method for solving jump-diffusion model for American options with local volatility using parameters given in Table 7.4.1 and $TOL = 10^{-5}$. Benchmark solution: 4.7194288.

| ϵ | Nodes | Error | Ratio |
|------------|-------|---------|-------|
| 10^{-2} | 80 | 7.33E-3 | *** |
| 10^{-3} | 80 | 7.67E-4 | 9.55 |
| 10^{-4} | 80 | 1.35E-4 | 5.66 |
| 10^{-5} | 80 | 7.41E-5 | 1.82 |
| 10^{-2} | 160 | 7.33E-3 | *** |
| 10^{-3} | 160 | 7.28E-4 | 10.06 |
| 10^{-4} | 160 | 8.16E-5 | 8.91 |
| 10^{-5} | 160 | 2.75E-5 | 2.96 |
| 10^{-2} | 320 | 7.33E-3 | *** |
| 10^{-3} | 320 | 7.21E-4 | 10.15 |
| 10^{-4} | 320 | 6.91E-5 | 10.44 |
| 10^{-5} | 320 | 8.26E-6 | 8.35 |

Table 7.4.5: Errors in spectral discretisation numerical method for solving jump-diffusion model for American options with local volatility; and the set of parameters given in Table 7.4.1 and $\epsilon = 10^{-6}$, $TOL = 10^{-6}$, Benchmark solution: 4.7194288

| N | $V(E)$ | Error | Ratio |
|-----|-----------|----------|--------|
| 20 | 4.6940173 | 2.54E-2 | *** |
| 40 | 4.7192926 | 1.36E-4 | 186.57 |
| 80 | 4.7193449 | 8.39E-5 | 1.62 |
| 160 | 4.7193995 | 2.93E-5 | 2.85 |
| 320 | 4.7194121 | 1.679E-5 | 1.74 |

of the penalty term and is nearly independent of the number of mesh points and is of order of $\mathcal{O}(\epsilon)$. We next investigate the convergence of our spectral method. we choose the time integration tolerance and the penalty to be 10^{-6} . From Table 7.4.5, we keep the tolerance fixed, vary the number of grid points, and report the value of the American put option under local jump-diffusion process at the strike price E , the

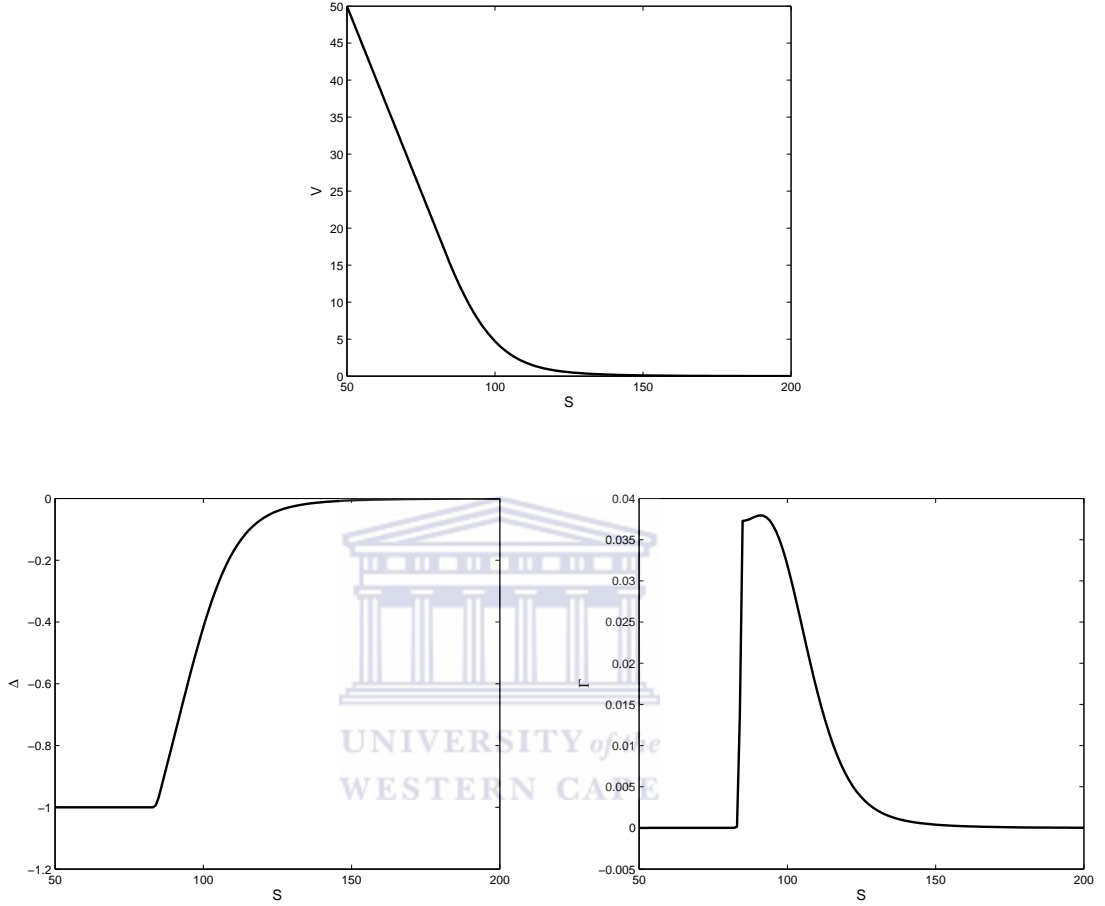


Figure 7.4.2: American put option under local volatility jump-diffusion process value (top), Δ (left bottom) and Γ (right bottom) using the data as in Table 7.4.1. The other parameters are $s_m = -1$, $s_M = 1$ and $\beta = 35$.

error and the ratio. We observe a very rapid decrease of the error as the number of grid points N increases. For instance, doubling the number of grid points from $N = 20$ to 40 results in reduction in the error by order two in magnitude. From $N = 160$ to 320, we observe a slow convergence. This is explained by the fact that the error achieves the order of the magnitude of the tolerance of the time integrator and that of the penalty parameter. The results reported in this case are similar to those of obtained for the first model where the volatility is a kept constant. Furthermore, from Figure 7.4.2, we observe that the numerical values of these options and their Greeks are free of spurious


oscillations around the strike price E which attests that the proposed method is robust even when these options have the local volatility.

7.5 Summary and discussions

We have presented a spectral collocation method based on the rational approximations and the Clenshaw-Curtis quadrature formulae with the penalty approach for pricing American put options under constant volatility and local volatility jump-diffusion process. The method is coupled with implicit fourth-order Lobatto time integration method. The total error depends on the spectral discretisation, the penalty parameter and the tolerance of the time integrator. By keeping the tolerance and the penalty parameter large enough, the fast convergence of the spectral method was observed. In fact, it was of the order the tolerance and the penalty parameter in both models. We have also computed the Greeks and found that they are free of oscillations. All these affirm that our spectral method is very accurate and robust for pricing American options under jump-diffusion process.

Chapter 8

Concluding remarks and scope for the future research



This thesis dealt with design and implementation of robust spectral methods for solving problems in computational finance. We have explored the use of classical spectral approaches and modified them suitably to provide exponentially accurate results (for the value of options and associated Greeks) for option pricing problems considered in this thesis.

We designed and implemented a fully spectral collocation method for solving European style vanilla and exotic options in Chapter 2. The method was initially designed to solve problems for European call and put, and then further extended to solve digital and supershare option pricing problems. The method was coupled with rational interpolation using prescribed barycentric weights and mapped Chebyshev points in asset (space) direction. We also investigated the convergence analysis of the proposed approach. Numerical results were checked against available analytical solutions and compared in a number of settings. In all experiments our rational collocation approach displayed an exponential convergence. We achieved satisfactory results with a very few mesh points.

In Chapter 3, we proposed a semi-discrete spectral method for solving models

present in Chapter 2. We realised that the semi-explicit spectral method gave the similar accuracy as that of the fully spectral method and therefore we continued exploring only the semi-discrete versions. The method in this chapter was based on a pseudo-spectral formulation of the PDE discretised by the means of an improved Lagrange formula. Implicit-Explicit (IMEX) Predictor-Corrector (PC) schemes were then used for time integration. We analysed the stability of the method and performed numerical experiments in order to illustrate the efficiency of the proposed method. Note that we have achieved significantly higher order accuracy using coordinate transformations that stretch points around the strike price.

In Chapter 4, we presented a robust rational spectral collocation method for pricing American options. Due to the free boundary conditions associated with the PDEs, we first reformulated the problem as a variational inequality. Then, by adding a penalty term, the resulting variational inequality was transformed into a nonlinear advection-diffusion-reaction equation on fixed boundaries. This nonlinear PDE was discretised in asset (space) direction by means of rational spectral collocation method, resulting into a system of stiff nonlinear ODEs which was then integrated using the implicit forth-order Lobatto time integration method. We carried out extensive comparisons with other results obtained by using some existing methods found in the literature.

After having solved the basic models, we then moved onto solving some more complex models. We considered European and American options ‘under local volatility, on both ‘dividend’ and ‘non-dividend’ paying assets in Chapter 5. In the case of European options, the PDE was discretised directly in space, by the mean of rational spectral method while a penalty approach was used to solve the partial differential complementary problem arising from American options resulting into a nonlinear partial differential equation. Then the nonlinear PDE was discretised in asset direction by means of a rational spectral collocation approximation on an adaptive grid. Through this discretisation, we obtained a system of ordinary differential equations that we solved using the implicit fifth-order RADAU time integration method. Several numerical results illustrating the robustness of our method were also presented.

Chapter 6 dealt with a more challenging problem which involved partial integro-differential equation (PIDE). The differential and integral parts of the PIDE are approximated by the rational spectral collocation and the Clenshaw-Curtis quadrature methods, respectively, resulting into a system of ODEs. We used the implicit-explicit predictor-corrector (IMEX-PC) schemes to integrate the ODEs in which the diffusion term was integrated implicitly, and the convolution integral, reaction and advection terms were integrated explicitly. We also analysed the stability of IMEX-PC and then performed several numerical experiments.

In Chapter 7, we extended the method proposed in the previous chapter to solve jump-diffusion models of American options. These type of problems were modelled by partial integro-differential complementary (PIDC) problems. We first reformulated the PIDC problem as a variational inequality, and then transformed it into a nonlinear partial integro-differential equation (PIDE) on fixed boundaries by adding a penalty term. We discretised the resulting nonlinear PIDE in asset (space) direction by means of a spectral method using suitable barycentric weights and transformed Chebyshev points. The system of ODEs that we obtained in this case was solved by using the implicit forth-order Lobatto time integration method. we obtained very promising numerical results.

In summary, we can mention that the applications of the rational spectral method for solving financial produced very accurate, robust and reliable methods. This method is very promising and can be consider as an alternative method for pricing financial derivatives. Furthermore, one of the other important issue that we would like to mention here is that the numerical results that we obtained for the Greeks were free of spurious oscillations which usually occurs when methods such as Crank-Nicolson are used.

As far as the scope for future research is concerned, we are currently extending our approach to solve problems of pricing linear and non-linear multi-asset options. Also we would like to investigate the effect of spectral filter and preconditioning on the convergence of our approach.

Bibliography

- [1] K. Al-Khaled, Sinc numerical solution for solitons and solitary waves, *Journal of Computational and Applied Mathematics* **130(1)** (2001), 283-292.
- [2] K. Al-Khaled, Numerical solution of the Fisher's reaction-diffusion equation by Sinc collocation methods, *Journal of Computation and Applied Mathematics* **137(2)** (2001), 245-255.
- [3] K. Al-Khaled, D. Kaya and M.A. Noor, Numerical comparison of the methods for solving parabolic equations, *Journal of Computation and Applied Mathematics* **157(3)** (2004), 735-743.
- [4] A. Almendral and C.W. Oosteele, Numerical valuation of options with jumps in the underlying, *Applied Numerical Mathematics* **53** (2005), 1-18.
- [5] L. Andersen and J. Andreasen, Jump diffusion processes: Volatility smile fitting and numerical methods for option pricing, *Review of Derivatives Research* **4** (2000), 231-262.
- [6] U. Asher, S.J. Ruuth and B.T.R. Wetton, Implicit-explicit methods for time dependent partial differential equations, *Numerical Analysis* **32(2)** (1995), 797-823.
- [7] U. Asher, S. Ruuth and R.J. Spiteri, Implicit-explicit Runge-Kutta methods for time dependent partial differential equations, *Applied Numerical Mathematics* **25** (1997), 151-167.

- [8] R. Baltensperger, J.P. Berrut and B. Noël, Exponential convergence of a linear rational interpolant between transformed Chebyshev points, *Mathematics of Computation* **68** (1999), 1109-1120.
- [9] R. Baltensperger and J.P. Berrut, The linear rational collocation method, *Journal of Computational and Applied Mathematics* **134** (2001), 243-258.
- [10] R. Baltensperger and J.P. Berrut and Y. Dubey, The linear rational pseudospectral method with pre-assigned poles, *Numerical Algorithms* **33** (2003), 53-63.
- [11] J. Barraquand and D. Martineau, Numerical valuation of high dimensional multivariate American securities, *Journal of Financial and Quantitative Analysis* **30(3)** (1995), 383-405.
- [12] A. Bayliss and E. Turkel, Mappings and accuracy for Chebyshev pseudo-spectral approximations, *Journal of Computational Physics* **101** (1992), 349-359.
- [13] A. Bensoussan and J.L. Lions, *Applications of Variational Inequalities in Stochastic Control*, *Studies in Mathematics and its Applications*, 12, North-Holland Publishing Co. 1982.
- [14] J.P. Berrut and H.D. Mittelmann, Lebesgue constant minimizing linear rational interpolation of continuous functions over the interval, *Computers and Mathematics with Applications* **33** (1997), 77-86.
- [15] J.P. Berrut and H. D. Mittelmann, Rational interpolation through the optimal attachment of poles to the interpolating polynomial, *Numerical Algorithms* **23** (2000), 315-328.
- [16] J.P. Berrut and H. D. Mittelmann, The linear rational pseudospectral method with iteratively optimized poles for two-point boundary value problems, *SIAM Journal on Scientific Computing* **23** (2001), 961-975.

- [17] J.P. Berrut and R. Baltensperger, The linear rational pseudospectral method for boundary value problems, *BIT Numerical Mathematics* **41** (2001), 868-879.
- [18] J.P. Berrut and H. D. Mittelmann, Linear rational interpolation and its application in approximation and boundary value problems, *Rocky Mountain Journal of Mathematics* **32** (2002), 527-544.
- [19] J.P. Berrut and L. N. Trefethen, Barycentric Lagrange interpolation, *SIAM Review* **46** (2004), 501-517.
- [20] J.P. Berrut, R. Baltensperger and H.D. Mittelmann, Recent development in barycentric rational interpolation, *Trends and Applications in Constructive Approximation, ISNM 151, Birkhäuser, Basel*, 2005.
- [21] F. Black and M. Scholes, Pricing of options and corporate liabilities, *Journal of Political Economy* **81**(3) (1973), 637-654.
- [22] A. Borici and H. Luthi, Pricing American Options by Fast Solutions of the Linear Complementarity Problem, in: *E. Kontoghiorghe, B. Rustem, S. Siokos (Eds.), Computational Methods in Decision-Making, Economics and Finance 2002*, 325-338.
- [23] A. Borici and H. Luthi, Fast solutions of complementarity formulations in American put pricing, *Journal of Computational Finance* **9**(1) (2005), 63-81.
- [24] S. Boscarino, On an accurate third order implicit-explicit Runge-Kutta method for stiff problems, *Journal of Applied Numerical Mathematics* **59** (2009), 1515-1528.
- [25] J.P. Boyd, *Chebyshev and Fourier Spectral Methods*, Dover, New York, 2001.
- [26] R. Breen, The accelerate binomial option pricing model, *Journal of Financial and Quantitative Analysis* **26** (1991), 53-164.

- [27] M.J. Brennan and E.S. Schwartz, The valuation of American put options, *Journal of Finance* **32(2)** (1977), 449-462.
- [28] M.J. Brennan and E.S. Schwartz, Finite difference methods and jump processes arising in the pricing of contingent claims: A synthesis. *Journal of Financial and Quantitative Analysis* **13(3)** (1978), 461-474.
- [29] M. Briani, C. La Chioma and R. Natalini, Convergence of numerical schemes for viscosity solutions to integro-differential degenerate parabolic problems arising in financial theory, *Journal of Numerical Mathematics* **98(4)** (2004), 607-646.
- [30] M. Broadie and J. Detemple, American option valuation: new bounds, approximations, and a comparison of existing methods, *Review of Financial Studies* **9** (1996), 1211-1250.
- [31] M. Broadie and P. Glasserman, Pricing American-style securities using simulation, *Journal of Economics and Dynamic Control* **21** (1997), 1323-1352.
- [32] M.P. Calvo, J. de Frutos and J. Novo, Linearly implicit Runge-Kutta methods for advection-reaction-diffusion equations, *Journal of Applied Numerical Mathematics* **37** (2001), 535-549.
- [33] M.P. Calvo and A. Gerisch, Linearly implicit Runge-Kutta methods and approximate matrix factorisation, *Journal of Applied Numerical Mathematics* **53** (2005), 183-200.
- [34] A. Kanevsky, M.H. Carpenter, D. Gottlieb and J.S. Heathaven, Application of Implicit-Explicit high order Runge-Kutta methods to discontinuous-Galerkin schemes, *Journal of Computational Physics* **225** (2007), 1753-1781.
- [35] C. Canuto, M.Y. Hussaini, A. Quarteroni, and T.A. Zang, *Spectral Methods in Fluid Dynamics*, Springer Series in Computational Physics, Springer-Verlag, New York, 1988.

- [36] M.H. Carpenter and C.A. Kennedy, Additive Runge-Kutta schemes for convection-reaction-diffusion equations, *Applied Numerical Mathematics* **44**(12) (2003), 139-181.
- [37] P. Carr and D. Faguet, Fast accurate valuation of American options, Technical Report, Cornell University, 1994.
- [38] J.R. Cash, Split linear multistep methods for the numerical integration of stiff differential systems, *Numerical Mathematics* **42** (1983), 299-310.
- [39] N. Clark and K. Parrot, Multigrid for American option pricing with stochastic volatility, *Journal of Applied Mathematics and Computation* **153** (2004), 165-186.
- [40] C.W. Clenshaw, The numerical solution of linear differential equations in Chebyshev series, *Mathematical Proceedings of the Cambridge Philosophical Society* **53**(1957), 134-149.
- [41] C.W. Clenshaw and A.R. Curtis, A method for numerical integration on an automatic computer, *Numerical Mathematics* **2** (1960), 197-205.
- [42] C.W. Clenshaw and H.J. Norton, The solution of nonlinear ordinary differential equations in Chebyshev series, *The Computer Journal* **6**(1963), 88-92.
- [43] T.F. Coleman, Y. Li and A. Verma, Reconstructing the unknown local volatility function, *Journal of Computational Finance* **2** (1999), 77-100.
- [44] R. Cont and E. Voltchkova, A finite difference scheme for option pricing in jumps diffusion and exponential Lévy models, *SIAM Journal on Numerical Analysis* **43**(4) (2005), 1596-1626.
- [45] G. Courtadon, A more accurate finite difference approximation for the valuation of options, *Journal of Financial and Quantitative Analysis* **17** (1982), 697-705.
- [46] J. Cox, S. Ross, The valuation of options for alternative stochastic processes, *Journal of Financial Economics* **3** (1976), 145-166.

- [47] J.C. Cox, S.A. Ross and M. Rubinstein, Option Pricing: A Simplified Approach, *Journal of Financial Economics* **7** (1979), 229-263.
- [48] C.W. Cryer, The solution of a quadratic programme using systematic overrelaxation, *SIAM Journal of Control and Optimization* **9** (1971), 385-392.
- [49] P. J. Davis and P. Rabinowitz, *Methods of numerical integration*, Academic Press Inc., Orlando, FL, 2nd edition, 1984.
- [50] J. de Frutos, Implicit-explicit Runge-Kutta methods for financial derivatives pricing models, *European Journal of Operational Research* **171** (2006), 991-1004.
- [51] J de Frutos, A spectral method for bonds, *Computers and Operational Research* **35** (2008), 64-75.
- [52] M.A.H. Dempster, J.P. Hutton and D.G. Richards, LP valuation of exotic American options exploiting structure, *Journal of Computational Finance* **2** (1998), 61-84.
- [53] E. Derman and I. Kani, Riding on a Smile, *RISK Magazine* **(1)** (1994), 32-39.
- [54] J. Dewynne, S. Howison and P. Wilmott, *Options Pricing: Mathematical Models and Computation.*, Oxford Financial Press, Oxford, U.K., 1993.
- [55] Y. d'Halluin, P.A. Forsyth and K.R. Vetzal, Robust numerical methods for contingent claims under jump diffusion processes, *IMA Journal of Numerical Analysis* **25(1)** (2005), 87-112.
- [56] B. Dupire, Pricing with a smile, *RISK Magazine* **1** (1994), 18-20.
- [57] E. Eliassen, B. Machehauer and E. Rasmussen, On a numerical method for integration of the hydrodynamical equations with a spectral representation of the horizontal fields, Report, Institut for Teoretisk Meteorologi, University of Copenhagen, 1970.

- [58] L. Feng and V. Linetsky, Pricing options in jump-diffusion models: an extrapolation approach, *Operations Research* **56**(2) (2008), 304-325.
- [59] N. Flyer and P.N. Swartrauber, The convergence of Spectral and Finite Difference Methods for initial-boundary value problems, *Journal of Scientific Computation* **23**(5)(2000), 1731-1751.
- [60] B. Fornberg, *A Practical Guide to Pseudospectral Methods*, Cambridge University Press, 1996.
- [61] P.A. Forsyth and K.R. Vetzal, Quadratic convergence of a penalty method for valuing American options, *SIAM Journal on Scientific Computing* **23**(6) (2002), 2096-2123.
- [62] R.A. Frazer, W.P. Jones and S.W. Skan, *Approximation to Functions and to the Solution of Differential Equations*, R&M 1799, Aeronautical Research Council, London, 1937.
- [63] R. Geske and H.E. Johnson, The American put option valued analytically, *Journal of Finance* **39** (1984), 1511-1524
- [64] R. Geske and K. Shastri, Valuation by approximation: a comparison of alternative option valuation techniques, *Journal of Finance and Quantitative Analysis* **20** (1985), 45-71.
- [65] D. Gottlieb and S.A. Orszag, *Numerical Analysis of Spectral Methods*, Society for Industrial and Applied Mathematics, Philadelphia, 1977.
- [66] A. Greenberg, *Chebyshev Spectral Method for Singular Moving Boundary Problems with Application to Finance*, PhD thesis, California Institute Of Technology, 2002.

- [67] I. Grooms and K. Julien, Linearly implicit methods for nonlinear PDEs with linear dispersion and dissipation, *Journal of Computational Physics* **230** (2011), 3630-3650.
- [68] E. Hairer and G. Wanner, *Solving Ordinary Differential Equations, II: Stiff and Differential-Algebraic Problems*, Springer-Verlag, New York, 1996.
- [69] N. Hale, *On the Use of Conformal Maps to Speed Up Numerical Computations*, PhD Thesis, St. Hugh's College, Oxford University, 2009.
- [70] M.J. Harrison and D.M. Kreps, Martingales and arbitrage in multiperiod securities markets, *Journal of Economic Theory* **20(3)** (1979), 381-408.
- [71] H. Han and X. Wu, A fast numerical method for the Black-Scholes equation of American options, *SIAM Journal on Numerical Analysis* **41(6)** (2003), 2081-2095.
- [72] P. Henrici, *Essentials of Numerical Analysis with Pocket Calculator Demonstrations*, Wiley, New York, 1982.
- [73] S. Heston, A closed-form solution for options with stochastic volatility with applications to bond and currency options, *Review of Financial Studies* **6** (1993), 327-343.
- [74] D.J. Higham, Nine Ways to Implement the Binomial Method for Option Valuation in MATLAB, *SIAM Review* **44(4)** (2002), 661-677.
- [75] N.J. Higham, The numerical stability of the barycentric Lagrange interpolation, *IMA Journal of Numerical Analysis* **24** (2004), 547-556..
- [76] J. Hull and A. White, The pricing of options with stochastic volatilities, *Journal of Finance* **42** (1987), 281-300.
- [77] J.C. Hull, *Options, Futures and other Derivatives*, 4th ed., Prentice-Hall, New Jersey, 2000.

- [78] W. Hundsdorfer and S.J. Ruuth, IMEX extension of linear multistep methods with general monotonicity and boundedness properties, *Journal of Computational Physics* **225** (2007), 2016-2042.
- [79] P. Jaillet, D. Lamberton, B. Lapeyere, Variational inequalities and the pricing of American options, *Acta Applicandae Mathematicae* **21**(1990), 263-289.
- [80] N. Ju and R. Zhong, An approximate formula for pricing American options, *Journal of Derivatives* **7(2)** (1999), 31-40.
- [81] A. Kanevsky, M.H. Carpenter, D. Gottlieb and J.S. Heathcote, Application of implicit-explicit high order Runge-Kutta methods to discontinuous-Galerkin schemes, *Journal of Computational Physics* **225** (2007), 1753-1781.
- [82] L.V. Kantorovich, On a new method of approximate solution of partial differential equations, *Doklady Akademii Nauk SSSR* **4** (1934), 532-536.
- [83] A.Q.M. Khaliq, D.A. Voss and S.H.K. Kazmi, A linearly implicit predictor-corrector scheme for pricing American options using a penalty methods approach, *Journal of Banking and Finance* **30** (2006), 489-502.
- [84] J. Kim and P. Moin, Application of fractional-step method in incompressible Navier-Stokes equations, *Journal of Computational Physics* **59** (1985), 335-356.
- [85] R. Kosloff and H. Tal-Ezer, A modified Chebyshev pseudospectral method with a time step restriction, *Journal of Computational Physics* **104** (1993), 457-469.
- [86] S.G. Kou, A jump diffusion model for pricing options, *Management Science* **48** (2002), 1086-1101.
- [87] M. Koulisianis, T. Papatheodorou, Valuation of American Options Using Direct, Linear Complementarity-Based Methods, *Proceedings of the ICCSA* **3** (2003), 178-188.

- [88] H.O. Kreiss and J. Oliger, Comparison of accurate methods for the integration of hyperbolic equations, *Tellus* **24**(1972), 199-215.
- [89] Y. Kwok, *Mathematical Models of Financial Derivatives*, Springer-Verlag, Singapore, 1998.
- [90] R. Lagnado and S. Osher, Reconciling Differences, *RISK Magazine* **1** (1997), 79-83.
- [91] J.L. Lagrange, Leçons élémentaires sur les mathématiques, données à l'Ecole Normale en 1795, *Journal de l'École polytechnique* **7** (1795), 183-287.
- [92] C. Lanczos, Trigonometric interpolation of empirical and analytical functions, *Journal of Mathematical Physics* **17**(1938), 123-199.
- [93] S.T. Lee and H.W. Sun, Fourth order compact boundary value method for option pricing with jumps, *Advances in Applied Mathematics and Mechanics* **1(6)** (2009), 845-861.
- [94] D.L. Lewis, J. Lund and K.L. Bowers, The space-time Sinc-Galerkin method for parabolic equations, *International Journal of Numerical Methods Engineering* **24(9)** (1987), 1629-1644.
- [95] D. Li, C. Zhang, W. Wang and Y. Zhang, Implicit-explicit predictor corrector schemes for nonlinear parabolic differential equations, *Applied Mathematical Modelling* **35** (2011), 2711-2722.
- [96] F.A. Longstaff and E.S. Schwartz, Valuing American options by simulation: A simple least-squares approach, *The Review of Financial Studies* **14(1)** (2001), 113-147.
- [97] J. Lund and C.R. Vogel, A fully-Galerkin methods for the numerical solution of inverse problem in parabolic partial differential equation, *Inverse Problems* **6** (1990), 205-217.

- [98] J. Lund and K.L. Bowers, *Sinc Methods For Quadrature and Differential Equations*, SIAM, Philadelphia, 1992.
- [99] D.B. Madan and E. Seneta, The variance gamma model for share market returns, *Journal of Business* **63** (1990), 511-524.
- [100] A. Mayo, Methods for the rapid solution of the pricing PIDEs in exponential and Merton models, *Journal of Computational and Applied Mathematics* **222** (2008), 128-123.
- [101] B.J. McCartin and S.M. Labadie, Accurate and efficient pricing of vanilla stock options via the Crandall-Douglas scheme, *Applied Mathematics and Computation* **43(1)** (2003), 39-60.
- [102] R.C. Merton, Option pricing when the underlying stocks are discontinuous, *Journal of Financial Economics* **5** (1976), 125-144.
- [103] G. Meyer and J. van der Hoek, The Valuation of American Options with the Method of Lines, *Advances in Futures and Options Research* **9** (1997), 265-286.
- [104] M. Muhammad and M. Mori, Double exponential formulas for numerical indefinite integration, *Journal of Computational and Applied Mathematics* **161** (2003), 431-448.
- [105] B.F. Nielsen, O. Skavhaug and A. Tveito, Penalty and front-fixing methods for the numerical solutions of American option problems, *Journal of Computational Finance* **5** (2002), 69-97.
- [106] C.W. Oosterlee, C.C.W. Leentvaar and X. Huang, Accurate American option pricing by grid stretching and higher order finite differences, Technical Report, Delft Institute of Applied Mathematics, Delft University of Technology, The Netherlands, 2005.

- [107] S.A. Orszag, Numerical methods for the simulation of turbulence, *Physics of Fluids* **12**(1969), 250-257.
- [108] S.A. Orszag, Transform method for calculation of vector coupled sums: Application to the spectral form of the vorticity equation, *Journal of the Atmospheric Sciences* **27**(1970), 890-895.
- [109] S.A. Orszag, Comparison of pseudospectral and spectral approximations, *Studies in Applied Mathematics* **51**(1972), 253-259.
- [110] J. Persson and L. von Sydow, Pricing multi-asset options using a space-time adaptive finite difference method, Department of information technology, Uppsala University, Technical report 2003-059, ISSN 1404-3203.
- [111] A. Quarteroni C. Canuto, M.Y. Hussaini and T.A. Zang, *Spectral Methods: Fundamentals in Single Domains*, Springer, 2006.
- [112] S. Raible, Lévy Processes in Finance: Theory, Numerics and Empirical Facts, PhD Thesis, Institut für Mathematische Stochastik, Albert-Ludwigs-Universität Freiburg, Germany, 2000.
- [113] L.C.G. Rogers, Monte Carlo valuation of American options, *Mathematical Finance* **12**(3) (2002), 271-286.
- [114] M. Rubinstein, Implied Binomial Trees, *Journal of Finance* **49** (1994), 771-818.
- [115] S.J. Ruuth, Implicit-explicit methods for reaction-diffusion problems in pattern formation, *Journal of Mathematical Biology* **34** (1995), 148-176.
- [116] E.W. Sachs and A.K. Strauss, Efficient solution of a partial integro-differential equation in finance, *Applied Numerical Mathematics* **58** (2008), 1687-1703.
- [117] I. Silberman, Planetary waves in the atmosphere, *Journal of Meteorology* **11** (1954), 27-34.

- [118] J.C. Slater, Electronic energy bands in metal, *Physical Review* **45**(1934), 794-801.
- [119] A. Solomonoff and E. Turkel, Global properties of pseudospectral methods, *Journal of Computational Physics* **81** (1989), 239-276.
- [120] F. Stenger, *Numerical Methods Based on Sinc and Analitic Functions*, Springer-Verlag, New York, 1993.
- [121] F. Stenger, A Sinc-Galerkin methods for solution of boundary value problems, *Mathematics of Computation* **33**(1979), 85-109.
- [122] S. Suh, *Orthonormal Polynomials in Pricing Options by PDE and Martingale Approaches*, PhD thesis, University of Virginia, 2005.
- [123] S. Suh, Pseudo-spectral methods for pricing options, *Quantitative Finance* **9**(6) (2009), 705-715.
- [124] E. Tadmor, The exponential accuracy of Fourier and hebyshev Differencing Methods, *Journal of Numerical Analysis* **23**(1) (1986), 1-10.
- [125] H. Takahasi and M. Mori, Double exponential formulas for numerical integration, *Publications of the Research Institute for Mathematical Sciences Kyoto University* **9** (1974), 721-741.
- [126] D.Y. Tangman, A. Gopaul and M. Bhuruth, Numerical pricing of options using higer-order compact finite diffence schemes, *Journal of Computational and Applied Mathematics* **218** (2007), 270-280.
- [127] D.Y. Tangman, A. Gopaul and M. Bhuruth, Exponential time integration and Chebychev discretisation schemes for fast pricing of options, *Applied Numerical Mathematics* **58** (2008), 1309-1319.
- [128] D. Tavella and C. Randale, *Pricing Financial Instruments: The Finite Difference Method*, John Wiley and Sons, New York, 2000.

- [129] T.W. Tee, *An Adaptive Rational Spectral Method for Differential Equations With Rapidly Varying Solutions*. Ph.D. Thesis, Exter College University of Oxford, 2006.
- [130] T.W. Tee and L.N. Trefethen, A rational Spectral collocation method with adaptively transformed Chebyshev grids points, *Journal of Scientific Computation* **28(5)**, 1798-1811.
- [131] J.A. Tilley, Valuing American options in a path simulation model, *Transactions of the Society of Actuaries* **45**(1993), 93-104.
- [132] J. Toivanen, Numerical methods for European and American options under Kou's jump-diffusion model, *SIAM Journal on Scientific Computing* **30(4)** (2008), 1949-1970.
- [133] J.V. Villadsen and W.E. Stewart, Solution of boundary value problems by orthogonal collocation, *Chemical Engineering Science*, **22** (1967), 1483-1501.
- [134] D.A. Voss and M.J. Casper, Efficient split linear multistep methods for stiff ODEs, *SIAM Journal on Scientific and Statistical Computing* **10** (1989), 990-999.
- [135] D.A. Voss and A.Q.M. Khaliq, A Linearly implicit predictor-corrector methods for reaction-diffusion equations, *Computers Mathematics with Applications* **38** (1999), 207-216.
- [136] M. Webb, L.N. Trefethen and P. Gonnet, Stability of the barycentric interpolation formulas, *SISC Journal of Scientific Computing* **24(4)** (2010), 547-556
- [137] J.A.C. Weideman, Spectral methods based on nonclassical orthogonal polynomials, *International Series on Numerical Mathematics* **131**(1999), 238-251.
- [138] W. Werner, Polynomial interpolation: Lagrange versus Newton, *Mathematics of Computation* **43** (1984), 205-217.

- [139] R.J. Williams, *Introduction to the Mathematics of Finance*, American Mathematical Society, Rhode Island, 2006.
- [140] P. Wilmott, S. Howison and J. Dewynne, *The Mathematics of Financial Derivatives*, Cambridge University Press, 1995.
- [141] P. Wilmott, *Derivatives*, Wiley, New York, 1998.
- [142] P. Wilmott, *Quantitative Finance*, John Wiley & Sons, 2000.
- [143] M. Willyard, *Adaptive Spectral Element Methods to Price American Options*, PhD Thesis, Florida State University, 2011.
- [144] K. Wright, Chebyshev collocation methods for ordinary differential equations, *The Computer Journal* **6**(1964), 358-365.
- [145] L. Wu and Y.K. Kwok, A front-fixing finite difference method for the valuation of American options, *Journal of Financial Engineering* **6**(2) (1997), 83-97.
- [146] X. Wu, Z. Ding, Differential Quadrature Method for Pricing American Options, *Numerical Methods for Partial Differential Equations* **18** (2002), 711-725
- [147] K. Zhang and S. Wang, Pricing options under jump diffusion processes with fitted finite volume method, *Applied Mathematics and Computation* **201** (2008), 398-413.
- [148] Y.L. Zhu, X. Wu and I.L. Chern, *Derivatives Securities and Difference Methods*, Springer, New York, 2004.
- [149] W. Zhu, *A Spectral Element Method to Price Single and Multi-asset European Options*, Phd thesis, The Florida State University College of Arts and Sciences, 2008.
- [150] W. Zhu and D.A. Kopriva, A spectral element method to price European options. I. Single asset with and without jump-diffusion, *Journal of Scientific Computing* **39** (2009), 222-243.